ANL-5680

ARGONNE NATIONAL LABORATORY
P. O. Box 299
Lemont, Illinois

ANNUAL REPORT

1956

Operated by The University of Chicago
under
Contract W-31-109-eng-38

DISCLAIMER

TABLE OF CONTENTS

		Page
PREFACE		4
PHYSICAL SCIENCES		6
REACTOR SCIENCES		38
BIOLOGICAL AND MEDICAL SCIENCES		71
LABORATORY ADMINISTRATION AND SERVICES		96
APPENDIX	Scientific Publications of the Staff of Argonne National Laboratory since the Previous Annual Report	107

PREFACE

The staff of the Argonne National Laboratory feels that the year 1956 has been a most successful one. A number of significant developments have materialized from both our basic research and our engineering development programs. In this, our second Annual Report to be issued, accounts of some of these accomplishments - ones which have reached a stage where a summary would be of general interest - have been given. Accordingly, this report describes, for the most part, a different set of activities from that included in the last Annual Report (ANL-5610). We have purposely avoided the format of a progress report in order to present a more readable account of scientific and technical achievement. The reader who wants more details about the work summarized here or about the many ANL projects not mentioned in this report should consult the various progress and topical reports issued by the Laboratory during 1956, as well as the professional literature accepted for publication by the scientific journals. A list of the latter, in alphabetical order by author, is given as an appendix.

A section summarizing the administrative and financial activities for Fiscal Year 1956 has also been included. Additional data is presented to permit comparison with the actual costs for Fiscal Year 1955 and the projected costs for Fiscal Year 1957.

PART I

PHYSICAL SCIENCES

	Page
NEUTRON PHYSICS	6
Resonance Parameters of Pu^{239}	6
A New Delayed-Neutron Period with a Bromine Precursor	8
NUCLEAR STRUCTURE AND PROPERTIES	9
Capture Gamma-Ray Spectrum of Gold	9
The Rotation of Elongated Nuclei	11
Lifetime Measurements from Recoil Studies	14
Paramagnetic Resonance Spectrum of Curium	15
Decay Schemes of Short-Lived Radioactive Nuclides	15
Reformulation of Quantum Field Theory	16
STOPPING POWER OF GASES FOR HELIUM IONS	18
SECONDARY EMISSION OF BERYLLIUM IONS	20
STRUCTURE OF SOLIDS	22
Hydrides	22
Uranium Oxides	22
Paramagnetic Resonance in Irradiated KCl Crystals	22
RESEARCH IN CHEMISTRY	23
Decay Kinetics of I_2^-	23
Activation of Phosphorus Compounds	24
Fluorine Chemistry	24
Fused Salt Chromatography	27
Separations of the Rare Earth Elements	28
Solvent Extraction Behavior of Lanthanides and Actinides	28
Differential Electrochromatography	28
Tritium Labeling	30
The Heat of Vaporization of Liquid He^3	30
RESEARCH INSTRUMENTS AND METHODS	31
The Particle Accelerator	31
Recoil-Type Neutron Spectrometer	32
Scintillation Counters	34
Particle-Size Analysis by Radioactivation	35
Sixty-Inch Cyclotron Facility	36

Resonance Parameters of Pu^{239}

The neutron velocity selector (fast chopper) described in the preceding Annual Report (ANL-5610) has been employed in making direct and independent measurements of all partial widths of the low-energy resonances of Pu^{239}. These measurements allow computation of the average values of the resonance parameters, which are important both for nuclear theory and for application in reactor engineering.

All quantities were measured with the same system in order to obviate the difficulties encountered in relating the partial cross sections when measured by different groups using different equipment. The resolution was much better than in previous work because of the large flux of neutrons from the CP-5 reactor and because of improvements in the chopper, the time analyzer and the detecting system (Fig. 1).

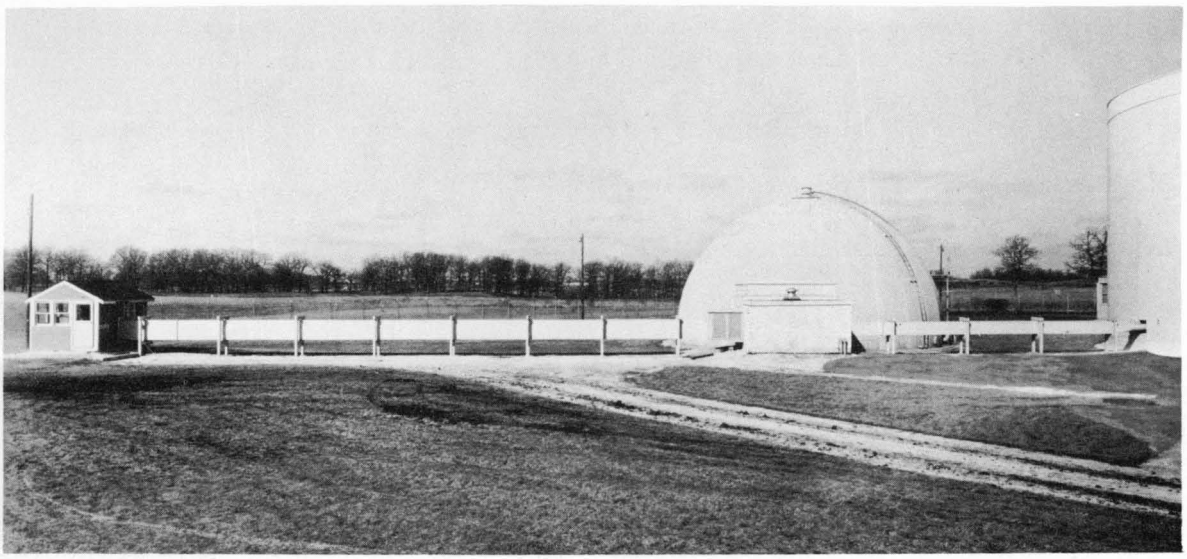

Fig. 1. Flight tube and detector stations for the fast chopper. The source of the neutrons is the research reactor CP-5 housed in the building at the right. The small buildings, which house the detectors, are respectively 25 meters and 60 meters from the chopper. The speed of the neutrons, which varies from 15 microseconds to 30 milliseconds, is found by electronically timing the flight from chopper to detector.

The individual experiments on Pu^{239} were the following:

(1) Using a boron-loaded liquid scintillator as the detector, the total cross section was found by neutron transmission measurements.

(2) A thin film (1 mg/cm^2) of plutonium was applied to the inner surface of a gas scintillation counter, the development of which was described in the 1955 Annual Report, and the fission fragments resulting from irradiation of this Pu^{239} by neutrons were counted. Pulses due to alpha particles from the radioactive decay of plutonium were rejected by a pulse-height analyzer, spurious large counts due to the almost

simultaneous passage of several alpha rays being avoided by the very short resolving time of this counter. The fission cross sections found directly from these measurements are plotted against the energy of the incident neutrons in Fig. 2. The fission widths of the resonances were found from the areas of the resonance peaks of this graph. This method is good at the resonances, but at positions removed from the resonances it is inaccurate because of poor statistics.

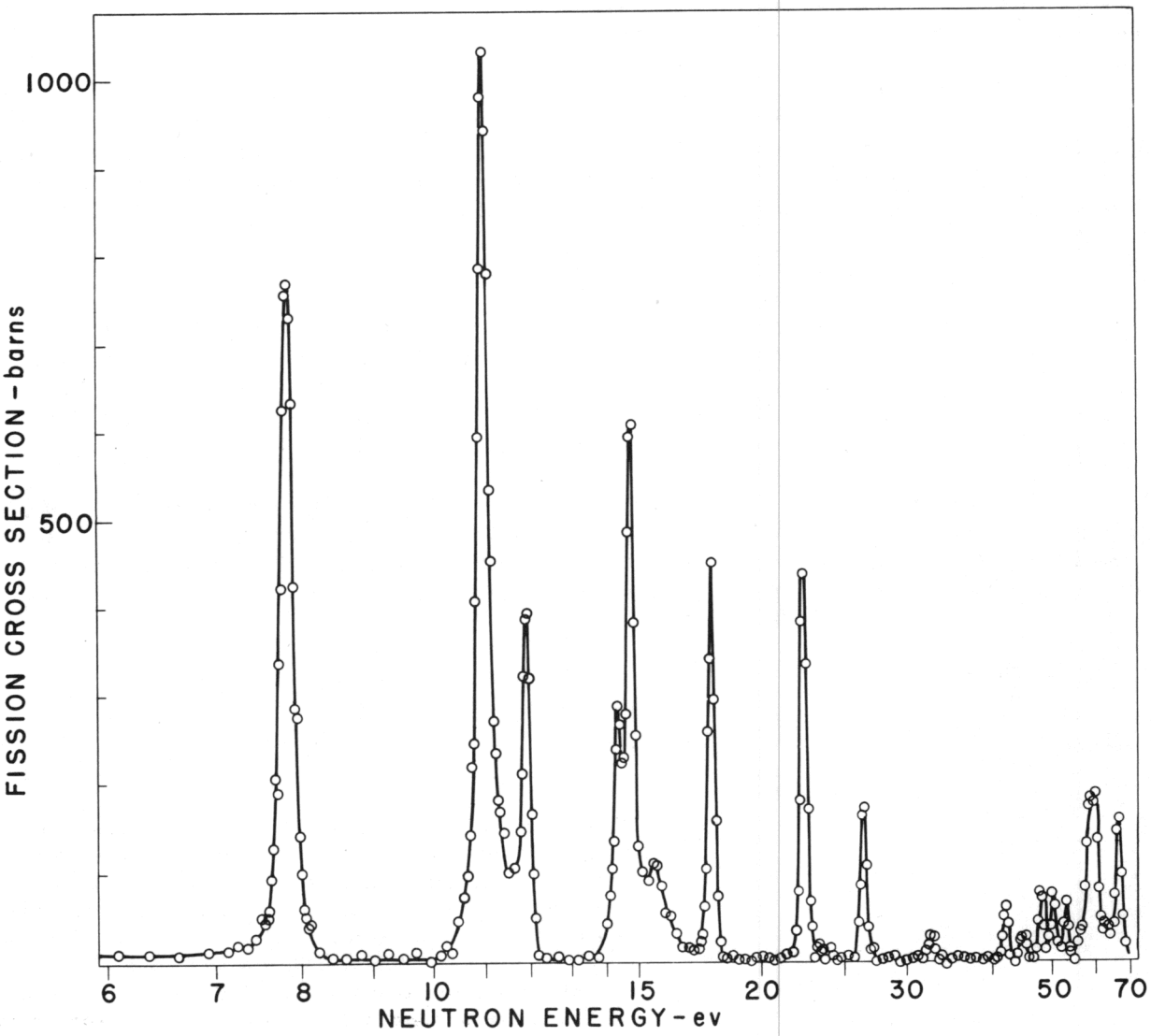

Fig. 2. The fission cross section of Pu^{239} as a function of the neutron energy.

(3) To achieve an adequate counting rate for the measurement of fission cross sections in off-resonance regions, it was necessary to use a thick sample. Since the short range of fission fragments makes them unusable except in the thin films, the fast neutrons from the fissions were counted instead. A sample of Pu^{239}, 3 mm thick, was placed between two liquid scintillation counters connected in coincidence. The fast neutrons from the fissions were detected by means of the recoil protons they produced in the liquid, while the scattered slow neutrons and products of radioactive disintegration were excluded by shields of B_4C and lead.

(4) A direct measurement was made of η, the number of fission neutrons produced per neutron absorbed by the fissionable material. The experimental arrangement was the same as in (3) except that the plutonium sample was thick enough to stop all the incident neutrons. The incident flux of neutrons was measured by a parallel-plate proportional counter with a thin layer of boron on one electrode. These direct measurements of η are in good agreement with the values of η computed from the resonance parameters found above, in contrast with the serious disagreement at thermal energies at the time of the Geneva Conference. Directly measured values of η have been obtained near the peaks of the nine levels at energies less than 23 ev. These measurements contain no known systematic errors greater than 2%.

Both the dependence of η on neutron energy in the neighborhood of resonance and the asymmetry found in a detailed study of the shapes of the peaks in the cross-section curves indicate the interference between levels which is characteristic of a very small number of exit channels for fission. It is barely possible that the asymmetry may be due to a chance occurrence of unresolved levels of just the right size and position.

A New Delayed-Neutron Period with a Bromine Precursor

In studying the energy spectrum of the delayed neutrons having Br^{87} as precursor, a small departure from pure exponential decay, indicating the presence of a component with a half-life of the order of 20 seconds, was observed. This suggested the presence of I^{137} with its well-known 22-second period, but the chemical separation of the bromine from other fission products made this explanation seem unlikely.

The continuous-flow system shown in Fig. 3 was therefore adjusted to enhance this short-period component, in comparison with the 54-second period having Br^{87} as precursor, by decreasing the average time between the formation of a bromine atom and its arrival at the CCl_4 vessel in which its decay was detected.

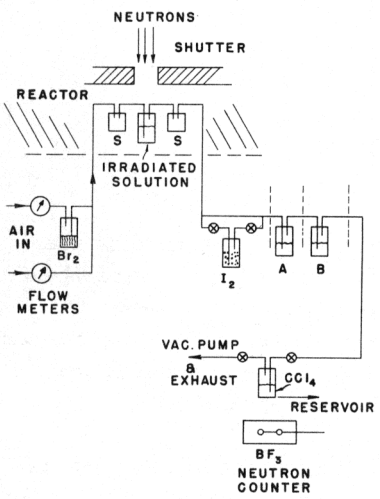

Fig. 3. System for the continuous-flow chemical separation of bromine. S, S are safety vessels to catch the radioactive overflow of irradiated solution in case of malfunction of the system. The I_2 is added as a "hold-back carrier" to ensure removal of the active iodine by the $KBrO_3$ solution in A. Vessel B, which contains a solution of $FeSO_4$ to trap bromine, was in the system only for an auxiliary experiment.

The active bromine was formed by the fission of U^{235} in the irradiated solution (Fig. 3) of enriched uranyl nitrate dissolved in dilute nitric acid. This solution, which was located in the thermal column of the research reactor, CP-5, also contained some potassium bromate for the two purposes of converting non-volatile bromides to bromine gas and of trapping iodine in the form of iodates. The active bromine was transported to the CCl_4 vessel, adjacent to the neutron counters, by a flow of air and carrier bromine. The active bromine formed by fission in the irradiated solution exchanged rapidly with the

carrier bromine and was swept out (except for the fraction in the BrO_3^-, with which exchange was negligible for the purposes of this experiment). The time elapsed between the formation of an active bromine atom and its arrival at the CCl_4 vessel was lowered to about 15 seconds by using only about 15 cc of uranyl nitrate solution and by keeping the flow rate as high as possible.

The decay curve obtained exhibited a short-lived activity whose half-life corresponded exactly to the previously determined 15.5-second period of the beta decay of Br^{88}. Hence, since the chemical separation eliminated the possibility of other elements, the sequence was quite clearly:

$$\xrightarrow{n} {}_{92}U^{235} \xrightarrow[\text{Fission}]{} {}_{35}Br^{88} \xrightarrow[15.5\ \text{sec}]{\beta^-} {}_{36}Kr^{88*} \xrightarrow[\text{prompt}]{n} {}_{36}Kr^{87} \quad .$$

This conclusion has been confirmed by a number of auxiliary experiments. The period had been missed by previous investigators since it cannot be distinguished from the 22-second period of I^{137} by the study of decay curves without chemical separation, and previous chemical separations had not been rapid enough to permit taking decay curves before this activity disappeared.

This delayed-neutron activity is remarkable in that the ${}_{36}Kr^{88}$ is the first even-even nucleus which has been found to be a neutron emitter. This nucleus indeed has a larger separation energy for the last neutron than its neighbors of odd neutron number, but the separation energies are relatively low for both odd and even neutron numbers just above the value of 50 for a closed shell. Moreover, the energy difference between the odd-odd ${}_{35}Br^{88}$ and the even-even ${}_{36}Kr^{88}$ is large enough so that the beta emission produces the latter in an excited state having sufficient energy for the emission of a neutron.

This method is being used to search for other delayed-neutron reactions.

NUCLEAR STRUCTURE AND PROPERTIES

Capture Gamma-Ray Spectrum of Gold

Careful tests followed by months of successful operation have shown that the Argonne 7.7-meter bent-crystal gamma-ray spectrometer described in the previous Annual Report fully measures up to its specifications. It can be used over the entire range from 20 kev to 7 Mev. Some idea of the potentialities of the instrument may be gained from Fig. 5, which is a line graph of a portion of the spectrum from Au^{198}. Of the 34 lines shown, only the lines marked R were known previously.

This is the beginning of a program to measure the capture gamma rays of as many as 90 per cent of the elements to accurately determine their lower energy levels. Such a systematic study should be an important guide to a fuller understanding of nuclear structure.

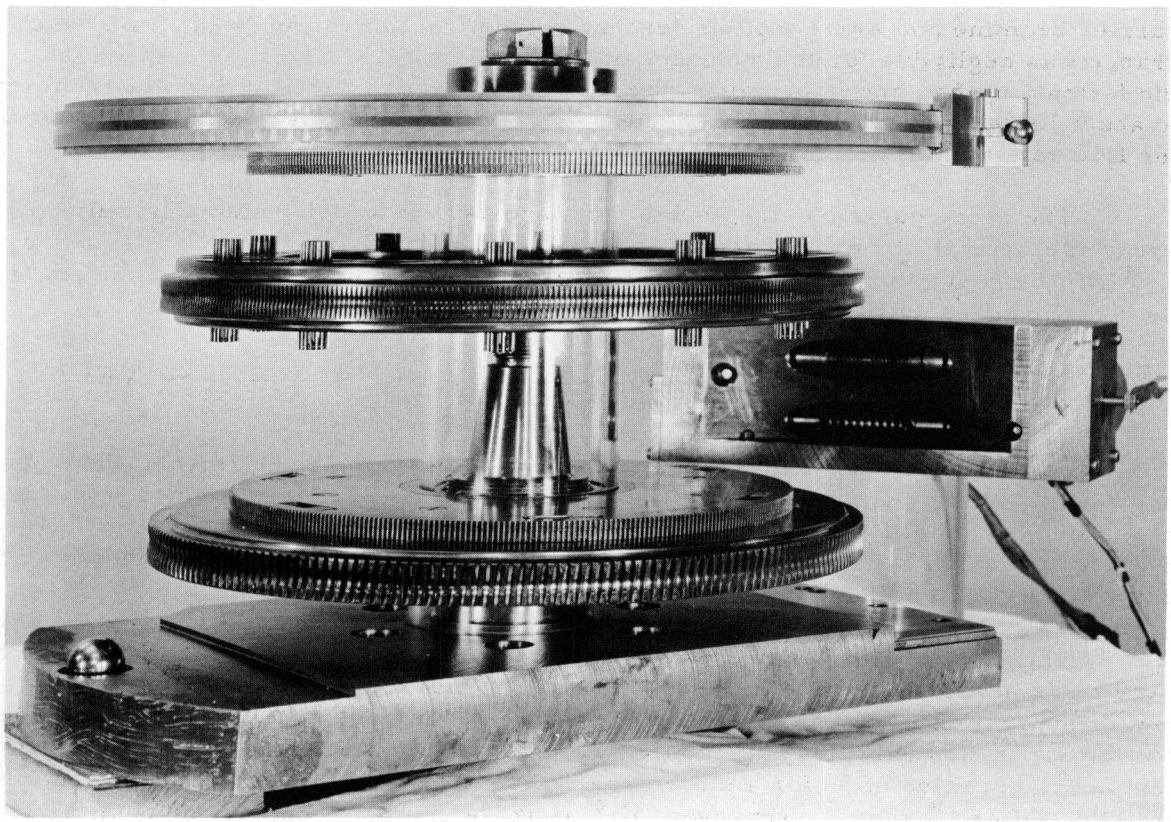

Fig. 4. The differential-gear system of the bent-crystal gamma-ray spectrometer. This arrangement provides the 1,296,000 to 1 reduction in speed needed to exploit the full resolution of the instrument. The worm (right center) is driven by a 27-rpm motor.

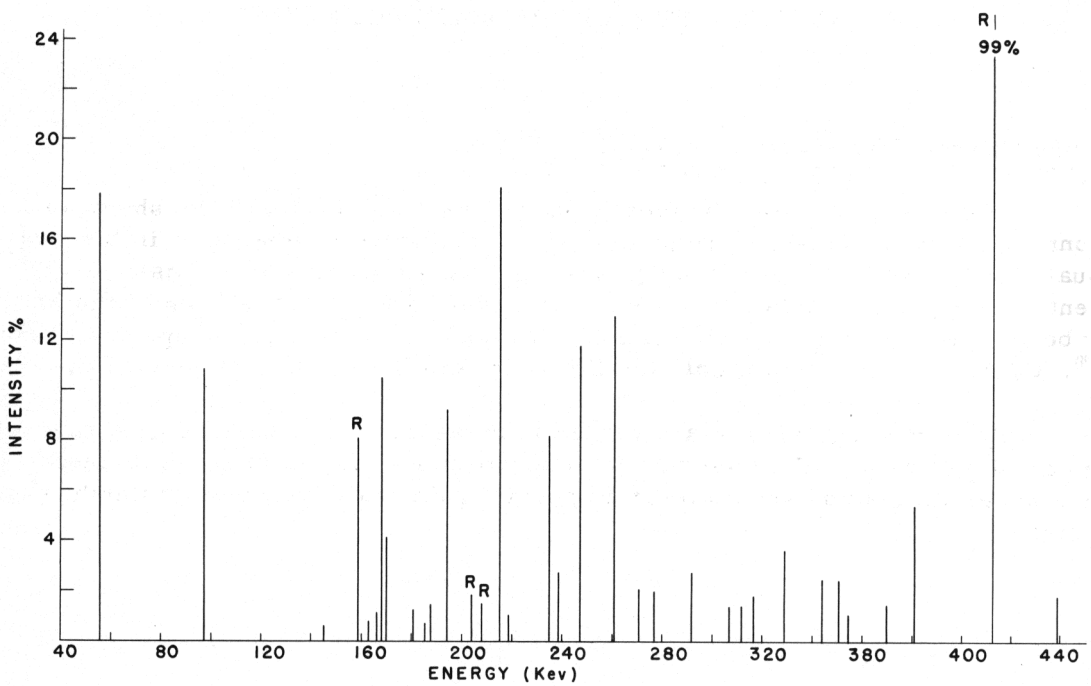

Fig. 5. Capture gamma-ray spectrum of Au^{198}. Some of the rays shown consist of closely-spaced unresolved lines. Only the lines marked R were known previously.

The Rotation of Elongated Nuclei

Some of the most interesting developments in nuclear physics are manifestations of the fact that most nuclei are not perfect spheres. The out-of-roundness was discovered in spectroscopic experiments on the "hyperfine structure" which showed that the energy of the atom depended slightly on the angle between the axis of the nucleus and the plane of the motion of an electron in a long and narrow elliptical orbit. The nuclei may be either oblate (somewhat flattened from spherical shape, like a doorknob) or prolate (somewhat elongated, like a watermelon) spheroids. The prolate shape is more common and more pronounced, extreme cases having their longest diameter almost 1.5 times their smallest diameter. The knowledge of nuclear shapes has been improved by the more recent molecular beam and magnetic resonance investigations.

To explain a number of phenomena observed in nuclear reactions, gamma radiation, and scattering experiments, as well as the fact that the density of nuclear matter is almost independent of the number of nucleons, theorists were led to assume that the forces between nucleons were effective only over a very short range - in close analogy with the forces responsible for surface tension in liquids. This is the basis of the "liquid drop" model of the nucleus developed by Niels Bohr and J. A. Wheeler.

To explain the deformations, it is necessary to consider the centrifugal forces exerted by the nucleons in their orbits inside the "droplet." Much as in the electron shells of atomic structure, the protons (and, almost independently, the neutrons) fill shells in the nucleus. A shell of protons (or of neutrons) consists of all the orbits having the same shape and energy but different allowed orientations. When a shell is filled (closed) the nucleons are uniformly distributed in space, i.e., the average distribution of the nucleons comprising a closed shell is spherically symmetrical but has a very fuzzy outer surface. A single open-shell nucleon in an orbit just inside the surface of the "droplet" is analogous to a small ball rolling around very fast inside a rubber balloon whose elasticity supplies the "surface tension." The ball tends to stretch the balloon where it pushes on it; if it moves so quickly that the rubber does not snap back before the ball returns, the balloon becomes somewhat flattened. This explains the oblate (flattened) nuclei.

When there are several open-shell nucleons, the nucleus is usually elongated instead. Although it is not quite so easy to make a valid picture showing why this happens, a good idea of the effect is given by thinking of two nucleons circling around inside the surface in planes normal to each other. Their paths intersect at two opposite poles, and at these poles, where they both are pushing the surface out, the bulge is greater, so the nucleus is elongated (prolate). Other properties of the wave functions and their nodes in a wave-mechanical description strengthen this tendency.

Since the nuclear fluid contains protons, it is electrically charged and tends to push itself apart. This disruptive tendency is opposed by the "surface tension" of the "droplet." Thus the strength of the surface tension can be determined from the fact that only for heavy nuclei like uranium does it fail to hold the nucleus together against the electric repulsion. This failure is the spectacular phenomenon of nuclear fission. The impressive fact for the present argument is that the strength of surface tension needed to explain fission is also just about right to explain the amount of deformation of elongated nuclei (such as rubidium and lutecium) and the associated quadrupole moments.

Evidence for the rotation of nuclei is obtained from experimental measurements of their allowed energy levels. Rotation has been observed only for nuclei with large deformations, and all large deformations are prolate (elongated). A wave-mechanical treatment of a rotator (such as a diatomic molecule or prolate nucleus) leads to the equation:

$$\begin{pmatrix} \text{Rotational} \\ \text{Kinetic Energy} \end{pmatrix} = \frac{J(J+1)}{2I}\left(\frac{h}{2\pi}\right)^2 ,$$

where I is the moment of inertia of the rotator, h is Planck's constant, and J is an integer. If the rotator is symmetrical (i.e., if the two atoms in the molecule are the same, as in O_2, or if the prolate nucleus has both ends the same size) so that a 180° rotation leaves the system unchanged, then J can only be even. The experimental discovery in some nuclei of sequences of 4 or 5 levels with energies proportional to J(J+1), within a fraction of a per cent, is striking proof of rotation.

The elongated nuclei containing an even number of protons and an even number of neutrons (the "even-even" nuclei) have energies proportional to 0, 6, 20, 42, etc., i.e., proportional to J(J+1) with J an even integer. The fact that J takes on only even values shows that the elongation is symmetrical for even-even nuclei. (Rotational patterns have also been observed for nuclei having an odd number of protons, but their analysis is much more complicated.)

The success of the liquid-drop model in the Bohr-Wheeler explanation of fission and the Rainwater explanation of the deformation of nuclei led Aage Bohr and Mottelson to apply it to the dynamics of nuclear rotation. They assumed that nuclear matter has constant density and behaves like a simple liquid with no viscosity. When such a liquid starts from rest and is set in motion by rotating the container, it moves in "irrotational flow." In two dimensions the flow is similar to that of water initially at rest in an elliptical wastebasket with vertical sides. When the wastebasket is set in rotation the water squishes around to fit the moving bulge, and a splinter floating on the surface moves in a small circle in fixed space without leaving its initial neighborhood or changing its orientation. Thus, although the water does not move with the container (as it would if it froze and became a rigid body), it is given some momentum by the rotation of the container and therefore contributes a moment of inertia. If ΔR is the difference between the largest and the smallest radii of the ellipse and R is the radius of a circle of the same area as the ellipse, then the effective moment of inertia of the water in irrotational flow is:

$$\begin{pmatrix} \text{Irrotational} \\ \text{Moment of inertia} \end{pmatrix} = \left(\frac{\Delta R}{R}\right)^2 \begin{pmatrix} \text{Rigid} \\ \text{Moment of inertia} \end{pmatrix}$$

(The water would have the rigid moment of inertia if it were frozen.) The nuclear moment of inertia calculated by this model has only about one-fifth of the value deduced from the observed electric quadrupole moments.

Theoretical work at Argonne has led to the adaptation of the shell model of the nucleus to explain why there should be such a discrepancy. In the shell model, each nucleon is thought of as moving in a potential determined by the averaged-out effect of all the other nucleons in the nucleus. For a closed shell the distribution of nucleons (and the associated potential) is spherically symmetric - so that the motion of a nucleus corresponds to a small ball rolling in a round potential bowl. In a nucleus with open shells the "droplet" is distorted, so a nucleon moves in an elongated potential bowl (similar to an elliptical celery dish). For convenience in computation, a harmonic

oscillator potential was assumed - one with a weaker restoring force (producing a lower frequency) along the longer axis and a stronger restoring force (higher frequency) at right angles to this. In an elliptical potential bowl at rest, the normal modes correspond to motions along either the major or the minor diameter. If the particle is not started along one of these lines, it traces out a complicated path called a "Lissajous figure" which is compounded from the two normal modes and involves both frequencies.

Now imagine that the bowl rotates counterclockwise about a vertical axis through its center. If the ball is started rolling toward the center along the major axis, it tends to roll in a straight line in fixed space - which means that it tends to deflect toward the right as seen by an observer moving with the bowl, as shown in Fig. 6. Thus an attempt to roll the ball directly along the long (low frequency) axis fails and both frequencies are involved in the motion. To make the motion a fairly simple one with a single frequency, the ball must be started in a direction somewhat to the right of the long diameter. Then the greater slope due to the greater curvature along the short diameter will push the ball to the left; and if the ball is started properly this leftward push will just compensate the tendency of the ball to deflect toward the right due to the rotation of the bowl. The resulting motion relative to the bowl will be an ellipse on which the motion repeats with a single frequency. If the rate of rotation of the bowl is much smaller than the frequency of the orbital motion of the ball, the ball will move in a narrow ellipse hugging the long diameter,and the frequency is only slightly lower than the frequency along that diameter in the absence of rotation. The faster the rotation of the bowl, the farther toward the right must the ball be started to get this compensation, the fatter must be the ellipse, and the more will the frequency be lowered.

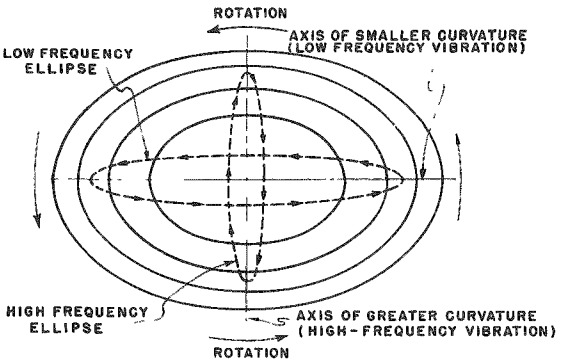

Fig. 6. Motions in a rotating elliptical celery-bowl potential. The fatter ellipses (drawn solid) are evenly spaced equipotentials ("contour lines" on the potential bowl).

Starting the ball to the right of the long diameter when the bowl has a counterclockwise rotation means that the ball traverses the ellipse in a counterclockwise direction also, so its orbital motion increases the angular momentum of the system. Because the ball traverses the ellipse many times while the bowl is making one revolution, it has much more angular momentum than it would have if it were rigidly attached to the bowl at the same average distance from the center. Thus the ball contributes much more than its share to the total moment of inertia (which measures the angular momentum for a given angular speed of the bowl). This is the key to understanding how nuclear moments of inertia can be larger than calculated from the "liquid drop" model neglecting the orbital motion of individual nucleons.

There is also an elliptical motion about the short diameter of the bowl, with a frequency near that of the high-frequency motion along this diameter in the absence of rotation. A similar analysis shows that this orbital motion relative to the bowl is clockwise when the rotation of the bowl is counterclockwise; so this orbital motion decreases the angular momentum of the system and decreases the effective moment of inertia.

The relation of all this to nuclear behavior depends on the way in which closed shells are formed in nuclei. It takes 50 neutrons (or quite separately 50 protons) in a nucleus to fill one of the important closed shells, 82 to fill the next, and so on. The "magic numbers" at which shells are filled are 2, 8, 20, 50, 82, and 126. It is with numbers of neutrons or protons or both nearly half way between these numbers, particularly near 100, that the most elongated nuclei are found; and in these parts of the periodic table are also found the most striking examples of nuclear rotation.

As we have seen, a closed shell has a strong tendency to be spherical, but a few added nucleons may elongate it. These added nucleons tend to populate the states corresponding to motions around the long axis of the nucleus, because the low frequency of this vibration means that these are the low-energy states for the nucleons. But these are also the states in which the motion in the elliptical orbits is in the same direction as the rotation of the nucleus, so it adds to the angular momentum. The actual nucleon states are compounded of the simple motions near the two axes (and also in the third dimension that matters very little for this discussion). The first states populated consist entirely of the low-frequency ellipse; the next ones consist mostly of it. But as the shell gets more than half filled, it becomes necessary to put the nucleons in the higher-energy states that correspond mostly to ellipses about the short diameter. These motions are opposite to the rotation of the nucleus and subtract from the total moment of inertia. Thus it is that by the time the shell is filled, the counterclockwise elliptical motions are just compensated by the clockwise; and the closed shell has no residue of these individual nucleon effects, but only the amorphous moment of inertia characteristic of a fluid droplet.

In a nucleus the large majority of the nucleons are in closed shells which contribute only the small fluid-droplet result to the moment of inertia. The actual moment of inertia is about five times this large, but the rapid motion of the relatively few open-shell nucleons in their narrow elliptical orbits is so rapid that it is somewhat more than enough to explain this large difference. Computations now in progress indicate that it may be possible to remove the residual discrepancy by modifying the assumed harmonic-oscillator potential to a form with a flatter bottom and steeper sides - a potential in better conformity with current ideas of nuclear forces.

People have commonly spoken of nuclear rotation as a collective motion because it depends on the rotation of the axes determined by the shape of the nucleus as a whole. We see, however, that the motion leading to the angular momentum is far from collective, since the few nucleons outside of closed shells contribute most of the effect. It must be admitted, however, that the others do provide the collective environment - the rotating celery dish potential - in which these few can be so productive.

Lifetime Measurements from Recoil Studies

Nuclear reactions commonly leave the product nucleus in an excited state. The mean lifetime of such a state is a measure of the transition probability, which in turn indicates the multipolarity of the radiation. A measurement of the lifetime thus aids in the assignment of quantum numbers. When such mean lifetimes are in the range from about 10^{-10} to 10^{-14} second, they may be measured by use of the Doppler shift.

A beam of protons from the Van de Graaff accelerator was allowed to bombard a thin layer of Na^{23}, the only naturally occurring isotope of sodium, deposited as NaCl on the back side of a very thin metal foil. When the proton energy is 1.29 Mev, the inelastic scattering reaction

$$Na^{23}\,(p,p')\,Na^{23*}\,(\gamma)\,Na^{23}$$

exhibits a very strong resonance at which nearly all the recoiling sodium nuclei are excited to the 440-kev state and are projected forward with speeds between 0.1 and 1.2×10^8 cm/sec and with directions which lie within a 35° cone. Hence the Doppler effect introduces a difference of approximately 0.5% between the values of the gamma-ray frequency as observed looking, respectively, parallel and antiparallel to the direction of flight of the recoiling nuclei.

When the excited sodium nuclei (Na^{23*}) were allowed to recoil directly into a vacuum, they emitted gamma rays while traveling at full speed, so the full Doppler shift was observed. When the Na^{23*} nuclei recoiled into a gas in which they were brought to rest in about 10^{-9} second, experimental observation of the full Doppler shift showed that the excited state decayed before the speed had been reduced appreciably, so the lifetime is less than 10^{-9} second.

When the thin target was backed by a layer of tantalum thick enough to bring the recoils to rest, the Doppler shift was not observed experimentally. This indicated that most of the excited states decayed after the nuclei came to rest, so the lifetime is longer than the stopping time of about 10^{-12} second.

Finally, a somewhat thick NaCl target was used to slow the recoils to about half their initial speed before they emerged into the vacuum. In this case the Doppler shift was not appreciably reduced. Consideration of the average velocity of the recoils at the instant of decay under these circumstances indicates a lifetime somewhat shorter than the stopping time in NaCl.

In view of the large uncertainties in the measurements of target thickness and the magnitude of the Doppler shift and in the rate at which the recoiling nuclei slow down in the solid materials, these last two results should be interpreted as indicating that both the probable upper limit and the probable lower limit of the lifetime are in the neighborhood of the stopping time in Ta or NaCl. Thus the lifetime of the 440-kev excited state of Na^{23} is of the order of 10^{-12} second.

Paramagnetic Resonance Spectrum of Curium

The paramagnetic resonance spectrum of curium in anhydrous lanthanum chloride has been measured at room temperature for a wavelength of 3 cm. Seven lines can be clearly distinguished, confirming the assignment of seven 5f electrons to this element and a ground state of $^8S_{7/2}$, analogous to the spectrum of gadolinium, which contains seven 4f electrons. Radiation damage caused by the intense alpha activity of Cm^{242} caused all transitions to disappear within a few hours, except for the $1/2 \rightarrow -1/2$ transition, as a result of the destruction of the crystal lattice.

Seven lines were also observed in the spectrum of curium in a magnesium bismuth nitrate single crystal. The larger amounts of curium used in this case caused a much more severe radiation damage. Three intense lines caused by the radiation damage were particularly noted and attributed to the hyperfine structure of N^{14}, the only isotope in the crystal with unit nuclear spin.

Decay Schemes of Short-Lived Radioactive Nuclides

Just as the study of optical spectra gave the key to the theory of the electronic structure of atoms, it is to be hoped that nuclear spectroscopy will lead to a comprehensive theory of nuclear structure. In both cases the energy levels of the complex systems are inferred from the energies of the emitted quanta. One reason why nuclear

spectroscopy is more difficult is that it is not as easy to produce nuclei in excited states as it is to excite the electronic levels of the outer structures. One method, however, is incidental to radioactive decay - the daughter nucleus is often produced in a considerable array of excited states of different energies, and gamma rays are then emitted in transitions from higher to lower levels. In spite of the large amount of study already devoted to these so-called decay schemes of radioactive disintegration there is still much to be learned by this method. At the Argonne Laboratory emphasis has been placed especially on such studies of radioactive nuclei having half-lives of but a few minutes. These can be studied profitably only in close proximity to a source of the activated material, such as at the CP-5 reactor. Often, however, a short-lived activity is intimately associated with one of much longer half-life and it is necessary that both be studied carefully at the same time in order to understand either.

The work has been greatly helped by the development of a 256-channel pulse-height analyzer by the Electronics Division of the Laboratory. The analyzer used in conjunction with a crystal scintillator and photomultiplier makes a powerful gamma-ray spectrometer. It can be used first to survey the gamma-ray spectra and then, by using it in coincidence with a single-channel detector of gamma rays or beta rays, to determine which electrons and quanta are related in rapid sequential emission.

One such analysis recently completed is that of the decay scheme of Sn^{125} which is known to have two isomeric states having half-lives of 9.7 and 9.4 minutes, respectively. The sources used were prepared by neutron irradiation, in the CP-5 reactor, of tin enriched in Sn^{124}. The preliminary studies showed the presence of the 1.97, 1.41, 1.07, 0.90 and 0.81-Mev gamma rays, but the ones of lower energy were obscured by radiations associated with the decay of the Sb^{125} daughter. Chemical removal of the antimony permitted observation of the gamma rays of 0.340 and 0.470 Mev in the Sn^{127} spectrum. The level scheme deduced from coincidence measurements is given in Fig. 7. All gamma-gamma coincidences indicated in this scheme were observed. Further confirmation was obtained by studying beta-gamma coincidences where both the pulse-height distribution of beta scintillations in coincidence with selected gamma rays and the absorption in Al of the coincident beta rays were investigated.

Similar studies of Ca^{49}, Sc^{49}, Mo^{101} and Ce^{143} have been completed recently.

Reformulations of Quantum Field Theory

In 1935 Yukawa proposed an explanation of nuclear forces by a hypothetical meson field. Some consequences of the meson theory, in particular the existence of π-mesons, have been spectacularly verified, but no reliable quantitative verification of meson theory is available as yet. It is the first time in history that not a single observable number could be reliably deduced from a major theory. The reason is that the equations of this theory are meaningless if taken literally. Meaningful results can be obtained only by a hazardous process of re-interpretation and introduction of additional prescriptions which are not deducible from prime principles.

This procedure is known as "renormalization." The results, although meaningful, bear only slight similarity with reality. For instance, one of the latest and most sophisticated calculations on nuclear forces results in purely repulsive forces between nucleons. Fortunately for the theory, these calculations are also mathematically inadequate, i.e., they are not good approximations to the actual solutions (with renormalization).

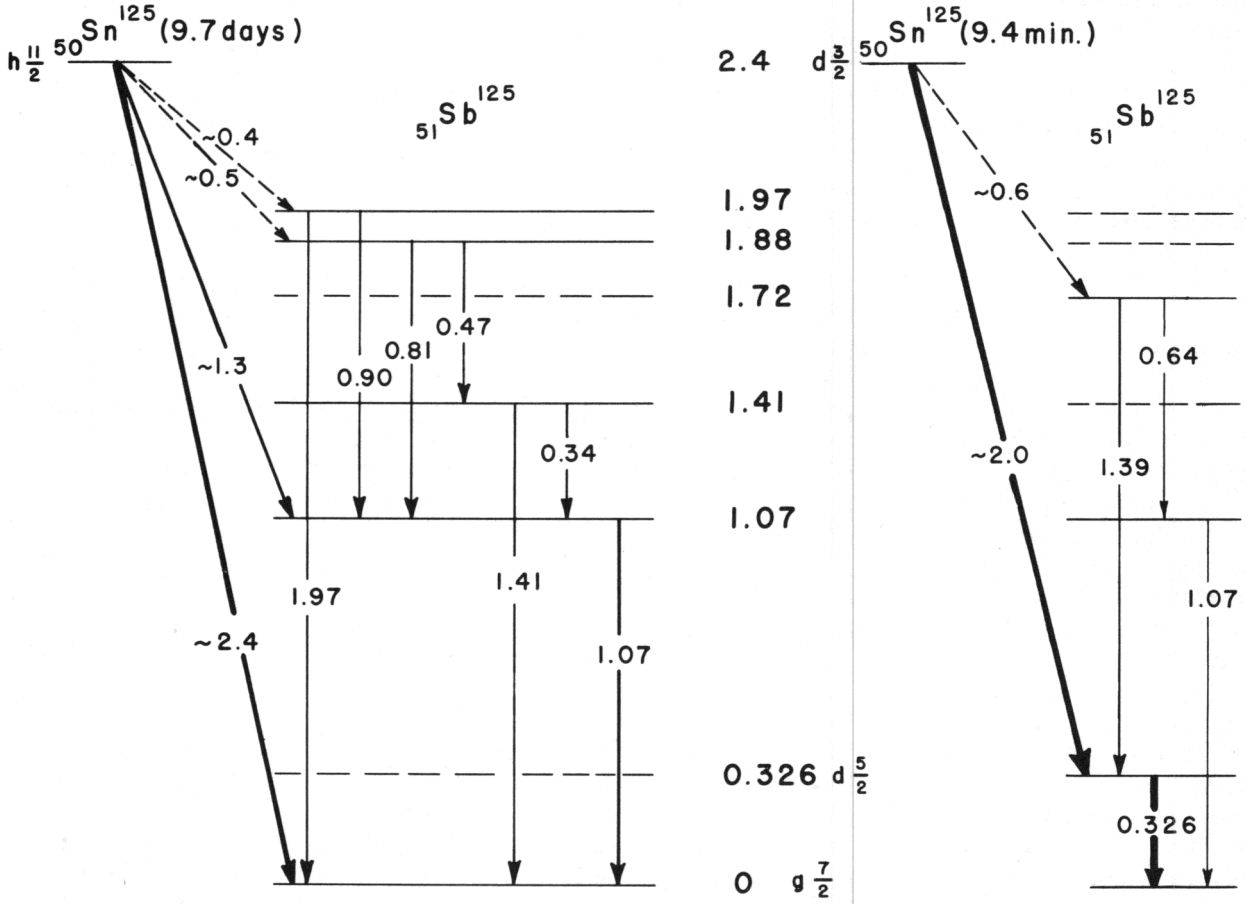

Fig. 7. Energy levels of $_{51}Sb^{125}$ in the decay of Sn^{125}.

Logical consistency in physics has never been up to the standards of mathematics except in dead fields, but lack of it has rarely prevented testing a major theory by comparison with experiment. At this point, however, there is a pragmatic need for more consistency. An effort is being made here to recast the theory so that an unambiguous comparison of its results with observation can be made.

What is the physical interpretation of quantum field theory? An approach made at Argonne is to propose a precise and unambiguous definition of observable particles, as distinguished from the "bare particles" which are usually introduced for mathematical convenience but which have no physical significance. In simple language, this definition says: physical particles are those entities which asymptotically (in the distant past and future) remain stable, i.e., conserve their four momenta and internal variables (spin, etc.). Starting from this definition, equations for the determination of scattering cross sections have been derived which differ in several respects from the conventional ones.

Since the general problem of field theory is quite complicated, we have considered, as a model, the simplest case: a fixed point nucleon interacting with charge-symmetric scalar mesons. In the usual formalism, this problem leads (in higher approximations) to divergent, i.e., nonsensical, results. In our reinterpretation, all observables calculated are finite.

One of the inconsistencies of the customary approach is the decomposition of state vectors into linear combinations of "basis states," each of which represents a given number of bare particles. However, the production of mesons by point sources is so copious that in any physical state the number of bare mesons is infinite. Hence, the coefficients in the expansions employed are all zero.

This difficulty is avoided by the "representationless" formalism, in which we consider only expectation values of operators with respect to physical states, and need no basis vectors for the purpose of representation.

We intend to apply this method to the most plausible meson theory, the pseudo-scalar theory with pseudo-scalar coupling, and to calculate at least the magnetic moment of the nucleon, so that the result may be considered as a reliable deductive consequence of the theory. Then, finally, the theory can be accepted or rejected by quantitative comparison with observation.

STOPPING POWER OF GASES FOR HELIUM IONS

For many experiments in nuclear physics it is important to know the rate of energy loss by various charged particles in a gas. Although the Bethe formula for the differential energy loss (dE/dx) due to inelastic collisions with electrons is adequate at energies at which the ion velocities are large compared to the velocity of the orbital electrons, there is no adequate formula for the lower energies at which other processes become significant (except for the special case of hydrogen ions in hydrogen gas). Other laboratories have measured the stopping power of gases for protons at the lower energies, at which stopping by charge exchange is appreciable. The research reported below studied the rate of energy loss of helium - the simplest ion which can be multiply ionized.

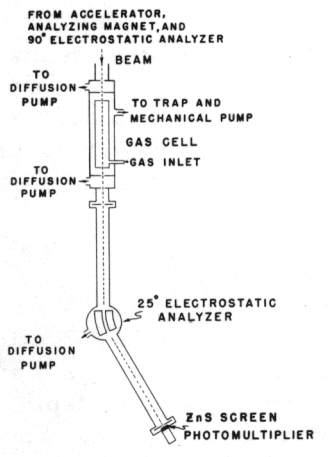

Fig. 8. Schematic diagram of apparatus for measuring the stopping power of gases.

The apparatus used is shown in Fig. 8. The ions were accelerated to the lower energies by the Kevatron at The University of Chicago, and to the higher energies by the Argonne Van de Graaff generator. Either singly or doubly-charged helium ions could be selected by the analyzing magnet, and those having just the desired kinetic energy were passed by the 90° electrostatic analyzer. The energy gap between the Kevatron and the Van de Graaff was bridged by using doubly-charged helium ions to double the kinetic energy available from the Kevatron. The ions then traversed the gas cell, after which their remaining energy was measured by the 25° electrostatic analyzer. In order to avoid the use of foils to confine the gas, a differentially pumped gas cell was used. The gas was admitted through a needle valve and could escape from the gas cell only through the two

0.40-mm diameter holes to an outer chamber exhausted continuously by a mechanical pump. At each end of the outer chamber was another small chamber evacuated by a diffusion pump to keep the gas from the rest of the system. The gas pressure in the inner cell was adjusted between about 0.3 mm and 1.5 mm Hg in order to keep the energy loss of the ions between 1% and 9% of the initial energy - which adequately approximates a true differential energy loss.

The results are shown in Fig. 9 and Fig. 10. Figure 9 shows the expected rapid increase of stopping power with atomic number and the general similarity of the curves.

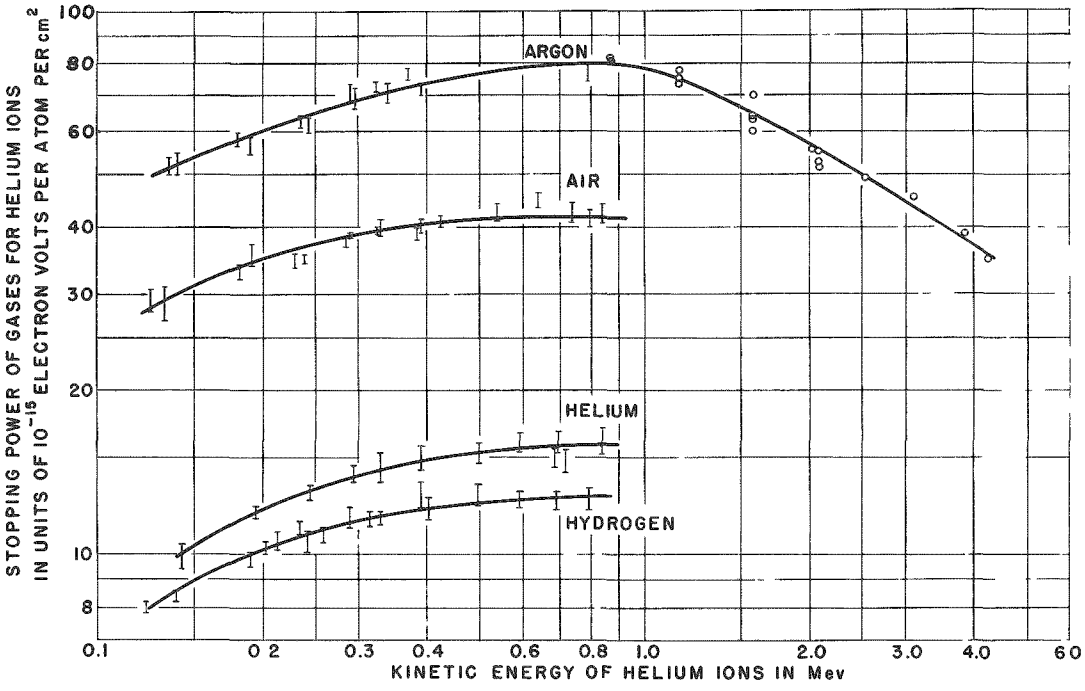

Fig. 9. Stopping power vs kinetic energy of helium ions for various gases. (Data below about 400 kev were obtained by Weyl at the University of Chicago.)

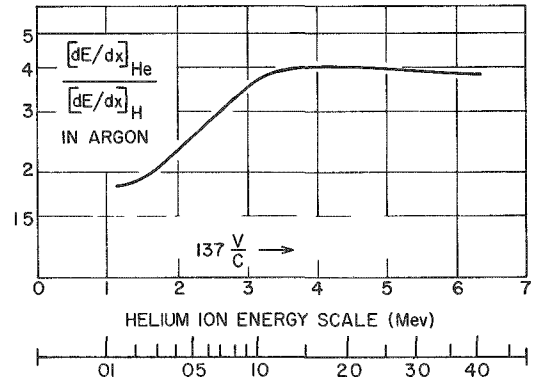

Fig. 10. Ratio of rate of energy loss of helium ions to that of hydrogen ions vs speed of ions (v = speed of ion, c = speed of light).

Figure 10, which was deduced from these and other similar data, shows that above about 1.2 Mev the energy loss per centimeter of path in argon is about four times as great for He as for H ions at the same speed, indicating that the helium quickly became doubly ionized in the gas. At lower energies the doubly ionized fraction decreased rapidly. The degree of ionization was characteristic of the energy of the ions, independently of whether the ions were singly or doubly ionized initially.

SECONDARY EMISSION OF BERYLLIUM IONS

The nature and energies of ions originating in a solid beryllium target under bombardment by positive ions have been investigated with the modified form of double-focusing mass spectrometer shown in Fig. 11. The essential departures from previous designs consist of insulating the 90° electric deflecting system from the source and inserting between the electric deflecting plates and the 60° deflecting magnet an extra slit system to focus and accelerate the beam.

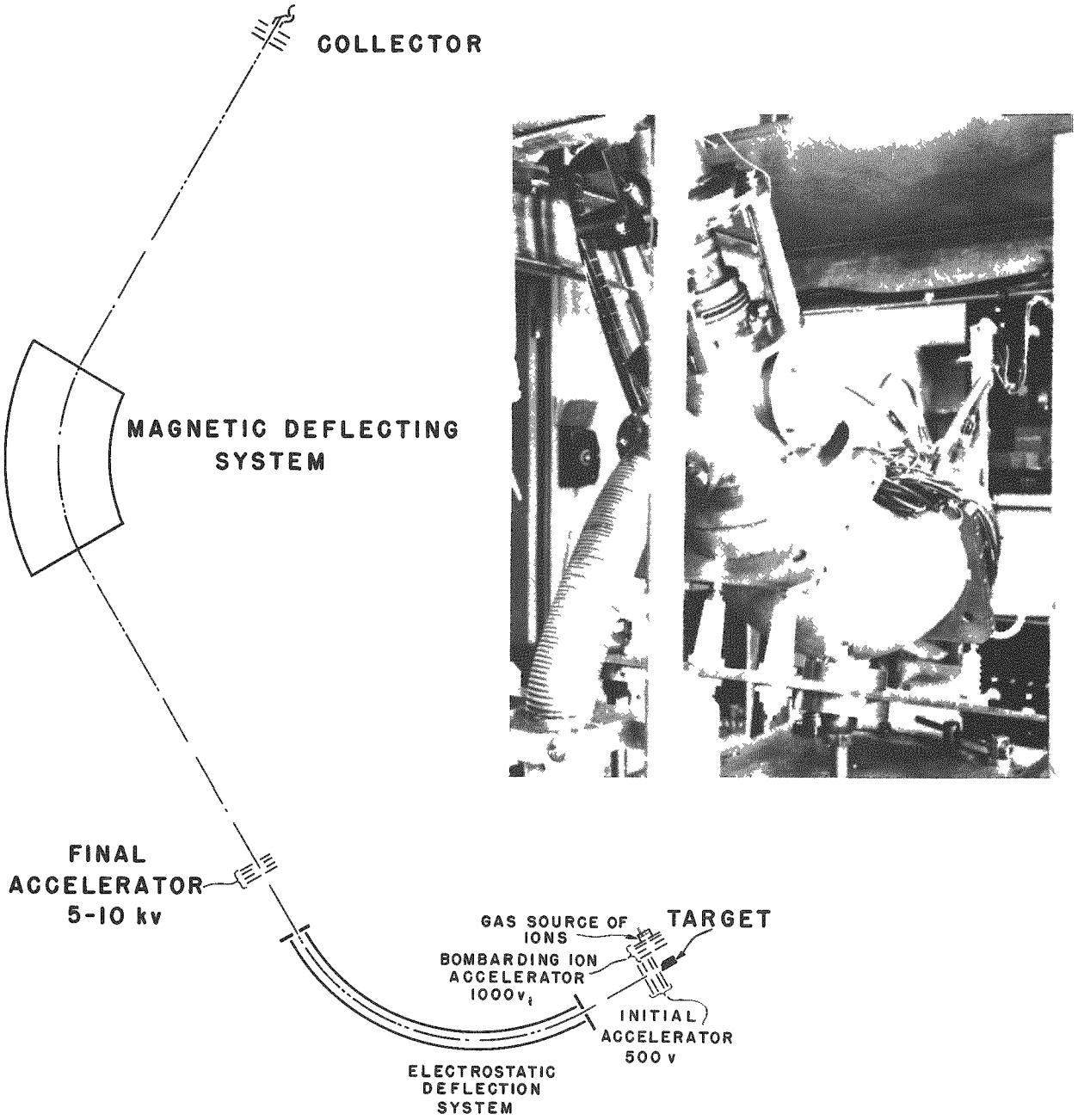

Fig. 11. Schematic diagram of the double-focusing mass spectrometer. The photographic inset shows the electrostatic deflection section used to obtain the kinetic energy spectrum of the ions.

With this design, the difference of potential between the point of origin of the ion and the electrical neutral of the condenser may be made small enough that the energy acquired by the ion in its process of formation becomes a significant fraction of its total energy as it enters the deflecting system. Hence the kinetic energy spectrum of the ions as they leave the target can be found from the energy spectrum measured by the electrostatic deflection. The masses of the ions having any given kinetic energy are identified by the magnetic deflection. The ions are detected by an electron multiplier feeding into a pulse-counting system and recorder.

The yield of beryllium ions, when the beryllium target was bombarded with 1000-ev ions, was found to be almost independent of the masses of the impinging ions. The kinetic energy distribution of the Be^+ ions resulting from bombardment with neon ions is shown in Fig. 12 along with the Maxwell distribution for 14,000° K, which seemed to give the best fit. For energies above 3 or 4 ev the discrepancy becomes rapidly worse, ions being detected with energies up to 300 ev. This failure to fit the data with a single Maxwell distribution was to be expected since thermal equilibrium should not be expected under the conditions of bombardment.

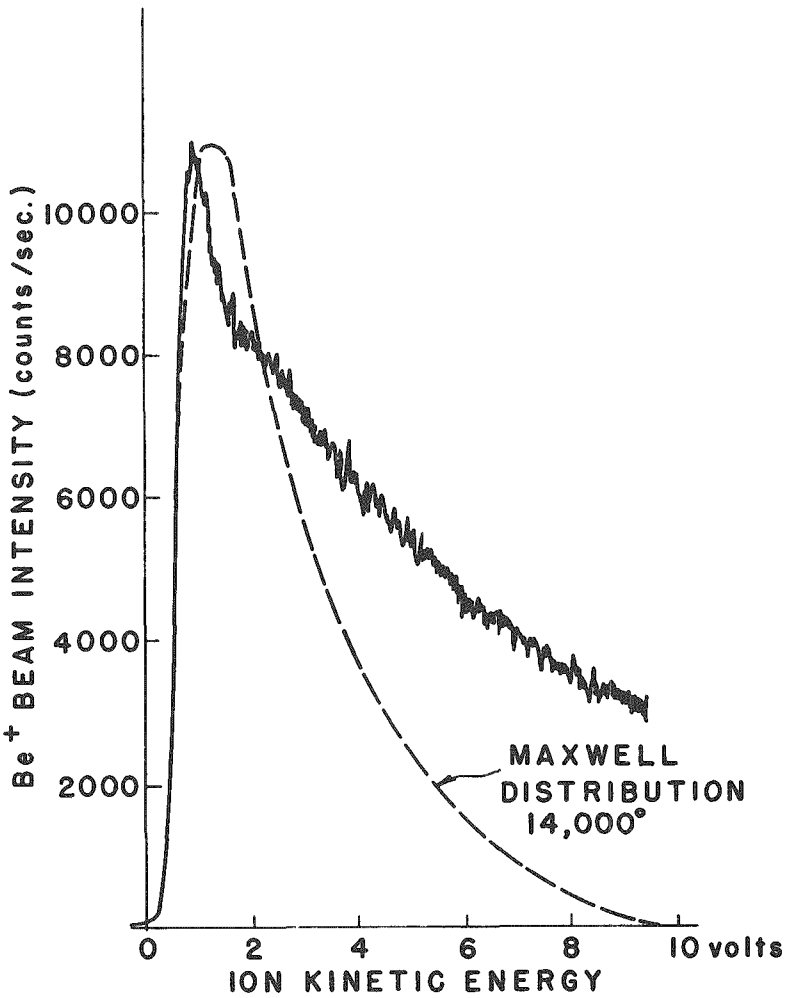

Fig. 12. Kinetic energy distribution of Be^+ ions resulting from bombardment with 1000-volt neon ions.

The kinetic energy distributions can, however, be explained on the assumption that an impinging ion produces a very small hot spot whose heat diffuses rapidly into

the target. On the surface, the expanding region of high temperature would evaporate ions until the temperature became too low. Thus the observed energy distribution would be the sum of a continuous sequence of Maxwell distributions corresponding to the decreasing temperatures. Although the relative importance of the different temperatures involved cannot be determined uniquely from the experimental data, reasonable assumptions based on the expected diffusion of heat in the target lead to a qualitative fit.

STRUCTURE OF SOLIDS

Hydrides

Studies of metal hydrogen systems by thermal, metallographic and X-ray diffraction methods usually reveal the formation of metal hydride phases, the dimensions of the unit cell, and the positions of the metal atoms. The difficulty or inability to locate the positions of the hydrogen atoms can be overcome, at least in simple non-magnetic systems, by utilizing the techniques of neutron diffraction, in which neutrons are scattered by the nuclei.

A structure analysis using a combination of X-ray and neutron diffraction techniques has been carried out for the hydrides of titanium and hafnium, using deuterium instead of the normal hydrogen isotope. It has been possible to determine the positions of the hydrogen atoms in the crystals, the nearest neighbor atoms, and their interatomic distances. A determination of the space available to the hydrogen in the lattices of these metals has led to the conclusion that the hydrogen must enter in ionic form.

Another characteristic of these hydrides is that the first pure hydride phase favors the CaF_2-type structure, with a fraction of the available atom sites unfilled. The metal-hydrogen bonds in this structure are anisotropic, and their directional nature becomes more pronounced when the face-centered cubic structure transforms to the face-centered tetragonal structure with contraction along one axis and expansion along the other two providing for shorter metal-metal atom bonds. The brittleness observed in these hydrides may be ascribed to these directional bonds rather than to the mechanical defects (such as the presence of pores, microcracks, fissures, and intergranular holes) generally mentioned in the literature.

Uranium Oxides

The exchange of oxygen between lattice and interstitial sites in the UO_2 structure has been studied over a range of interstitial oxygen concentrations corresponding to $UO_{2.05}$ through $UO_{2.20}$ and over a range of temperatures varying from 350° C to 1200° C. The exchange was followed by two reactions: CO reduction and the exchange between CO_2 and interstitial sites, together with mass spectrometric analysis of products. Under the experimental conditions, the oxygen exchange was complete in 10 minutes or less, except in those cases where evidence existed of the U_4O_9 structure. The results indicate a very mobile anion sub-lattice.

Paramagnetic Resonance in Irradiated KCl Crystals

It has been known for some time that if an alkali halide crystal containing U-centers is exposed, at sufficiently high temperatures, to light absorbed by the U-centers,

F-centers are formed. Since a U-center is believed to be a hydride ion which has replaced a halide ion in the lattice, the conversion of a U-center to an F-center must also produce a hydrogen atom. The effects of ultraviolet irradiation of KCl-KH and KCl-KD single crystals at 80° K and 300° K have been investigated using paramagnetic resonance and optical absorption techniques to obtain information regarding the state of the hydrogen atoms produced in the photodecomposition of U-centers,

Crystals of KCl-KH irradiated at 80° K have been found to exhibit, along with the usual F-center spin resonance, a resonance doublet with a splitting of 500 $\pm$ 10 gauss and a line width of 68 $\pm$ 5 gauss; the doublet is presumed to be due to hydrogen atoms in the crystal. This conclusion is substantiated by the fact that crystals of KCl-KD, after a similar irradiation, exhibit a resonance triplet with a separation of outer components of 156 $\pm$ 10 gauss. Further results lead to the conclusions (1) that the hydrogen atoms produced by irradiation are located in interstitial positions in the lattice, (2) that these interstitial hydrogen atoms give rise to an optical absorption band (U_2-band) located at 236 mμ, (3) that a broad optical absorption band (U_1-band) extending to the long wavelength side of the U-band is due to interstitial hydride ions.

RESEARCH IN CHEMISTRY

Decay Kinetics of I_2^-

A detailed study of the decay kinetics of the unstable diiodide ion (I_2^-) from dilute buffered, air-free solutions of potassium iodide has been made by means of a flash spectrophotometry technique. A comparison of experiments at different pH but constant concentration of iodide ion (I^-) has shown that, although the amount of final product increases with decreasing pH, the lifetime of the I_2^- is invariant. It appears that the I_2^- does not disappear by reaction with hydrogen ion, but rather that the decay is in agreement with the following scheme:

(A) $I + I^- \rightleftharpoons I_2^-$

(B) $I + I_2^- \longrightarrow I_3^-$

(C) $I + I \longrightarrow I_2$

(D) $I_2^- + I_2 \longrightarrow I_3^- + I$

(E) $I^- + I_2 \rightleftharpoons I_3^-$.

The simultaneous solution of the rate equations for the disappearance of I_2^-, assuming that the two equations are approximately maintained in a steady state during the decay, shows that the disappearance of I_2^- obeys second-order kinetics. Experimental observations have shown that the decay obeyed a bimolecular law over the entire range of iodide ion investigated (3×10^{-5} M to 10^{-3} M) independent of hydrogen ion concentration. Further, the effective rate constant increases with decreasing iodide ion concentration, suggesting that reaction (D) is rate-controlling above 10^{-3} M KI, while at lower concentrations reactions (B) and (C) become of increasing importance. These results suggest that a re-evaluation of previous theories concerning the photo chemistry of iodide ions under continuous irradiation is in order.

Activation of Phosphorus Compounds

Radioactive phosphorus compounds are especially useful for investigation of the biological and chemical transformations of phosphorus and its derivatives. But attempts to prepare particular, radioactive, phosphorus compounds by neutron irradiation of supposedly suitable preparations have frequently yielded a variety of products. This variation of the activation products has now been related to various conditions, such as the state of oxidation of the irradiated substances, the chemical form of the irradiated substances, the action of the gamma rays that accompany the neutrons in the reactor, and the presence or absence of oxygen (air or vacuum). This information has, in turn, provided clearer concepts about the chemical reactions that accompany the nuclear activation process itself.

In vacuum, where easily oxidized, neutron-irradiation products should be stable, bombardment of anhydrous disodium phosphate with neutrons yielded principally phosphate itself. Traces of elemental phosphorus that were detected could be attributed to the action of gamma rays also present in the reactor. Neutron irradiation of oxyacids of phosphorus in lower valence states yielded complex mixtures of activated products. For example, in vacuum, neutron activation of anhydrous disodium hydrogen phosphite and sodium dihydrogen hypophosphite yielded mixtures of more reduced and more oxidized substances, including hydrogen, phosphorus, phosphate, phosphite, and hypophosphite.

In vacuum, gamma rays from the Argonne High-Level Gamma Irradiation Facility scarcely altered anhydrous disodium phosphate, yielding only traces of phosphorus. But these gamma rays promoted extensive alteration of anhydrous disodium hydrogen phosphite and sodium dihydrogen hypophosphite and produced the same intermolecular oxidation and reduction products as resulted from neutron irradiation.

In an atmosphere of oxygen, neutron or gamma irradiation of the anhydrous salts of the oxyacids produced oxidation products of the same valence as phosphate. These products were usually condensed modifications of orthophosphate or metaphosphate. In aqueous solution, either in the presence of oxygen or in vacuum, irradiation with neutrons or with gamma rays converted all the phosphorus compounds into orthophosphate.

These observations show that radioactive orthophosphate may be prepared most conveniently by the irradiation of phosphate in solution. Other radioactive oxyacids of phosphorus are not readily preparable in a state of high purity by direct irradiation of the acids or their salts. These observations, particularly those with the irradiation of anhydrous disodium phosphate, indicate that neutron irradiation of phosphate does not break most of the phosphorus-oxygen chemical bonds as has long been supposed.

Fluorine Chemistry

Measurements of the chemical equilibrium of the reaction

$$Br_{2(g)} + BrF_{3(g)} \rightarrow 3\ BrF_{(g)}$$

have been made. These were used to calculate the standard enthalpy (-75 kcal/mole) and free energy of formation (-57 kcal/mole) for bromine trifluoride. Theoretical and experimental evidence indicate that bromine does not react at an appreciable rate with bromine pentafluoride at 75° C.

Although numerous oxides or oxygen-containing compounds can be fluorinated smoothly with bromine trifluoride in the liquid phase near room temperature, there are, nonetheless, many substances which fail to react quantitatively, or indeed to react at all, with bromine trifluoride even at its boiling point, 127° C. Certain of these, it is true, can be completely fluorinated with bromine trifluoride at temperatures ranging from 200° C to 300° C, and at pressures which are so high as to present formidable and, at present, intractable apparatus problems. A number of addition compounds, in particular with potassium fluoride and antimony pentafluoride, appeared to present the possibility of utilizing the fluorinating capacity of bromine trifluoride without attendant disadvantages of high pressure.

Measurements of the melting points and dissociation pressures of $KBrF_4$ and of $BrF_2Sb_2F_6$ have shown that it is possible to achieve a considerable range of liquid phase without producing high pressures in a closed system.

The observed behavior of the reaction of various oxides with $KBrF_4$ and BrF_2SbF_6 can be related quite well with the acid-base properties of these reagents. In BrF_3 solution, KF functions as a base, while SbF_5 shows acid properties. Molten $KBrF_4$ can be considered as a basic flux and BrF_2SbF_6 as an acidic flux. The rate of fluorination with these reagents depends strongly on the acid-base properties of the reactants. With amphoteric oxides both reagents were found to be equally effective. The fact that the reactions can be made to yield a quantitative recovery of oxygen as molecular oxygen can be made the basis of analytical procedures for oxygen in a wide variety of compounds.

The crystal structure of $KBrF_4$ was determined by means of powder patterns, inasmuch as decomposition by moisture interfered too greatly in attempts to analyze single crystals. It was found that $KBrF_4$ is tetragonal, being similar to $BeSO_4 \cdot 4H_2O$. Measurements of density led to the conclusion that there are 4 molecules in the unit cell. The fluorine atoms are distributed in tetrahedral configurations about each bromine atom. Each potassium has 8 fluorine atoms as nearest neighbors (see Fig. 13).

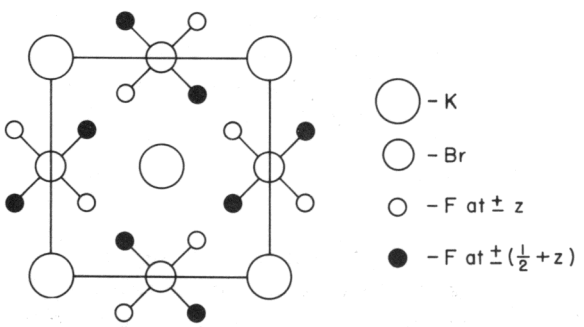

Fig. 13. Projection on C face of $KBrF_4$.

The interhalogen compounds, ClF_3 and BrF_3, have been shown by microwave spectroscopy to have the structure of a slightly distorted "T" with two different halogen-fluorine distances. This was an unusual discovery in view of the fact that all other molecules of the type XY_3 that have been extensively studied are either planar or pyramidal with a threefold symmetry axis, i.e., the three Y atoms are equivalent. The existing infrared and Raman data on these compounds had not been interpreted in terms of the C_{2v} symmetry of the "T" structure partly because of the great difficulty in obtaining both complete and reliable data with these highly reactive substances. Experience in this laboratory with various hexafluorides was helpful in permitting us to obtain reliable spectra on ClF_3 vapor from 275 to 1500 cm^{-1} and its Raman spectrum at 1200 mm pressure. All six of the fundamental vibrations required by the "T" structure have been identified from the infrared data, and all of the observed combination bands have been successfully explained in terms of these fundamentals. The two strongest Raman bands were also in agreement with the infrared fundamentals. Careful examination of the

infrared band contours showed them also to be in agreement with the "T" structure. Thus, the vibrational spectra may now be regarded as confirming this unusual structure for ClF_3. Less complete data were obtained for BrF_3 owing both to the higher temperatures required to vaporize it and to its greater instability. However, the major features of the ClF_3 spectra are also present in those obtained for BrF_3 and this may be taken as an indication of a similar structure.

Osmium hexafluoride is the electronic analogue of PuF_6, with the difference that its two nonbonding electrons are 5d rather than 5f electrons. Its melting point and boiling point are markedly higher than one would estimate by interpolation from the properties of the hexafluorides of the neighboring elements tungsten, rhenium, and iridium; rather, the interpolated values are close to those reported for osmium octafluoride. This observation suggested that the volatile yellow solid identified by Ruff and Tschirch in 1913 as OsF_8 is in reality the hexafluoride and that their less volatile green hexafluoride was also incorrectly identified. To test this possibility, fluorine was passed over osmium metal at 200 to 250° C; a volatile yellow solid was obtained in quantitative yield that had the same physical properties as Ruff and Tschirch's octafluoride. However, vapor density measurements yielded a value for the molecular weight that corresponded to the formula OsF_6 rather than OsF_8. Infrared and Raman spectra demonstrated the purity of the compound and corroborated the hexafluoride formula. It therefore seems very likely that the octafluoride of osmium has not yet been prepared and in fact may not exist.

The paramagnetic susceptibility of solid NpF_6 has been measured from 64° K to 295° K. After correction for the diamagnetism of the electrons in the compound the molar susceptibility of the Np^{+6} ion is given by

$$M\chi_{Np^{+6}} = \frac{0.0361}{T} + 387 \times 10^{-6} \quad .$$

The value for the susceptibility at 295° K, 509×10^{-6}, is considerably smaller than that found for isoelectronic compounds; for example, in $NaNpO_2(C_2H_3O_2)_3$ the susceptibility for Np^{+6} at 295° K is 1680×10^{-6}. This result can be explained on the basis of a strong interaction between the octahedral electric field provided by the six fluoride ions and the nonbonding 5f electron in NpF_6 that results in a doubly degenerate ground state of small susceptibility. In PuF_6, where two nonbonding electrons are present, the splittings produced by the octahedral field result in a nondegenerate ground state and only a small, temperature-independent paramagnetism is observed:

$$M\chi_{PuF_6} = 173 \times 10^{-6} \quad .$$

The complete removal of the degeneracy is not possible for NpF_6 since Kramer's theorem shows that for odd numbers of electrons the degeneracy cannot be completely removed by an electric field alone. The magnetic properties of NpF_6 and PuF_6 are very striking examples of the very different behavior of the nonbonding electrons in the actinide elements as compared with both the rare earth (4f) and transition series (3d, 4d and 5d) electrons. In the rare earths the total angular momentum characterizes the susceptibility while in the transition series the "spin only" susceptibility is the predominant characteristic. By contrast, for the actinides, detailed consideration of crystalline and molecular field splittings must be taken into account before even a qualitative explanation of the susceptibility is possible.

Fused Salt Chromatography

Chromatography is a well-known method for the separation of materials from aqueous or organic solutions. This classical method has now been extended to fused salt systems, opening up a new field of investigation in the general area of high temperature separations processes. The procedure consists of allowing a solution of fused $LiNO_3$-KNO_3 eutectic (melting at 132° C) containing metal ions to flow through a column of alumina, the salts being maintained in the molten state and the temperature of the column kept constant by flowing vapors of high-boiling organic liquids around the supporting Pyrex tube.

The transition metal ions Fe(II), Co(II), Ni(II), Cu(II) and U(VI) can be adsorbed on alumina and may be eluted with fused $LiNO_3$-KNO_3 eutectic containing various complex-forming anions, like Cl^-, Br^-, $SO_4^=$ and CN^-. Separation of Co(II) from Ni(II) is accomplished by addition of KCl to the $LiNO_3$-KNO_3 eutectic because of the formation in the melt of chlorocomplexes of different stabilities.

The capacity of the column and the elution properties of specific cations have been measured in relation to various complexing anions, their concentration, and the temperature of operation of the column. The adsorption and ion exchange behavior of some oxides other than alumina and silicates have also been studied.

Some preliminary spectrophotometric studies have been made of complex ions in fused salts using a Beckman Model DU spectrophotometer adapted for use at elevated temperatures.

In fused $LiNO_3$-KNO_3 eutectic and in the absence of Cl^-, the Co(II) spectrum is similar to that in aqueous perchloric acid solution. Addition of anhydrous KCl to the melt causes pronounced spectral changes (see Fig. 14) which have been interpreted as being due to a change from hexacoordinated to tetracoordinated cobalt. In the pure nitrate melt Co(II) is thought to be surrounded by six nitrate groups. In the presence of Cl^-, however, the stepwise replacement of NO_3^- by Cl^- occurs resulting finally in the formation of the tetrahedral complex ion $CoCl_4^=$.

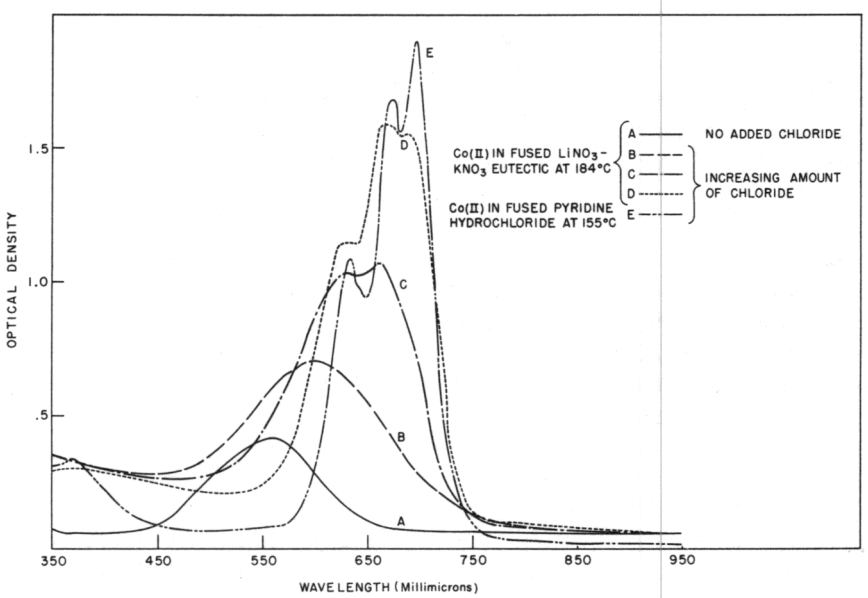

Fig. 14. Absorption spectra of cobalt in fused salts.

Absorption spectra in fused salts have also been obtained for the ions Mn(II), Fe(II), Fe(III), Cr(III), U(IV), U(VI), Np(II), Np(VI), Ni(II), Cu(II), Pr(III), and Nd(III). Changes occur in the spectra of these ions also when complexes are formed. The complex ions $UCl_6^{=}$ and $NpCl_6^{=}$ have been observed.

Separations of the Rare Earth Elements

Under constant operating conditions, the elution method of separation of rare earths on a cation resin column gives rise to a characteristic pattern wherein each peak or band as it is eluted tends not only to be broader (that is, lower in the concentration of rare earth), but also relatively further displaced from that of its immediate predecessor than the latter had been from the band ahead of it (see Fig. 15a). As a result, when conditions are chosen so that satisfactory separation of the earlier bands is attained, the later ones are found to be inordinately slow in eluting and are unsatisfactorily low in concentration. Some success has been obtained elsewhere in overcoming these difficulties by gradually raising the pH during the progress of a separation this procedure served to increase the concentration of the complex-forming organic acid ion responsible for eluting the bands down the column.

Limited data in the literature indicate that, as the temperature is increased, the dissociation of the organic acids used as eluting agent generally decrease. Since this is so, it should be possible to obtain increased anion concentrations by starting separation runs at a high operating temperature and allowing the column to cool slowly during the period of the experiment. Figure 15 shows the results of experiments demonstrating that this technique can be used to obtain a gradient elution effect.

Solvent Extraction Behavior of Lanthanides and Actinides

Studies of di(2-ethyl hexyl) orthophosphoric acid, HDEHP, have demonstrated its value in fractionations of lanthanides and actinides. Thus, in a system involving HDEHP in a carrier solvent and with aqueous mineral acid as the opposing phase, the lanthanides and actinides may be extracted, presumably as $M(DEHP)_3$, in a precisely controllable manner. The distribution coefficient, K, is directly proportional to the third power of the free HDEHP concentration in the organic phase and inversely proportional to the third power of the H^+ ion concentration in the aqueous phase. For the lanthanides, a plot of log K vs atomic number Z, for a specific system utilized in actual separations, is a straight line of positive slope such that the ratio of K's of adjacent lanthanides is approximately 2.6. This value is sufficiently large to render the system practical for large-scale separation. The actinides may be fractionated similarly.

In systems involving an aqueous phase of extremely high acidity, HDEHP may be used to effect sharp differentiation between lanthanides or actinides of different valences, such as between M(III) and M(IV). Thus, it has been possible to isolate, in highly purified form, berkelium as Bk(IV) from trivalent lanthanides and actinides including americium. Also, americium as Am(VI) has been efficiently separated from trivalent lanthanides and actinides.

Differential Electrochromatography

Differential electrical migration in moist paper has provided effective separations of mixtures of various inorganic cations. As a general rule, mixtures of ions of different groups of the periodic table are readily separable, but it is difficult to separate ions of

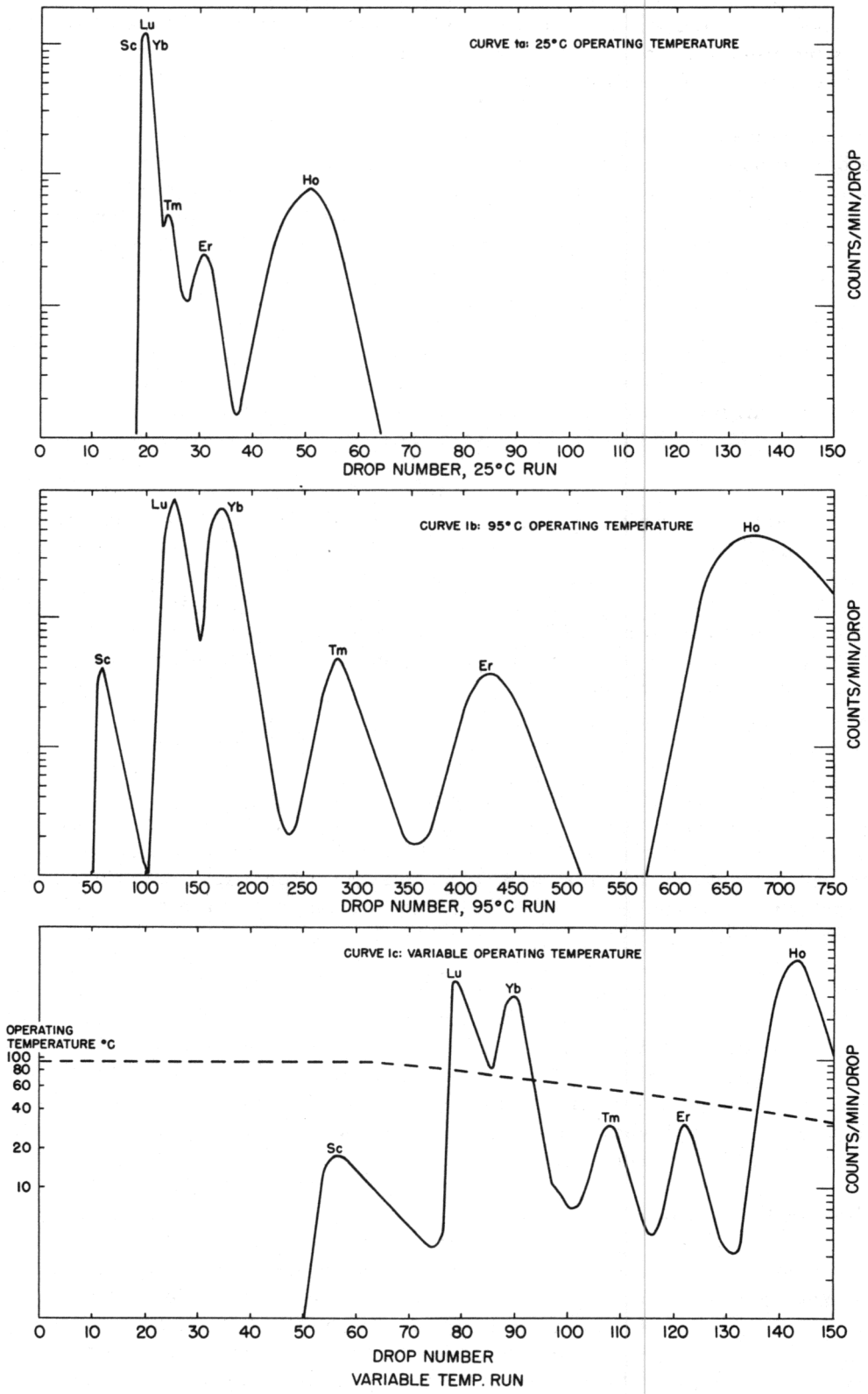

Fig. 15. Effect of operating temperature on the elution of rare earths from Dowex-50 with ammonium d-hydroxy isobutyrate.

the same group. Because of its promise in the development of a systematic scheme of chemical analysis based upon electrochromatography, the possibilities of the formation of complexes by means of various polyvalent acids have been tested as an aid in the separation of mixtures of alkali and alkaline earth.

The experimental results were found to vary greatly with the compositions and pH's of the background electrolytic solutions employed. In most acidic solutions, both the alkali and alkaline earth ions migrated rapidly, but there was much cross contamination of the zones. In weakly acid and alkaline solutions of complex-forming acids, such as citric and ethylenediaminetetraacetic acids, the alkaline earth ions formed complexes that migrated as anions and separated completely from the uncomplexed alkali metal cations.

The separation of barium, strontium, calcium, and magnesium from one another was most complete when these ions were but partially in the complex form. In acid solutions, barium migrated most rapidly, followed closely by strontium, calcium, and magnesium. In weakly acid and alkaline solutions of the polybasic acids this order was reversed.

The separation of the alklai metal ions from one another was not affected by variation of the background electrolytic solution. Under all the conditions tested, cesium, rubidium, and potassium formed a single, rapidly migrating zone, followed by sodium and lithium in turn. A practical technique for the separation of radioactive cesium and rubidium from other nuclear fission products could be based on this effect. Also an effective separation and analysis of lithium, sodium, and potassium can be based on electrical migration techniques.

Tritium Labeling

An attractive method for tritium labeling by self-induced exchange has been found to occur when organic materials are exposed to tritium gas. The incorporation of as much as one per cent of the tritium per day has been observed. This method of labeling appears to be widely applicable, and it is possible to prepare materials containing higher concentrations of tritium with little or no radiation damage than are possible by the triton-recoil method.

The self-induced exchange reactions occur at room temperature in subatmospheric pressures of tritium. Preferably, the hydrogen content of the tritium should be low, but it is not necessary to remove the helium-3 formed by decay. The tritium recovered from an exposure may be re-used, but increased formation of by-products may occur if the gas is not purified. Although there are no limits to the quantity of organic material that may be employed, use of the smallest amount which can completely absorb the radiation offers some advantages.

Heat of Vaporization of Liquid He^3

Calorimetric measurements have been made of the heat of vaporization of liquid He^3 in the temperature range 1.2 to 2.1° K in order to provide more accurate values of the entropy. Although the heat capacity of liquid He^3 has been measured down to 0.23° K it is not possible to make a reliable extrapolation from this temperature to absolute zero to obtain the entropy. The entropy of the liquid, however, can be determined at a given temperature from the entropy of the gas (known from the Sackur-Tetrode equation) and the heat of vaporization at that temperature. The heat capacity data can be combined with this to obtain the entropy at other temperatures.

Heretofore the only values of the heat of vaporization that have been available were derived from vapor pressure measurements and were subject to as much as 2% error because of uncertainties in the temperature scale and the second virial coefficient. Although the quantity of He^3 vaporized in the present experiments was at most 0.009 mole, the estimated probable error in the heat of vaporization is only 0.2%. The measured heat of vaporization at 1.5° K was 10.39 ± 0.02 cal $mole^{-1}$, and from this value the entropy of the liquid at 1.5° K was computed to be 2.60 ± 0.03 cal deg^{-1} $mole^{-1}$. The entropy previously obtained from vapor pressure measurements was 2.52 ± 0.17 cal deg^{-1} $mole^{-1}$.

RESEARCH INSTRUMENTS AND METHODS

The Particle Accelerator

At the request of the Atomic Energy Commission, the Laboratory is concentrating the efforts of the recently established Particle Accelerator Division on the design of a semi-conventional accelerator which is expected to be in operation within a reasonably short time - about five years. For the time being, the development of the accelerator of a novel type discussed in the Annual Report for 1955 will be de-emphasized.

Under design is a proton synchrotron of 12.5 Bev, an energy high enough to be significantly above the threshold of production of every known subnuclear particle. Output currents of substantially 10^{12} ions per pulse are expected, which will put the machine in the "high intensity" class. The magnetic field guiding the particles as they follow their orbits around the accelerator will be produced in a ring-shaped magnet of 8 sectors arranged in a circle of 600-foot circumference and weighing about 6400 tons. The field will differ from that in existing synchrotrons in that it will be built as homogeneously as possible, i.e., there will be no radial gradient. With such a design, it will be possible to attain a field of at least 20,000 gauss, as compared to the three-fourths of this figure obtainable in the usual design, thus leading to a more compact machine for a given energy. Studies with model magnets have verified the feasibility of reaching fields of this magnitude, and even higher.

Although a homogeneous field supplies radial focussing forces to the orbits of the protons, it does not contribute to vertical stability, so that this sine qua non must be reached otherwise. In the present design, the necessary vertical restoring force will be obtained by cutting the ends of each of the eight magnet sectors in such a way that the equilibrium orbit makes an angle of 77 degrees with the magnet face, thereby introducing the required component of radial gradient at each of sixteen "lenses" so that vertical stability is brought about.

This zero-gradient design (a special case of the more usual constant-gradient type mentioned above) has been chosen rather than the alternating-gradient pattern (which requires considerably less iron) for several reasons: first, it will be possible to inject protons into the machine for about 100 turns, thus leading to a much larger yield of high energy particles (alternating-gradient accelerators are limited to one-turn injection); secondly, the program of model magnet studies will be very substantially reduced; and thirdly, the tolerances in magnet alignment will be considerably eased.

Protons will be injected into the magnet from a 50-Mev linear accelerator. Although this choice involves the expense and effort of building such an injector,

it has considerable advantage over the purchase of a commercially available 5-Mev Van de Graaff generator. The frequency of the accelerating voltage applied to the ions while in the ring magnet will range over a factor of only 3.2 rather than about 10, thus greatly simplifying the problems of generation and control of the accelerating fields at radio frequency; the deleterious effects of proton loss due to scattering by residual gas will be very greatly reduced; and finally, recent progress in construction and design of proton linear accelerators at other institutions indicates that no insuperable difficulties should be encountered in producing a machine with the desired characteristics.

Acceleration in the magnet will be accomplished by the use of four cavities, all operating in phase and tuned to the fourth harmonic of the frequency of revolution of the particles. Tuning will be effected by loading the cavities with rectangular frames of ferrite and by appropriate variation of a direct current which produces a biasing magnetic field in the ferrite, thus altering its permeability. Extremely close tracking of the desired frequency will be required, this being determined by the instantaneous value of the guiding magnetic field. Means of continuously monitoring the guide field are under development. In the later portions of the acceleration cycle, after the protons have become well bunched, it is planned to sense the passage of the bunches and to use this signal to drive the amplifiers feeding the cavities, so that tracking will be automatic.

Detailed studies of the properties of several brands of ferrite over the required frequency range have been carried out and a full scale model of a cavity will be constructed soon.

The problem of stability of the foundation for the magnet and for the radiation shielding has been approached through study of soil characteristics obtained from many borings; seven test piles of three different types have been driven to depths ranging from 50 to 90 feet, so that subsidence and rebound characteristics under application and removal of load may be studied throughout the coming several months.

Detailed requirements for the associated buildings and structures are being drawn up.

Recoil-Type Neutron Spectrometer

The recoil-proton technique has been extended to produce a neutron spectrometer which operates successfully in the previously inaccessible energy range between 50 kev and 1 Mev. The instrument consists of three interconnected proportional counters arranged along the line of flight of the incident neutrons as shown in Fig. 16. Recoil protons, produced when neutrons strike hydrogen atoms in the methane (CH_4) gas with which the counters are filled, lose their energy by ionizing the gas along their paths.

When a neutron suffers a head-on collision so that the proton recoils along the line of flight of the neutron, the entire kinetic energy of the neutron is transferred to the proton. This group of protons is selected by connecting counters A and B (Fig. 16) in coincidence so that the count includes only those recoil protons passing through the collimator holes from A to B. The pulse from proportional counter A is added to that from B to yield a sum-pulse which is proportional to the energy lost by a recoil proton in both counters (neglecting the small amount lost in the collimator channel). If the proton stops in the gas of counter B, the energy dissipated in ionizing the gas is the total energy of the proton which, for the protons counted, is equal to the energy of the incident neutron. On the other hand, protons which continue on into counter C lose only part of their energy in the gas in A and B and thus produce a "tail" on the low-energy side of

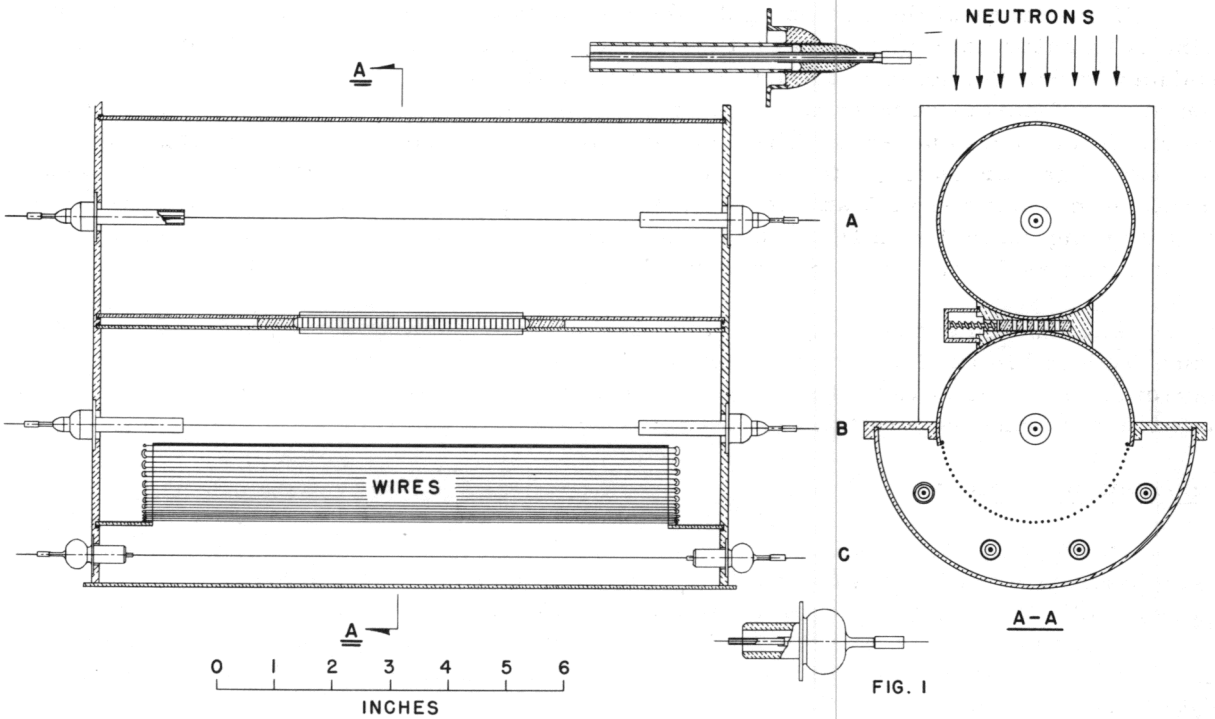

Fig. 16. Recoil-type neutron spectrometer for 0.05 to 1 Mev.

a peak as shown by curve AB in Fig. 17. When these protons are eliminated from the tally by connecting C in anticoincidence with A and B, this tail (and the concomitant loss of resolution) disappears as shown in curve ABC in Fig. 17. At low energies, for which the range of protons is short, this anticoincidence feature is quite unimportant, as shown by Fig. 18 in which the circles represent data taken with the anticoincidence feature and the triangles are for data taken without it.

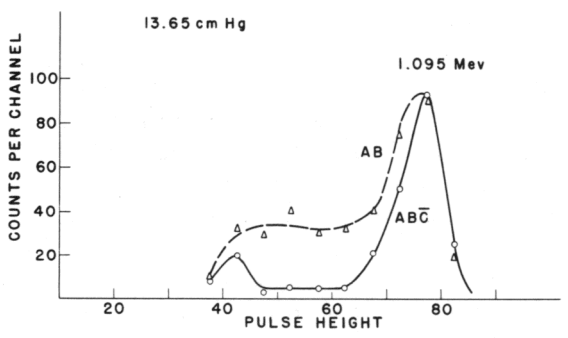

Fig. 17. Peak at 1.095 Mev, showing the need for the anticoincident counter C. Curve AB (triangles) was taken without use of C; curve ABC (circles) shows the greatly improved resolution when C is used.

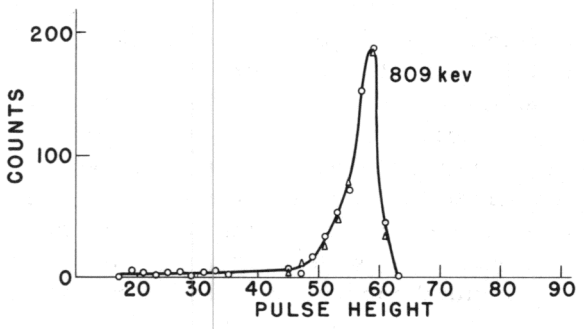

Fig. 18. Peak at 809 kev showing the small effect of the anticoincidence feature at lower energies. The circles were taken with counter C in the circuit, the triangles without it.

If the range of the protons gets short enough to be comparable with the length of the collimator holes (3/16 inch), the correction to be made for the loss of the ions produced within the holes becomes excessive; as the range becomes greater than the diameter (8.9 cm) of counter B, the efficiency falls because of protons penetrating into anticoincident counter C. The energy range of the counter may be changed by a change of gas pressure, 8 to 140 mm Hg being a useful range. At higher pressures a neutron may scatter in A and again in B, producing a spurious pulse. There is no point in going below 8 mm Hg because the cross section for (n,p) scattering is too low at energies for which such pressures would give a suitable range for the protons.

The instrument is being used to study the energy spectrum of delayed neutrons produced in fission and to measure the neutron-energy spectrum of reactors (especially fast reactors). It is suitable for any investigations of nuclear reactions in which neutrons are emitted with energies between 50 kev and 1 Mev.

Scintillation Counters

Both liquid and plastic scintillators consist of a base material (solvent) with a small admixture of fluorescent solutes (sometimes called "activators" by analogy with the activators used in organic phosphors). A study of a series of activators, which were developed elsewhere for use in liquid scintillators, resulted recently in the development at Argonne of plastic scintillators of lower cost and greater versatility than those hitherto available.

The usefulness of a scintillator may be improved by the addition of special elements to make it sensitive to a particular radiation. Recently, efforts have been directed toward loading liquid and plastic scintillators with heavy elements to increase the photoelectric response to gamma rays. In both liquid and plastic scintillators, the addition of a compound of a heavy element involves the problems of (1) its solubility and (2) its quenching of the light output. In a plastic, a compound of a heavy element introduces the additional problems of (1) its compatibility with polymerization, and (2) its stability at the polymerization temperature; but these added problems are offset somewhat by their smaller quenching effect in plastic scintillators. This is illustrated for the case of mercury added as diphenylmercury in Fig. 19.

The ability of a scintillating material to emit light is frequently impaired (quenched) when foreign substances are added (as in the case of the diphenylmercury shown in Fig. 19). Experiments elsewhere, with liquid scintillators from which dissolved gases were quite completely removed, have shown that the oxygen component of the dissolved air also has a marked quenching effect in many scintillators. In order to study the properties of the scintillators in the absence of this quenching and to eliminate the variable quenching due to unknown concentrations of dissolved atmospheric oxygen, an apparatus was constructed in which the concentration of solutes can be varied over a wide range, and their light output under beta-ray excitation can be studied under conditions of equilibrium with various controlled atmospheres. In particular, the quenching effect of dissolved oxygen has been studied as a function of the concentration of various activating solutes - the light output under a non-quenching atmosphere (such as argon) being used as a reference. As predicted by theory, oxygen greatly reduces the ability of the solvent to transfer its energy of excitation to the fluorescent solute. However, detailed studies indicate that some modifications in the theory may be necessary.

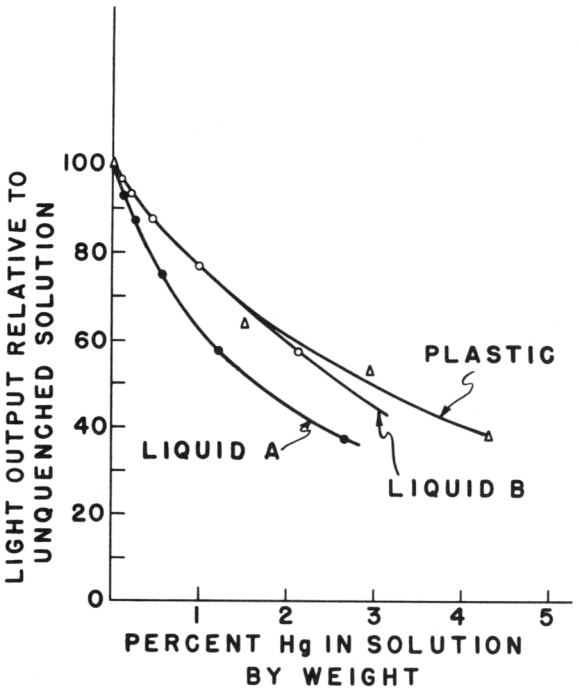

Fig. 19.

Light output of two liquid and one plastic scintillators vs concentration of added heavy element quencher. Plastic scintillator is polyvinyltoluene plus 2% 2-phenyl-5-(4-biphenylyl)-1,3,4-oxadiazole (PBD) and 0.05% 2,5-di-(4-biphenylyl)-oxazole (BBO). Liquid A is toluene plus 20 grams/liter PBD. Liquid B is toluene plus 280 grams/liter naphthalene plus 20 grams/liter PBD.

Particle-Size Analysis by Radioactivation

Of the various techniques developed for the determination of particle sizes by sedimentation analysis, none are easily adapted for use with liquid metal dispersants. In all cases the difficulty arises in attempting to measure the amount of material in suspension as a function of time. A modification of the light-scattering method by substitution of gamma rays for visible light has not been found to be entirely satisfactory, because such a technique is fairly insensitive to small changes in composition and furthermore requires that the stopping power of the suspended material be greatly different from that of the dispersing medium.

A radioactivation method has been developed to make use of the activity generated in suspended particles by neutron bombardment. During irradiation, the engendered activity in a particle is proportional to the number of susceptible atoms. Consequently, the relative activity between two particles will be equal to their relative weights. Similarly, in a lamina of a suspension undergoing settling, the relative activity in the lamina at two different times will be equal to the relative weight of material in the lamina at those times.

When the lamina is defined by a collimating slit at a fixed distance from the top of the suspension, then, by use of Stokes' law, it is possible to calculate the time t_i for a particle of diameter x_i to settle past the slit. The ratio of the activity at time t_i to the initial activity, when the suspension was uniform, will be equal to the weight fraction of material whose particles are of diameter smaller than x_i.

The sources of error peculiar to this method are due to counting statistics, incomplete dispersion, and scattering of radiation. The latter can be largely eliminated by suitable geometric arrangement and electronic discrimination. Nonuniformity of dispersion can easily be checked by scanning the length of the tube with the counter while stirring. The counting statistics actually limit the accuracy of the method. The largest weight fractions will be determined with the greatest precision.

Experiments have shown that this radioactivation method is comparable in accuracy with more conventional sedimentation techniques. The method is rapid, capable of being adapted to automatic operation and to taking close size intervals. It is particularly suited to reactive systems that must be handled in vacuo or in an inert atmosphere.

Sixty-Inch Cyclotron Facility

During 1956 an external quadrupole lens focussing system was designed, constructed and put into operation. Briefly, the magnetic lenses accept and focus 10% of the total deflected beam into an area of about 0.15 cm^2. This beam can be focussed either in the cyclotron vault or in the experimental tunnel, 35 feet from the cyclotron tank. Such a system permits the set-up of targetry and instrumentation in the experimental tunnel during irradiation of targetry in the vault. This will decrease the machine "dead time" and increase the "beam on" time.

With this system functioning a scattering program has been initiated to measure the angular distribution of elastically and inelastically scattered particles. In addition, the focussed beam is being used to determine deuteron, proton and alpha-induced fission cross sections of heavy nuclides.

PART II

REACTOR SCIENCES

Page

THE BOILING WATER REACTOR PROGRAM 38

The Experimental Boiling Water Reactor 38
BORAX-III and BORAX-IV 44

THE POWER BREEDER REACTOR PROGRAM 46

Experimental Breeder Reactor-II 46
Experimental Breeder Reactor-I 50
A Coupled Fast Thermal Power Breeder 51

NAVAL REACTOR PROGRAM 53

THE RESEARCH REACTOR CP-5 53

REACTOR DEVELOPMENT PROGRAMS 55

The Argonaut 55
The Mighty Mouse 57
ALPR 58

BASIC PHYSICS INVESTIGATIONS 59

Fission Energetics 59
Neutron Lifetimes 60
The Doppler Temperature Effect 61
Reactor Physics Constants Center 61

SUPPORTING RESEARCH AND DEVELOPMENT 62

Heat Transfer Studies 62
Control Rod Drive Development 62
The Plutonium Metallurgy Research Laboratory 63
Multi-Crucible Furnace 64
Studies of Dispersion and Coalescence 64
Metal Oxidation and Ignition 65
Fluidization Processes 65

THE ARGONNE HIGH-LEVEL GAMMA-IRRADIATION FACILITY 68

THE BOILING WATER REACTOR PROGRAM

Since 1953 the Laboratory has pursued the problems relating to the development of economical power from boiling water reactors. The various Borax experiments were carried out to gain experience under conditions closely simulating operation of an actual power plant. In 1956 these efforts culminated in the completion of construction and operation of the Experimental Boiling Water Reactor.

The Experimental Boiling Water Reactor

The Experimental Boiling Water Reactor (EBWR) reached its rated electric power output of 5,000 kilowatts on December 29 and thereby became the first reactor in the Atomic Energy Commission's Power Reactor Development Program to go into operation.

Power generation itself is not a primary objective of the EBWR. Rather, the installation is an experimental plant intended to provide practical information for future use in designing large central station units, particularly as regards the direct coupling of the reactor proper with the power-generating equipment.

Construction of the EBWR began at its site at Argonne National Laboratory in June 1955. The gas-tight steel cylindrical structure containing the reactor was completed and tested near the end of 1955. General construction work on the remainder of the plant then began.

Details of construction are not reported here. Only those highlights having technical significance will be mentioned with particular attention given to those items which were not described in the previous Annual Report.

The reactor vessel arrived at the site in May 1956. It was installed in the hollow octagon which had been excluded from the original construction contract pending completion of a study by the Armour Research Foundation on consequences of an explosive metal-water reaction.

The most important features of the design adopted as a result of the Armour study are shown in Figs. 20 and 21. In the absence of proof that metal-water reactions cannot occur following an uncontrolled reactor excursion which melts the fuel, it was assumed that 25% of the metal of the core would react explosively. The Armour study indicated that the sudden release of 8×10^8 calories of energy in this manner would certainly rupture the pressure vessel below the water line and reduce the surrounding concrete shield to rubble. Pressures developed in the steam dome, however, would be in the range of feasible restraint. Accordingly, a design evolved which would allow the pressure to relieve itself by blowing downward while the upper part of the pressure vessel remained intact.

The flat cover of the pressure vessel is held down by a 6-inch thick steel plate backed up by three tremendous, horizontal, steel H-beams. The H-beams are pinned with steel wedges to six huge, vertical, steel columns which pass down through the reactor shield to anchors buried deep in the 7-foot thick concrete filler in the bottom of the steel containment building. The vertical columns are protected against radial shock waves by thick laminated wood-steel blast shields interposed between the columns and the reactor.

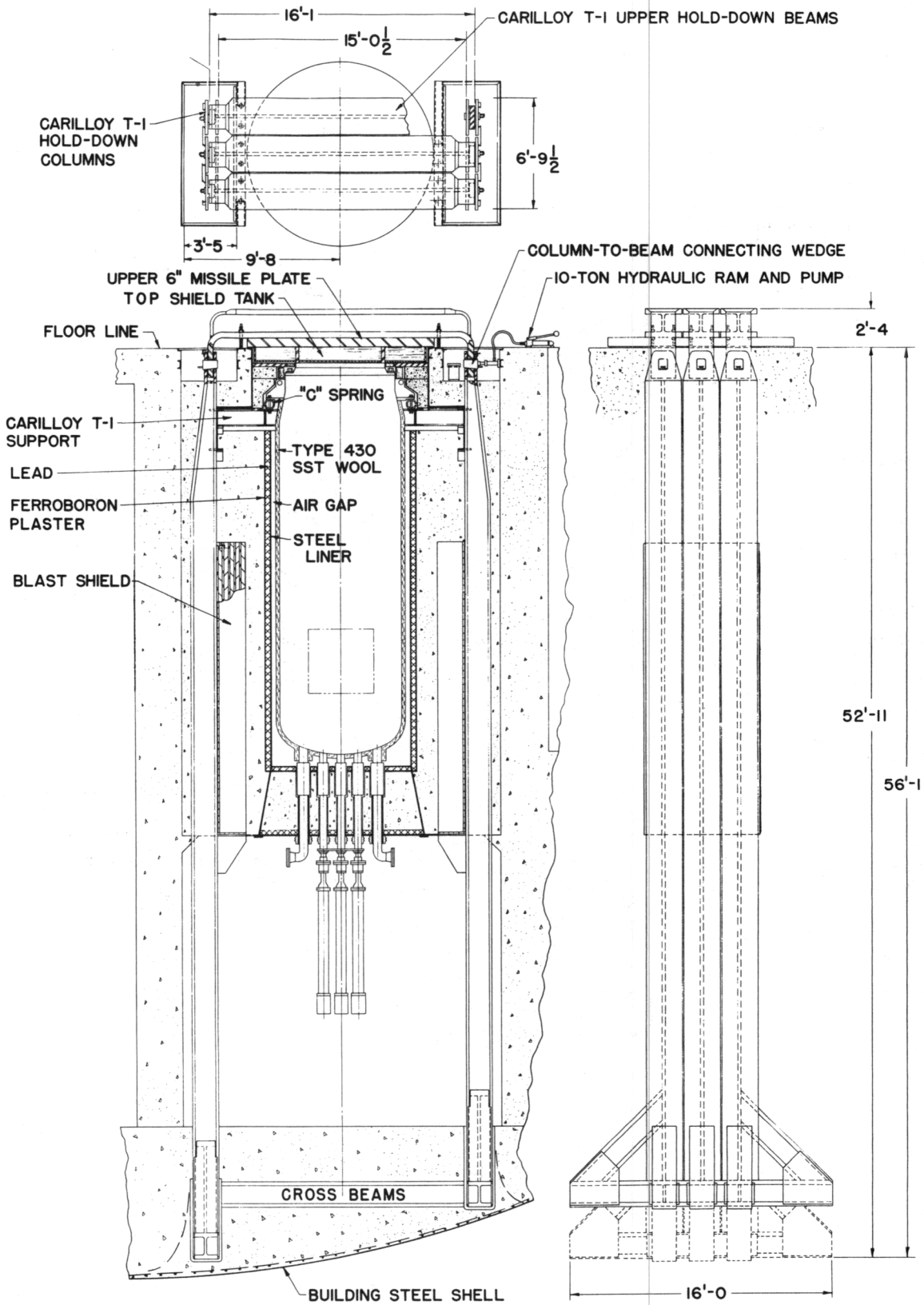

Fig. 20 The hold-down structure of the pressure vessel for EBWR

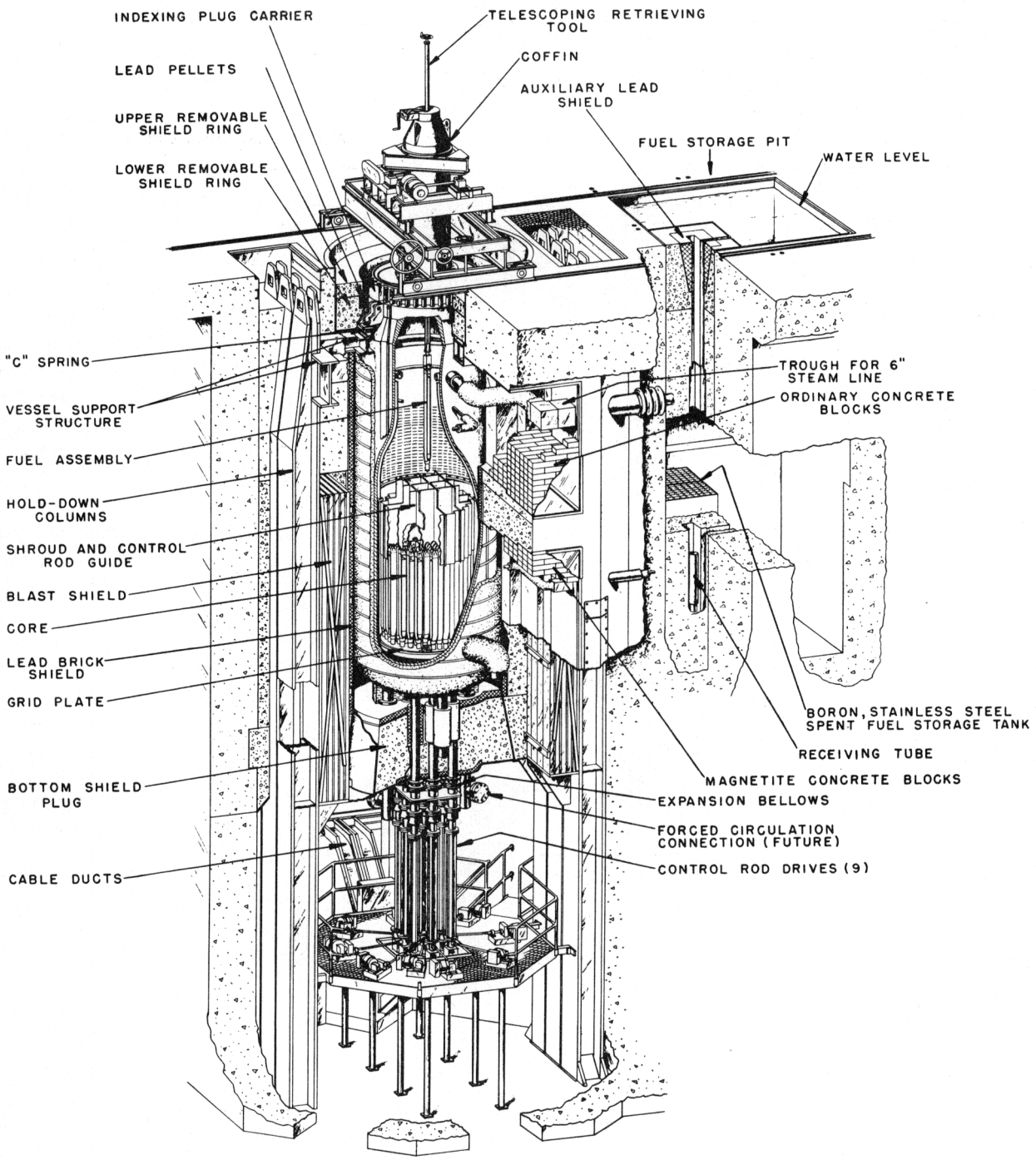

Fig. 21 A cutaway pictorial of the EBWR reactor and its components

The method of structural support of the reactor pressure vessel is shown in Figs. 20 and 21. The 7-foot ID, 23-foot high vessel is suspended at its upper end from a steel framework which is attached to the vertical steel columns described above.

The reactor pressure vessel is surrounded by a 3-inch thickness of stainless steel wool insulation, 3 inches of air space, and a cylindrical carbon steel tank which serves as an inner form for the shielding. Cooling coils are embedded in the 3-inch thick layer of lead outside the steel cylinder. Outside the lead, the biological shield consists of magnetite concrete with steel punchings added, magnetite concrete, or ordinary concrete, depending on the estimated radiation intensity at the point concerned.

The cover of the pressure vessel is a 9-inch thick plate which is bolted and gasketed to the vessel proper. Some difficulty was encountered in achieving a satisfactory seal. A special set of Flexitallic gaskets with Teflon filler, installed with steel retainer ribbons, has proven to be satisfactory thus far, but long term experience is lacking.

All fuel for the EBWR was fabricated by the Metallurgy Division of Argonne using a process developed by this Division. Since no critical experiments had been run, four different types of fuel elements were fabricated so that uncertainties in core characteristics would not hold up the program. Two thicknesses (Fig. 22) of fuel plates were used in different assemblies so that the volume ratio of water to uranium could be varied in the core. Both natural uranium and slightly enriched (1.44% U^{235}) uranium assemblies were provided. Zircaloy-2 cladding was used.

All fuel plates were tested for integrity of the cladding in autoclaves maintained at 500F for two weeks. Only three plates out of 970 failed this test. The test was repeated on all completed fuel assemblies without any failures.

Loading of fuel into EBWR began November 26 and criticality was first achieved December 1. A long series of calibrations and rearrangements of the core were made to arrive at a 4-foot diameter core with enough excess reactivity for operation at 20 megawatts heat output (at 600 psig) and with a void coefficient of reactivity which is just slightly negative at room temperature.

Because of existing uncertainties in nuclear constants, as well as imperfections in theoretical methods, a probable error of about ± 3% k was estimated for the reference fuel loading for EBWR. This loading consisted of enriched and natural uranium assemblies in the ratio of 76: 36. The most probable number of such assemblies required for the reactor to go critical was calculated to be 42; actually, 81 assemblies were required. This increase in critical mass corresponded to a difference in k of about 3%. Thus, the actual error was equal to the estimated probable error. This experience indicated once again that theory alone cannot be relied upon to give the nuclear characteristics of a core accurately. Having available a variety of fuel which had been fabricated in anticipation of the possibility of such a discrepancy between theory and experiment, the ratio of enriched to natural assemblies was promptly adjusted to give the required extra reactivity.

A cross section of the core as it was finally loaded for full power operation is shown in Fig. 23. This core, loaded with 106 enriched and 8 natural uranium assemblies, had about 7% reactivity at room temperature. This appears to be slightly more than is needed for operation at a 20-megawatt heat output (600 psig) and may be reduced by substitution of natural for enriched uranium assemblies.

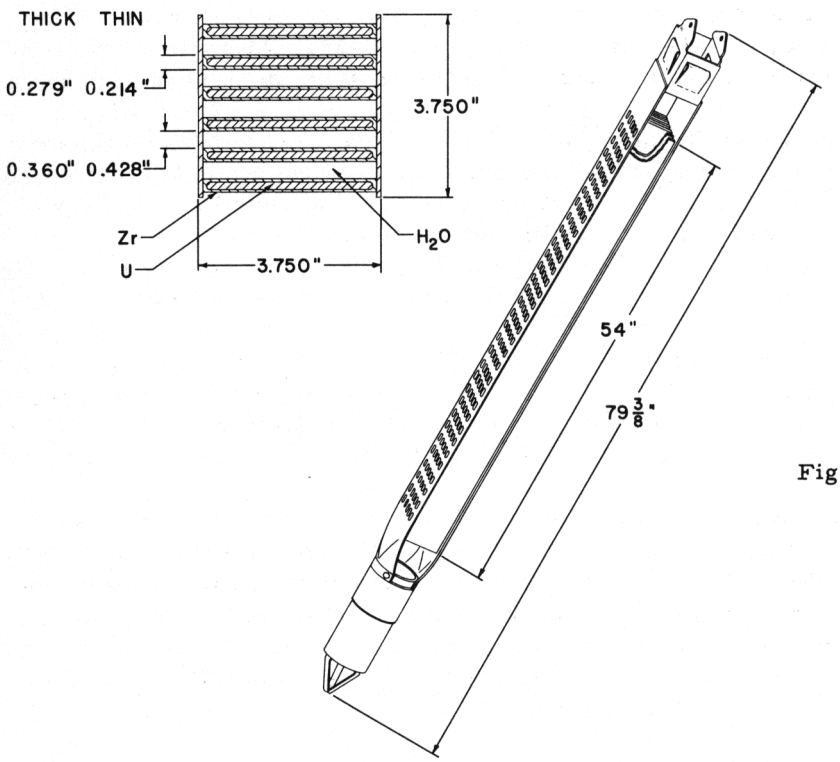

Fig. 22 The EBWR fuel assemblies

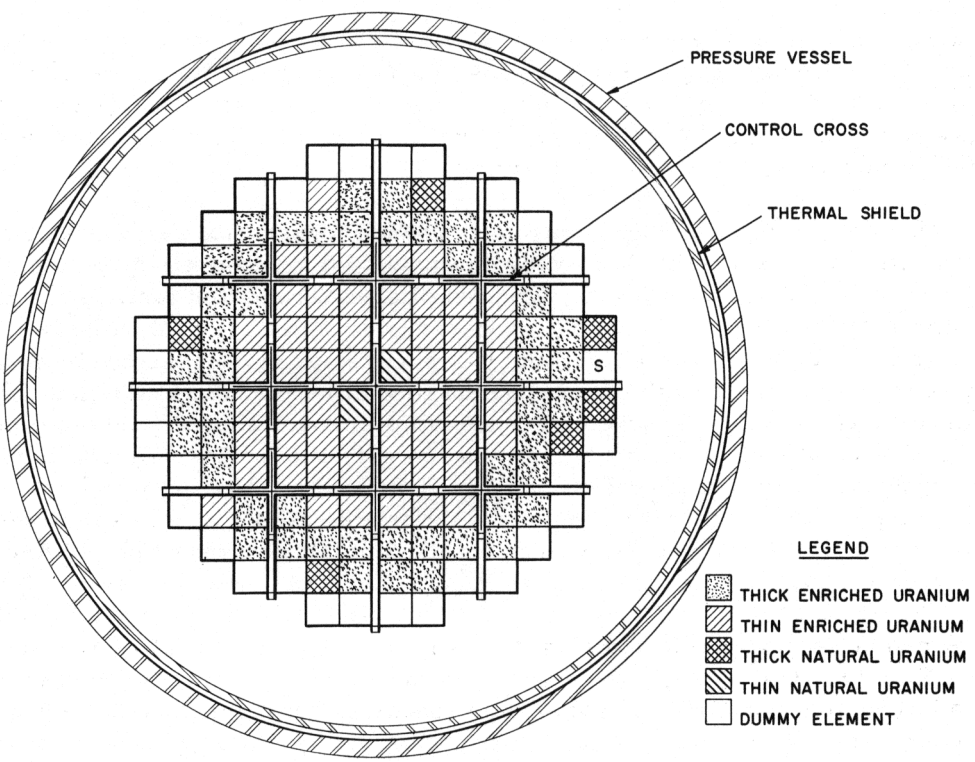

Fig. 23 A cross-sectional representation of the EBWR core as it was loaded for full power operation

Changes of moderator density and steam bubbles in the core were simulated by adding Styrofoam (expanded polystyrene) strips between fuel plates. In such calibration tests it was determined that the coefficient of reactivity of the steam voids was negative at room temperature, even with all thin-plate assemblies at the center of the core. Since it is desirable to reduce the magnitude of the negative void coefficient without actually running the risk of its becoming positive, the thin-and thick-plate assemblies were arranged as shown in Fig. 23, with all thin assemblies in the central part and all thick assemblies in the outer region.

Prior to critical tests it was verified that no large openings existed in the steel containment vessel. Upon completion of the criticality experiments and before operation of the reactor at significant power levels, a three-day leakage test was performed on the completed plant. The measured leakage rate at an internal pressure of 15 psig was well within the specified maximum of 1,000 ft^3/day.

Other features of the EBWR reactor and power plant as constructed can be seen in Figs. 24 and 25. The grid, guide, and shroud (Fig. 24) within the reactor pressure vessel serve to hold the fuel assemblies in their proper position as well as to guide the nine control rods. Structures within the active region of the core are fabricated of zirconium, while portions outside the active region are made of stainless steel.

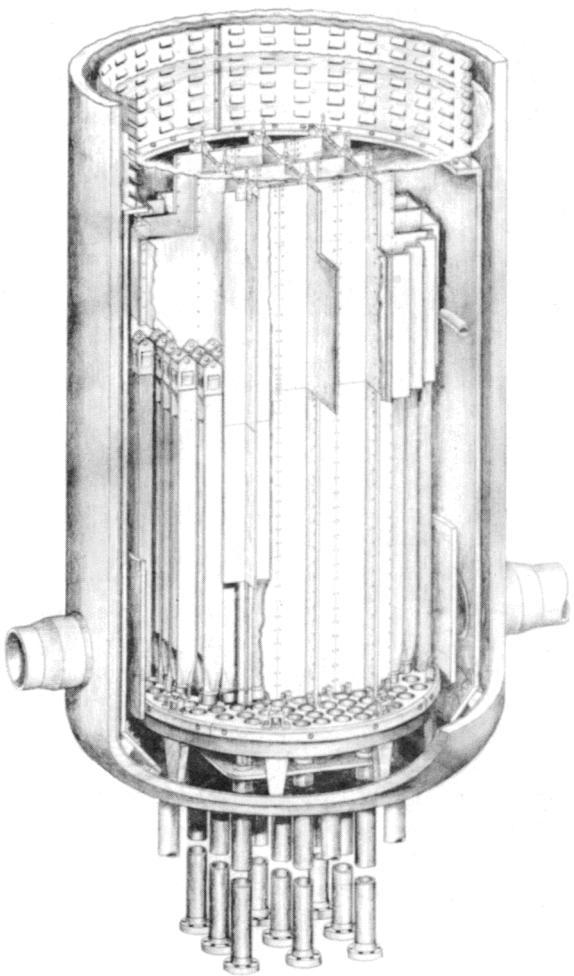

Fig. 24 Perspective of the reactor core utilized in the experimental boiling water reactor

Mechanisms for driving the control rods are located outside the shield below the reactor. Five control rods are made of hafnium; the other four are of relatively inexpensive borated stainless steel which was developed during 1956.

Operation of the reactor at significant power levels began on December 22. The first generation of electricity occurred the following day. The full 20-megawatt power output of the reactor was achieved on December 28, and 5,000 kilowatts of electricity were generated on December 29. Except in a few relatively minor respects, test operation of the EBWR power plant as a whole was highly satisfactory. Operation on a continuous full power basis should begin early in 1957.

Future plans for the EBWR include installation of pumps for obtaining higher power levels by use of forced circulation of the coolant. The plant is designed for future conversion to a heavy water system after the feasibility of keeping leakage rates at acceptably low levels has been verified with light water in the system.

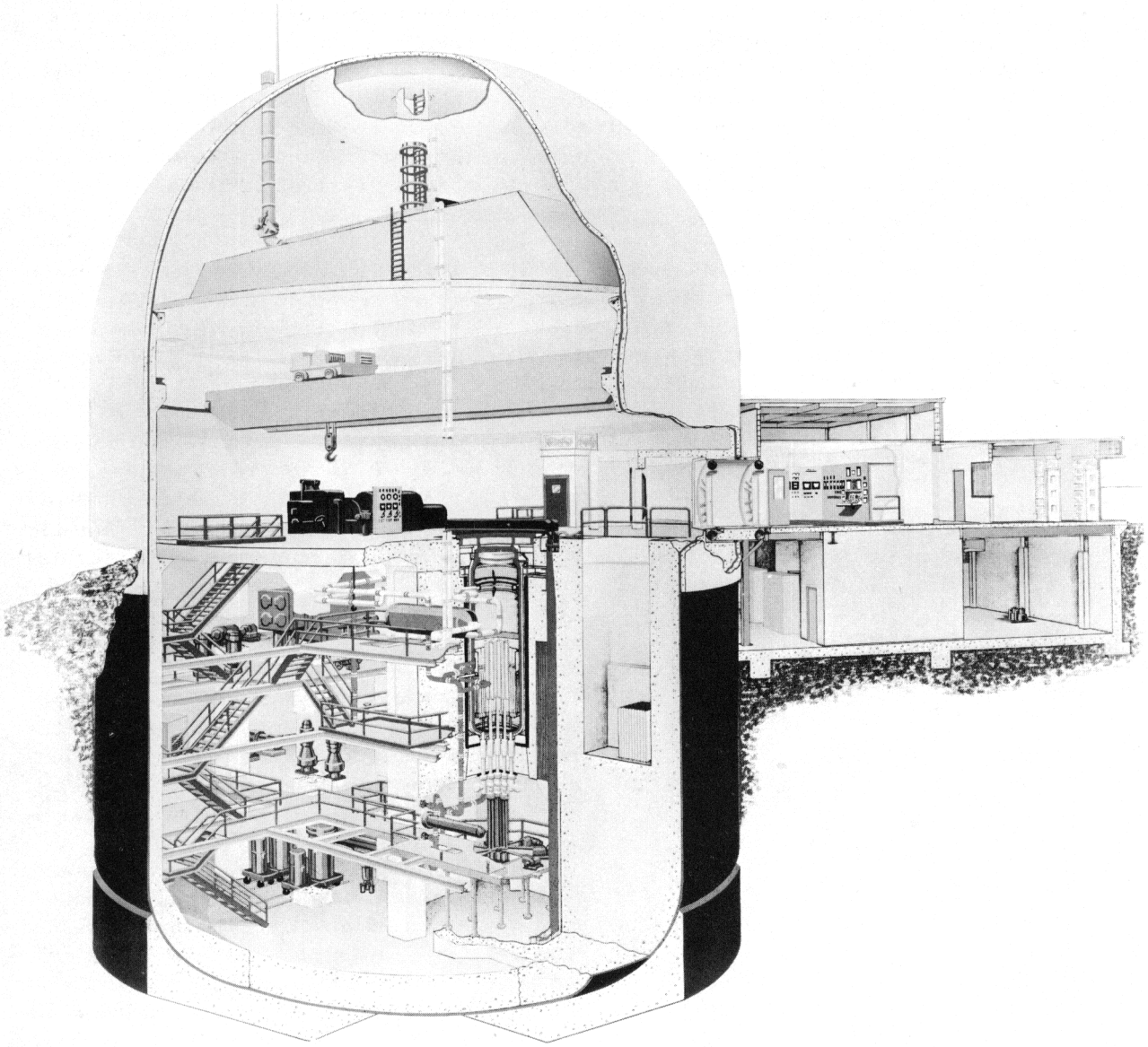

Fig. 25 Perspective of the power plant of the experimental boiling water reactor

BORAX-III and BORAX-IV

The BORAX-III reactor was continued in operation at 300 psig during the early part of the year at power levels between 8 and 12 Mw. It was primarily used to continue experimental studies of the various parameters and conditions which influence the operation of power plants utilizing boiling water reactors. Efforts to outline and solve the problems connected with the reactor water represented one of the major aims of the BORAX-III program.

The rate of decomposition of the water in BORAX-III was measured quantitatively by collecting the noncondensable gases by water displacement during sampling of the steam flowing to the turbine. The rate was found to vary with the pH of the reactor water, ranging from 64 cc of total gas per liter of condensed steam at a pH of 8.1 to 197 cc of total gas per liter of condensed steam at a pH of 5.2. Fig. 26 is a graphical

representation of the observations. These high rates, at first attributed to impurities in the reactor water, are now believed to be caused by the sweeping out of the gases by the boiling action in the reactor.

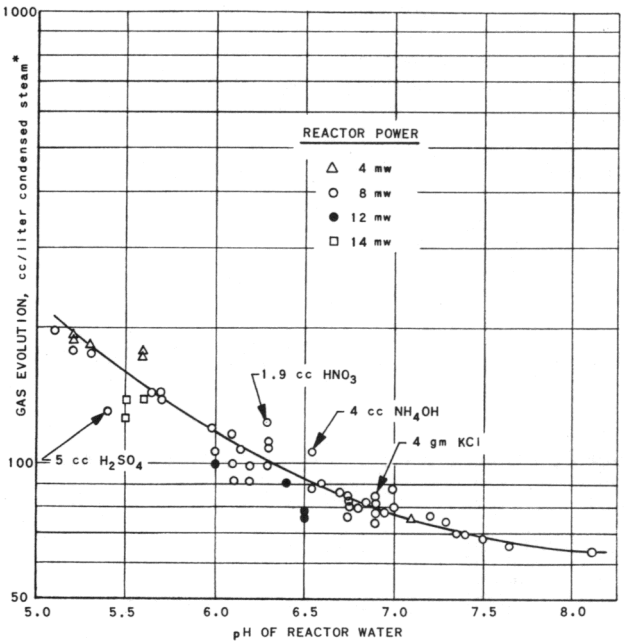

Fig. 26 Non-condensable gas collected in BORAX-III operations

The purity of the water was controlled by continuous circulation through filters and ion-exchange columns. By using separate columns of anion and cation resins in parallel, it was possible to operate the reactor with water having a specific resistance of 150,000 ohms per cm^3. By using a mixed bed column, water having a specific resistance of 900,000 ohms per cm^3 and a pH of 6.75 was obtained. The decontamination factor (ratio of activity of reactor water to that of the effluent) across the cation column varied from 90 to 330, while that across the mixed bed ranged from 1000 to 1400. The data from BORAX-III indicate that there should be no trouble in maintaining reactor water of high quality in EBWR.

The major radioactive isotope in the reactor water after decay of N^{16} (formed by neutron interaction with O^{16}) was Na^{24}. Other radioactive isotopes that have been identified were O^{19}, Cl^{38}, A^{41}, Ca^{45}, Mn^{56}, Cu^{64}, and Zn^{65}.

Entrainment of water in the steam does not appear to be a serious problem with respect to contamination of the system. The fact that samples of condensed steam from the reactor outlet and of condensate from the turbine hot well had practically the same activity after 20 hours of decay time indicated that little, if any, radioactivity was being deposited in the turbine. The activity of the exhaust end of the turbine 12 hours after the final shutdown of BORAX-III was only 1 to 1.5 mr/hr on contact.

The principal source of radioactivity in the steam was N^{16}, and its level varied with changes of operating conditions. The lowest measured activity occurred when the pH of the reactor water was increased to 8.1. The results of many experiments led to the conclusion that N^{16} does not come over in the steam solely as nitrogen gas, but rather as a mixture of nitrogen and various oxides of nitrogen. Changes in the concentration of N^{16} in the steam appear to be due to shifts in the equilibrium distribution of these substances between the steam and the reactor water. These could be caused by either or both (1) the changes in solubilities of the compounds in the water and (2) the oxidation or reduction conditions present in the reactor water and steam.

The high gas content of the steam, particularly that attributable to oxygen, has caused much concern about the corrosion of the reactor and the electrical generating equipment. In an investigation of methods to reduce this problem, it has been found that by introducing hydrogen into the feedwater at high flow rates the oxygen content of the steam can be reduced to values below that observed in the feedwater (see Fig. 27).

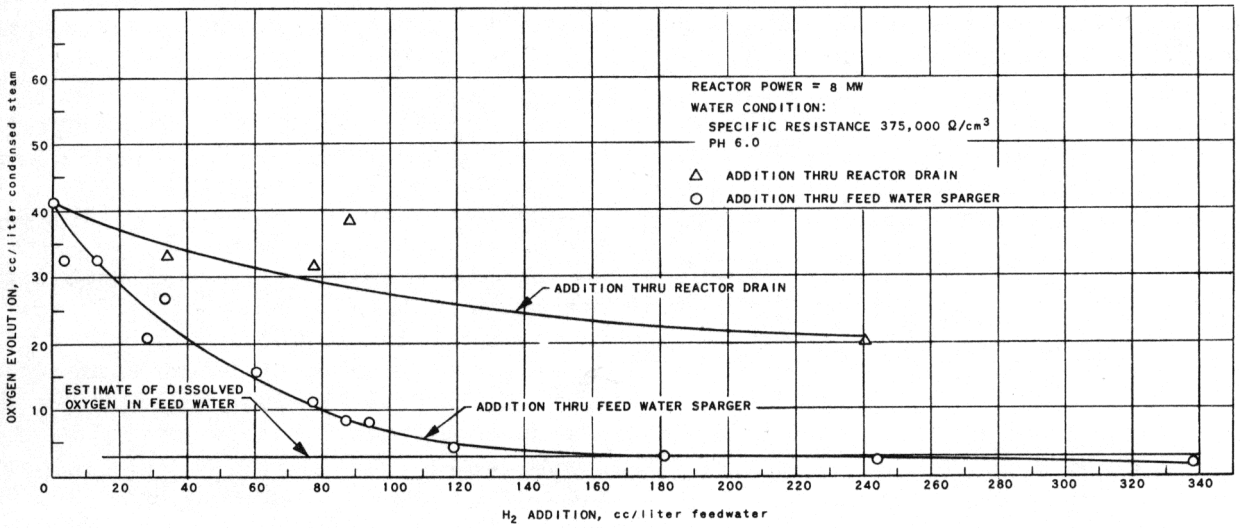

Fig. 27 Effects of addition of hydrogen on the production of oxygen during operation of BORAX-III

BORAX-III was shut down after 600 megawatt-days of operation. Initially, the reactor had a total reactivity of 7.5% in the cold, clean condition. At the completion of operation there was 5% reactivity available at room temperature without xenon.

A second core of oxide instead of metallic fuel has been prepared and has been utilized in continuing the experiments on boiling water reactors as BORAX-IV. The fuel elements are composed of thoria-enriched urania pellets contained in a jacket of aluminum containing one weight per cent of nickel. The annulus between the outer surfaces of the pellets and the inner surface of the tube is filled with lead to improve the heat transfer characteristics.

Since this type of fuel element has a higher heat capacity and a longer time constant for heat transfer than were the cases for elements used in previous Borax reactors, there is some question as to the stability of BORAX-IV under actual boiling conditions. At present only initial testing and calibrations have been carried out.

THE POWER BREEDER REACTOR PROGRAM

The Laboratory's program for the development of economical nuclear power from unmoderated power breeder reactors has continued. The major goal has been the completion of the Experimental Breeder Reactor-II (EBR-II) during 1958. Simultaneously, fundamental investigations of the characteristics of reactors using fast neutrons have been studied.

Experimental Breeder Reactor-II

The EBR-II, described in the last Annual Report, is to be built at the National Reactor Testing Station in Idaho. A contract has been placed with the H. K. Ferguson Company to perform the necessary services as Architect-Engineer.

The physical arrangement of the facility is depicted in Fig. 28. The reactor and primary cooling system (utilizing sodium instead of the sodium-potassium alloy used in EBR-I,) as well as the reactor auxiliaries, are located in the large, cylindrical gas-tight containment vessel in the center. The steam generator is located in the small structure connected by piping to the reactor building and to the power plant, which is the conventional building placed in the left foreground. The control room for the operation of the complete power cycle is located in the power plant building. The fuel processing facility is located to the right of the reactor building and contains the equipment for processing and fabricating the reactor fuel.

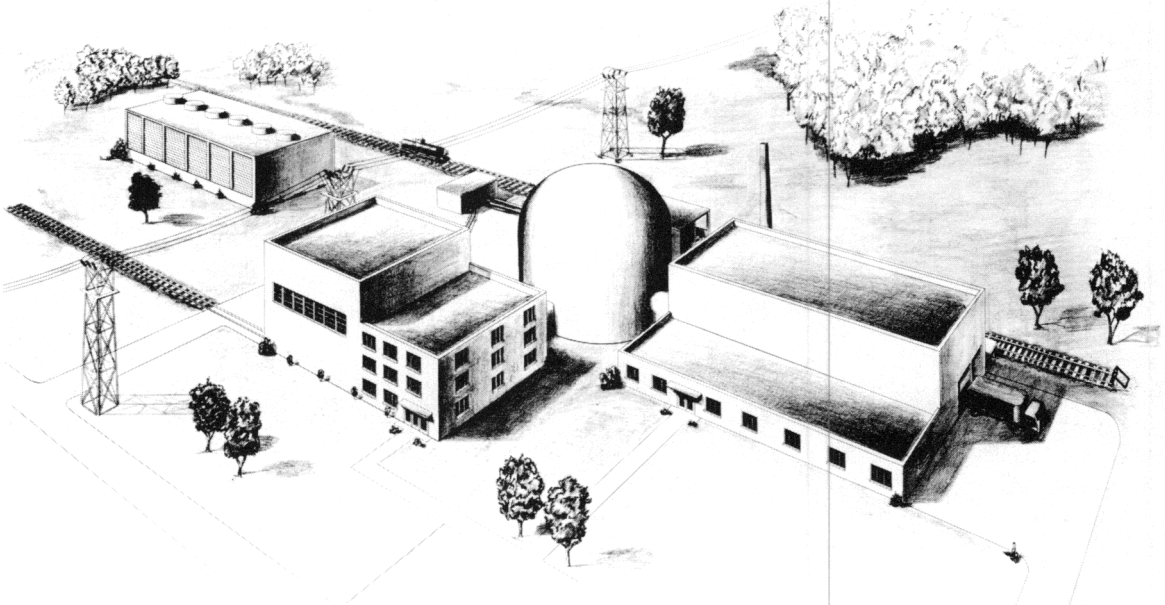

Fig. 28 A conception of the plant designed for EBR-II

Originally designed in the approximate shape of a right cylindrical shell, the geometry of the reactor core has been changed to that of a solid cylinder in order to avoid possible undesirable kinetic behavior. It has not been possible to prove that there would be no motion of the fuel toward the hollow center during operation, thereby causing an increase in reactivity. Accordingly, the safer configuration has been adopted.

Another modification in the original design has been the replacement of the large, single pump of the primary cooling system with two circulating pumps operating in parallel. This change will increase the reliability of the cooling system.

The emphasis in the engineering program associated with the EBR-II has shifted from developmental work to the actual testing of prototypes of components. The greatest effort has been expended in testing the largest liquid sodium pumps in existence and the associated piping systems. Included in the program have been an A.C. linear induction electromagnetic pump (Fig. 29), a centrifugal (mechanical) pump (each of a design rating satisfying the requirements of the EBR-II secondary sodium system), and a D.C. electromagnetic pump with characteristics satisfying the requirements of the primary sodium system.

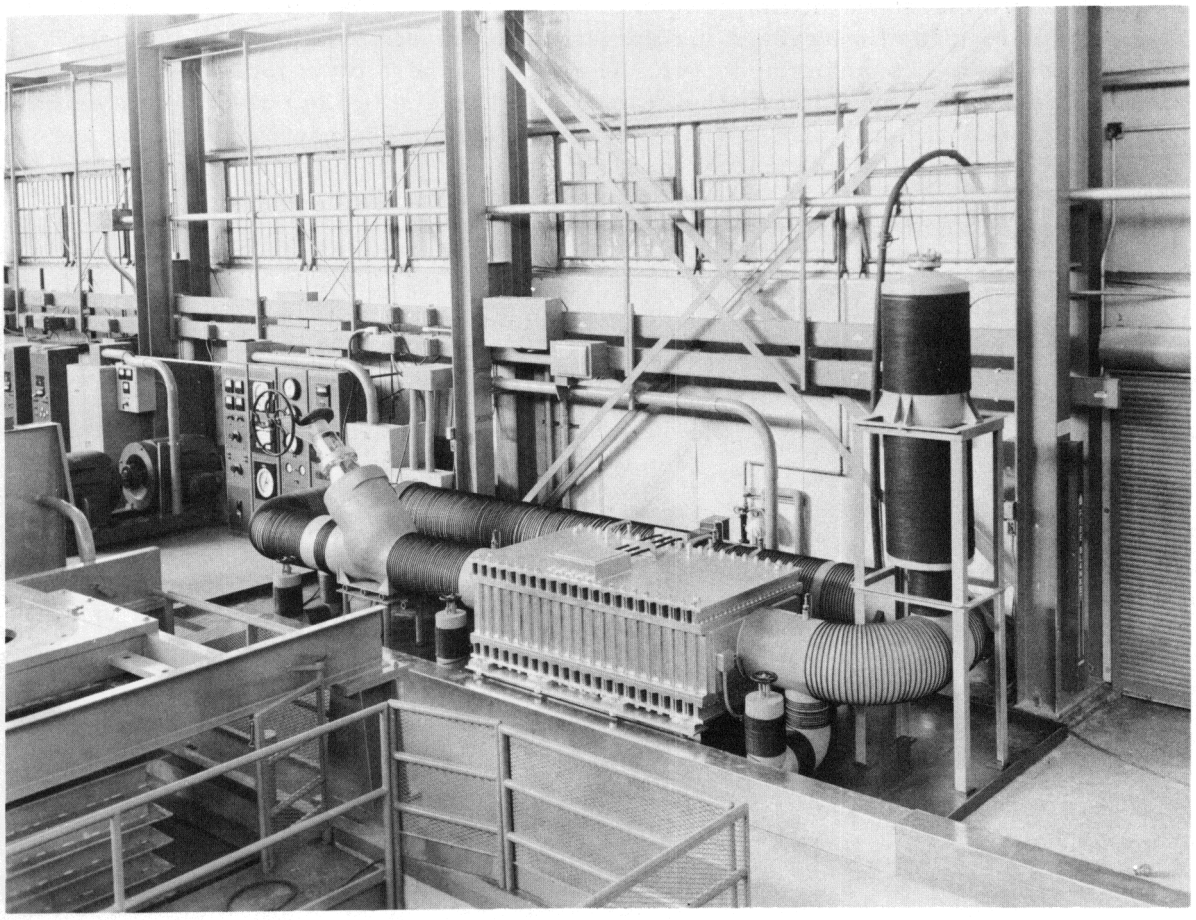

Fig. 29 The A.C. linear induction electromagnetic pump which has been undergoing tests for possible application to EBR-II

The EBR-II Working Model, described in the last Annual Report, has operated satisfactorily since the correction of minor difficulties encountered early in its tryout. The prototype 1000-gpm D.C. electromagnetic pump has operated for more than 4000 hours under conditions comparable to those anticipated in the EBR-II primary cooling system.

The development of high power-density reactors, of which EBR-II is a prototype, and of high burn-up fuels is expected to aggravate the problems of reprocessing spent fuel. Conventional methods require extended cooling periods of the fuel prior to reprocessing in order to avoid the deleterious effects of irradiation of materials. Therefore, research and development work on pyrometallurgical or high temperature processes has been undertaken in an effort to find a suitable way of processing briefly cooled, highly irradiated fuels. If the irradiated fertile and fissionable materials can be processed as molten metals, the usual need for converting uranium or plutonium salts back to metal would be avoided.

Melt refining of irradiated uranium by oxide drossing removes the volatile fission products, the alkaline metals, the rare earths and (partially) the transition metals, but does not appreciably separate the more noble metals from uranium. If a

reactor fuel is recycled through a reactor-processing plant, the accumulated elements will eventually have to be removed. While this removal can be effected by physical dragout of a portion of the fuel, a pyrometallurgical method is being sought. Preliminary experiments indicate that a fractional crystallization from a solvent metal such as zinc seems to offer promise.

Melt refining of uranium is usually done in crucibles made of ceramic oxide. Accordingly considerable study has been made of the interaction of uranium and its alloys with such materials. A sessile drop method was utilized to determine which oxides were wet by molten uranium. Actual liquations were performed in crucibles of alumina, magnesia, thoria, beryllia and lime-stabilized zirconia to obtain quantitative data for the corrosion reactions. Tests were made in the temperature range 1200 to 1300°C. (The melting point of uranium is 1132°C.) The data show two categories of reaction mechanisms. Aluminum and magnesium oxides react with uranium to form a layer of uranium dioxide and nearly equivalent amounts of aluminum in uranium solution, or magnesium vapor, respectively. The oxides of thorium, beryllium and zirconium react by preferential diffusion of oxide ions to form an interfacial layer which builds up from the ceramic oxide interface.

Plutonium made in the blanket of a power breeder reactor will have to be concentrated with respect to uranium before it can be used in the reactor core. Molten magnesium extraction of the plutonium from molten uranium alloys and from uranium metal powdered by hydriding and dehydriding has been shown to be a rapid and effective means of effecting this concentration. The plutonium can then be separated from the magnesium by distillation.

Various pilot plant components have been constructed and tested for use in the EBR-II reprocessing cell. This cell will be shielded by massive walls and filled with a protective atmosphere of argon.

The pilot plant will include facilities for storage of irradiated fuel elements, furnaces for melt refining of fuel elements by oxide drossing, and equipment for magnesium extraction of plutonium from uranium, and subsequent distillation of magnesium to concentrate the plutonium. Also, facilities for purifying the cell atmosphere will be provided. Facilities for refabrication of the fuel will be included. Apparatus inside the cell will be operated remotely. A remotely operated uranium furnace has been constructed and tested (see Fig. 30).

When the jackets of EBR-II fuel pins are removed, a small amount of the sodium bond adheres to the surface. Experiments have shown that the oxygen concentration in the cell atmosphere should be less than twenty parts per million to prevent excessive corrosion of sodium-coated pins, which are at an elevated temperature resulting from heat liberated in the decay of the fission products. The indicated permissible concentration for nitrogen is about 5 per cent. It may be possible to maintain this concentration by purging from the cell atmosphere; however, if chemical removal of nitrogen is necessary, calcium at 600°C and sodium-activated calcium at 450°C have been shown to be effective for removing nitrogen.

When EBR-II fuel pins are melted, sodium adhering to the surface of the pins and certain fission products are volatilized. The sodium and condensible fission products (such as cesium and cadmium) will collect on cooler portions of the cell unless they are collected in the furnace. A number of materials of high surface area appear to be effective in trapping and retaining the condensibles. These include activated alumina, activated charcoal and "Molecular Sieves."

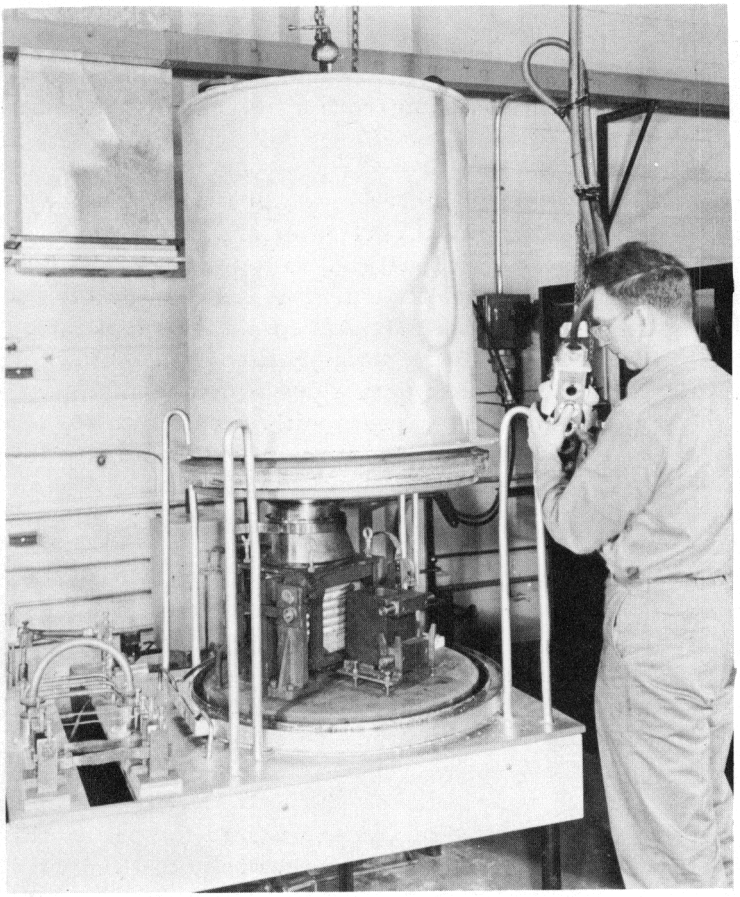

Fig. 30 A remotely operated furnace for the melting of uranium. The bell-jar cover is partially removed.

Synthetic alloys which are a close approximation to the anticipated composition of the fuel after many cycles in the reactor have been produced. These have been employed to test pyrometallurgical decontamination processes and to test the prototype equipment required for each stage in the fuel cycle. Irradiations of these alloys in the research reactor CP-5 under conditions simulating those anticipated in EBR-II have indicated that the stability of the fuel to irradiation damage is enhanced by the fission products which remain after processing.

Experimental Breeder Reactor-I

The EBR-I has been used for almost 5 years in an experimental program mostly devoted to the study of the physics of fast reactors. On November 29, 1955, during the course of an experiment on transient temperature coefficients in which the flow of the liquid metal coolant was deliberately stopped, the temperature of the fuel rose to a point where melting occurred. The fact that melting had occurred was established by the appearance of fission gases in the inert gas atmosphere of the reactor vessel some minutes after the transient, and by subsequent inspection of fuel elements which showed alloying of uranium and stainless steel.

Because of the resulting deformation of the fuel elements and the close clearances in the positioning and shield plates, it was not possible to remove them from the reactor in the normal manner. It thus became necessary to remove the reactor support structure from within the reactor tank and to cut off the fuel elements from below.

Since the elements were highly radioactive, a special temporary hot cell was constructed above the reactor tank. This cell was built with large portable shield blocks which were already on hand. The windows, lights, and manipulators were borrowed from existing facilities, and ventilation was provided by the use of a filter, building fan, and the high EBR stack.

The reactor core was removed from the structure with little difficulty. The outer rows of fuel rods were removed first, and then the extreme extent of the meltdown became evident (see Fig. 31).

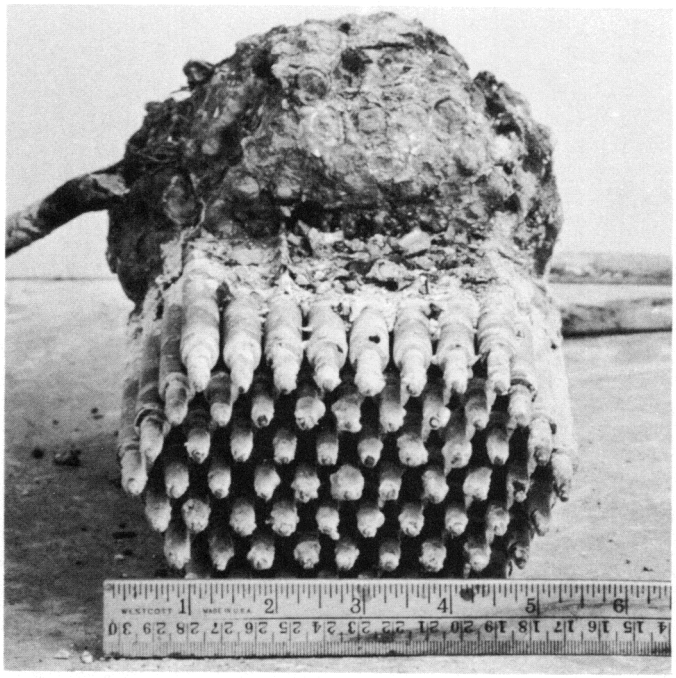

Fig. 31 A stage in the disassembly of the partially damaged core from EBR-I

At this point it was decided that the risk of fire was too great to proceed further in this manner. A thimble was placed around the remaining core rods and the space flooded with inert gas. The balance of the core was then removed as a unit by sawing off above the fuel and allowing it to drop into the thimble. This was then placed into a tight tank, which was filled with inert gas, and shipped to the Metallurgy Division of the Laboratory in a special coffin.

Final disassembly was accomplished in a special inert gas hot cell.

The temporary hot cell has been removed, the reactor's supporting structure placed in storage, and the reactor tank cleaned.

The next loading will be designated EBR-I, Mark-III, and will be used for further investigation of the instability of the reactor. By rebuilding the inner supporting structure, it will be possible to change the flow of coolant through the inner blanket and core to either parallel or series flow at will. This loading will be made as rigid as possible to eliminate bowing of the rods for the first series of tests and to allow bowing for the second series.

Instrumentation and some controls are being modified to provide a much better factor of safety in running the experiments so that another meltdown will not occur. Parts for the reactor are now being made, and a mock-up of fuel subassemblies will be made early in 1957.

A Coupled Fast Thermal Power Breeder

As part of the Laboratory's program of investigating new reactor types, a conceptual study was made of a power breeder reactor consisting of a fast assembly coupled to a thermal assembly. The aim was to obtain a system which combined the better features of each, such as the greater breeding ratio that is characteristic of fast assemblies and the relatively long neutron lifetimes in thermal assemblies. The essential problem in the design was to obtain sufficient coupling between the assemblies while at the same time introducing a barrier to isolate sufficiently the fast section from neutrons of thermal energy.

A system of some promise appeared to consist of a fast core surrounded by a natural uranium inner blanket which, in turn, is surrounded by moderator and, finally, by an outer blanket of depleted uranium. The inner blanket serves the multiple purposes of a core for the thermal system, of a barrier to the lower energy neutrons between the moderator and the fast core, and of a reflector for the fast core. The transition from a fast system to a coupled system basically involves only the replacement of some blanket material by moderator.

In order to gain experimental knowledge of the behavior of such coupled systems, and of fast reactors themselves, the Zero Power Reactor V (ZPR-V), known as the Half Fast Reactor, has been designed and constructed. In this facility (Fig. 32) the fissions necessary to sustain the nuclear chain reaction are caused in the central section by fast neutrons (ranging in energy from several kilovolts to several megavolts) and in the outer section by neutrons of thermal energies. The unmoderated central region consists of 35 volume per cent uranium, of 11 per cent iron (in the cans containing the uranium), and the rest of either sodium or "reduced density" aluminum to simulate sodium. The ratio of U^{238} to U^{235} can be varied from 3.1 to 7.1. The thermal fissions occur in an annular lattice of Al-U^{235} plates with water serving as moderator. A blanket of natural uranium of varying thickness is inserted between the unmoderated central region and the moderated annulus.

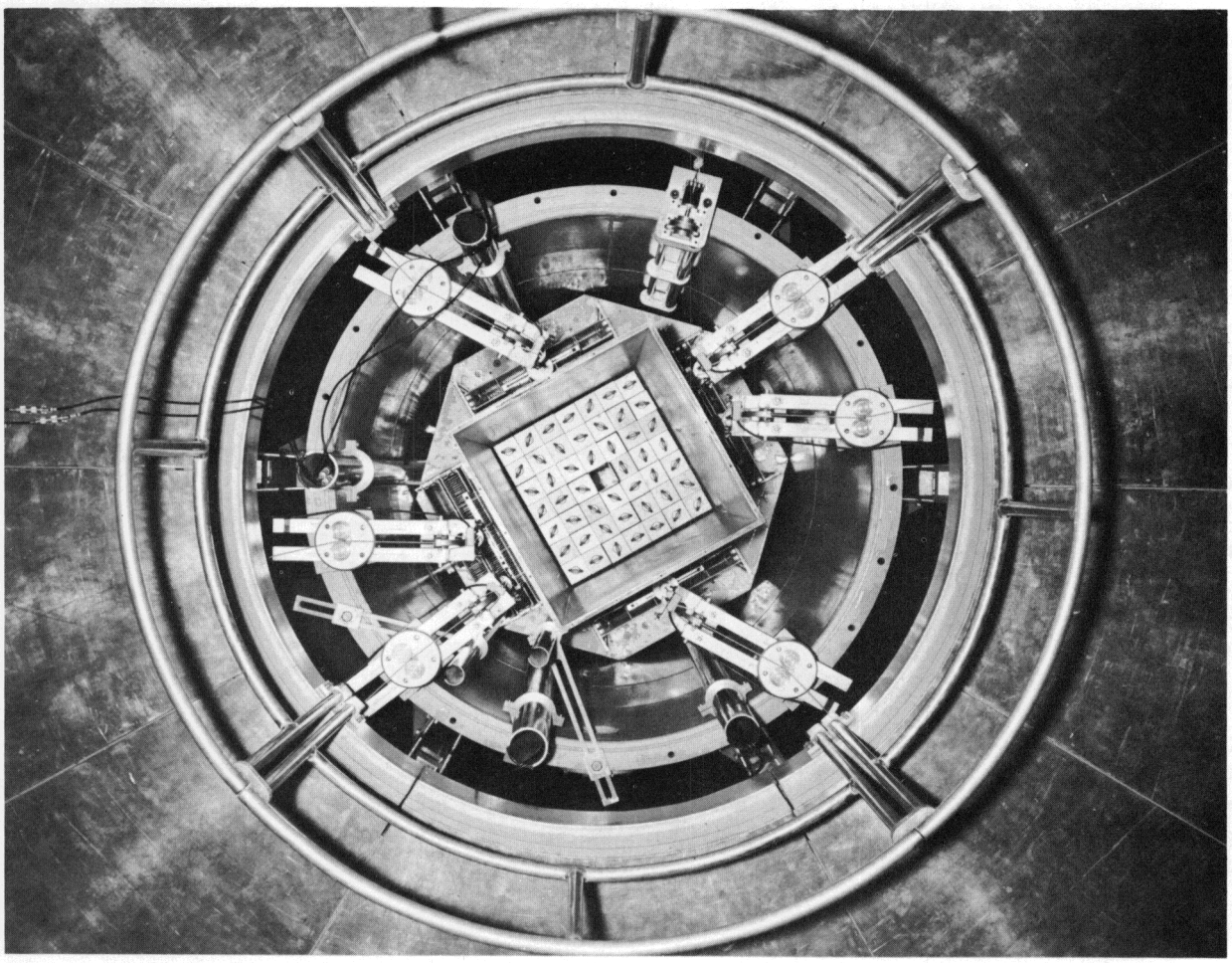

Fig. 32 First exponential loading of the "half-fast" reactor

The energy spectrum of the neutrons at the center of the reactor closely approximates that of a large fast breeder reactor, the range of composition of the core having been chosen to accomplish this. Thus, the experiments which depend only on the nature of this spectrum give the same results at the center of this reactor as at the center of an actual breeder, while the investment in fuel and the hazards of operation are greatly reduced.

NAVAL REACTOR PROGRAM

The Laboratory has terminated its participation in the Naval Reactor Program with the completion of a preliminary design study of a reactor plant cooled and moderated by an organic liquid for a fleet escort vessel. This study indicated that the low pressure requirements and lack of activation of the diphenyl coolant would result in significant savings of weight in comparison with a pressurized water plant. The less favorable heat transfer and the lower hydrogen density of diphenyl will require a somewhat larger reactor core. Indications are that make-up requirements due to the radiolytic breakdown of diphenyl will not place serious range limitations on such a vessel.

A concurrent experimental program verified the expected low corrosiveness and good lubricating properties of diphenyl. In over 4500 hours of static testing at temperatures up to 750F, uranium and high-uranium alloys showed considerably lower corrosion rates and no tendency toward catastrophic failure by comparison with their counterparts in high-temperature water. Corrosion of structural and cladding materials was, in general, equivalent to that of stainless steel in water.

THE RESEARCH REACTOR CP-5

Argonne's research reactor CP-5 has continued its impressive operational record in supporting work for all the scientific divisions of the Laboratory. All of the reactor facilities are used at capacity.

Originally operating with fuel in the form of aluminum-clad plates of uranium-aluminum alloy, a new loading of a cylindrical type of fuel assembly (Fig. 33) has been installed in CP-5. This assembly was developed to provide additional radiation facilities penetrating the reactor core and to provide further safety features permitting operation at power levels up to 4000 kw instead of at the 1000 kw level hitherto employed.

The fuel tube components of the assemblies were produced by a co-extrusion process which formed simultaneously the fuel section and its co-axial jacket with end closures all metallurgically bonded. The cylindrical shape of the assembly provides a generous axial cavity in which a vertical thimble can be installed for irradiating samples in high neutron fluxes especially rich in fast neutrons. Measurements of the thermal and fast neutron fluxes throughout the reactor core have given the values and distributions shown in Figs. 34 and 35.

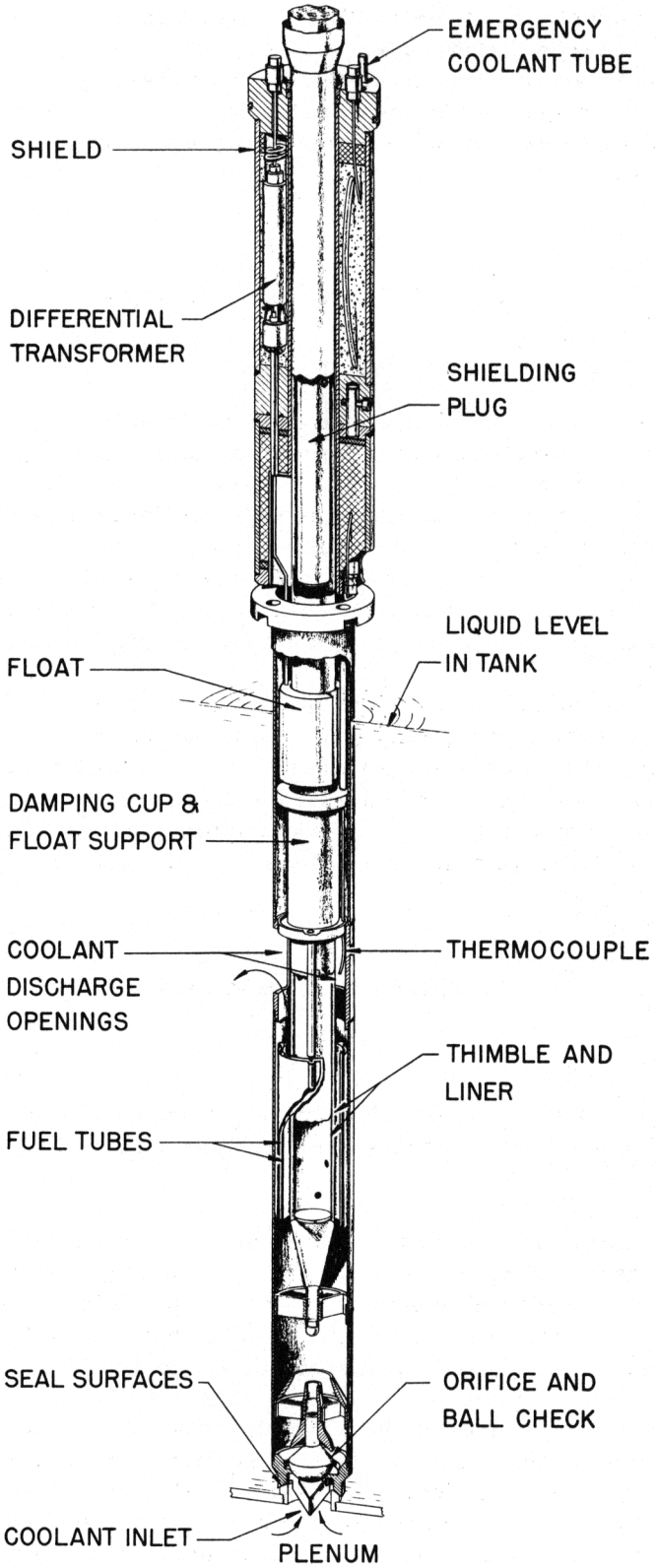

Fig. 33 A diagram of the new cylindrical type of fuel element now used in CP-5

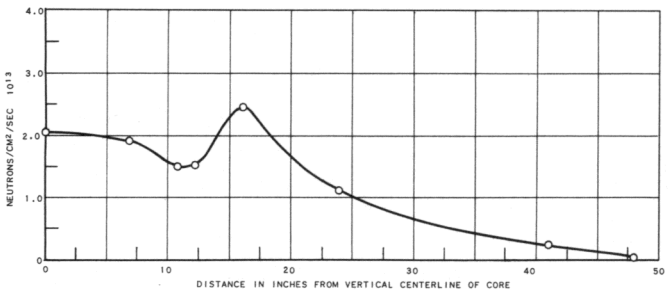

Fig. 34 Thermal neutron flux in CP-5 as measured with gold

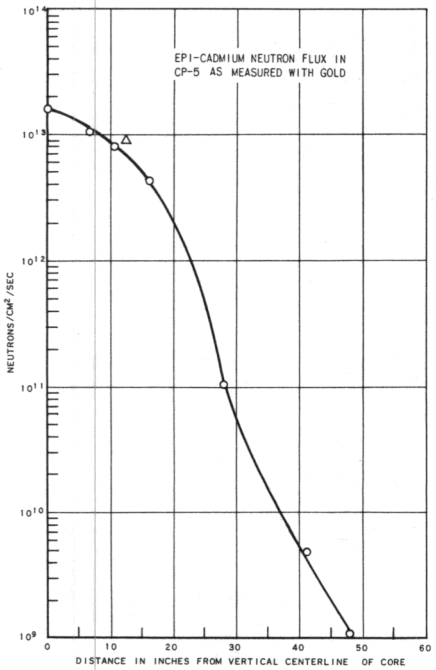

Fig. 35 Epi-cadmium neutron flux in CP-5 as measured with gold

A further improvement has been made by the addition of an emergency cooling system incorporated in the cylindrical fuel assembly. Cooling may now be supplied to the fuel assemblies for as long a time as necessary, even though the heavy water serving as moderator-coolant be lost from the reactor tank, whether deliberately or through some accident.

REACTOR DEVELOPMENT PROGRAMS

The Argonaut

The purpose of the Argonaut (Argonne Nuclear Assembly for University Training) project was to design a low-cost reactor with high flexibility for both training and reactor physics research. This has been achieved and the delivered price of $80,000 for the components seems well within the reach of the average engineering school.

The design and analysis of the system were facilitated by the construction and operation of a sub-critical assembly using parts identical with, or equivalent to, Argonaut components. By use of this experiment the static properties of the reactor

physics of Argonaut were verified and it was possible to adjust the design to avoid the effects from some minor surprises which were observed. All of this was accomplished without ever approaching criticality of the system to a close degree.

The reactor is thermal and heterogeneous, with an annular core of fuel, graphite and water, and with internal and external reflectors (Fig. 36). Moderation of the neutrons is provided by graphite segments between the fuel clusters and by water between the fuel plates within the clusters. The fuel is in the form of plates, similar in composition to those of the Geneva pool reactor, but with fabricating simplifications allowed by the less stringent thermal and irradiation requirements. The maximum flux is about 5×10^{11} neutrons per cm per sec at a power level of 10 kw, at which the heat generation is about 49 watts or 168 BTU per hour per plate. The critical loading is less than 3.6 kg of uranium-235. There are 17 horizontal experimental ports and five vertical ones.

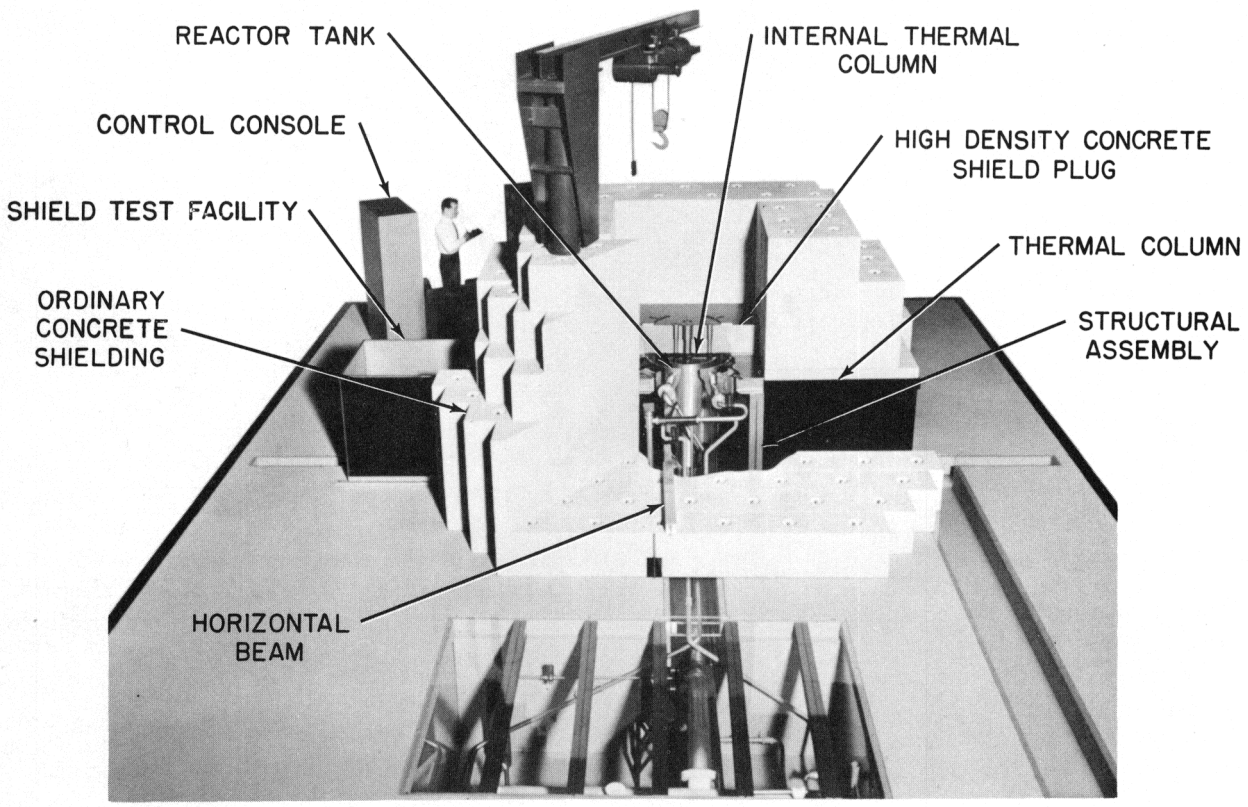

Fig. 36 Cutaway model of Argonaut reactor

The design has been developed on the "do-it-yourself" philosophy. A minimum of skilled help is needed for the erection and tryout. Argonaut is one of the "inherently safe" reactors. Experience at Argonne has been that an experimental physicist can be checked out as a pile operator after about four months of training; students working with an Argonaut can probably be trained in about four to six months, the time depending upon their skill.

A number of connected, smaller projects which owe their stimulus to the work done on, or for, Argonaut have been initiated and appear to be feasible for continued,

small scale effort. One such is the project, which incidentally evolved from the problems of design of the Argonaut's control rods, to develop general-purpose, rugged, and inexpensive control rod drives for application to critical experiments in general. Another of these side effects has been the application of the sub-critical multiplication experiment as a useful training facility in its own right, which may lead to proposing it as "the poor man's Argonaut." The International School of Nuclear Science and Engineering, located on the Argonne site, is cooperating in the design of just such a system.

The Mighty Mouse

Early in 1956 a study was initiated on the feasibility of providing the Laboratory with a research reactor of flux sufficiently high to constitute a new step in the development of such systems. Preliminary design specifications were necessarily vague, but the following general principles were adopted:

1. The reactor core should have a mean flux of about 10^{15} neutrons per cm^2 per sec.

2. There must be at least one experimental location where a flux as high as 5×10^{15} neutrons per cm per sec is attainable.

3. In case of conflict between users, preference was to be accorded in the design to those features making the system useful for pure research as opposed to materials development.

4. If at all possible, the reactor should have such a high degree of safety that the designers would be confident about recommending its location at the Argonne site.

While recognizing that these goals represent steps so large that nothing can be guaranteed, a design concept has been developed at the expenditure of about 15 man months of effort. This concept, known as "Mighty Mouse," is that of a 250-Mw CP-5 system. It appears that all the objectives are feasible and that a straightforward development effort without foreseeable snags may be expected to prove this within about a year. Changes from the CP-5 design have been drastic, but they seem practicable in view of the changed requirements:

1. A magnesium-base fuel element of large surface area is a highly desirable component. It will not corrode too badly according to present tests in water in which the pH is maintained at about 10.

2. In view of the lowered cost of heavy water and of the extensive research facilities which would be invested in such a system, the heavy water tank has been made appreciably larger and may end up with a diameter in excess of 13 feet.

3. In order to achieve a degree of safety comparable with that of CP-5 itself, it is desirable that the fission product content of the reactor should never exceed compositions which are orders of magnitude greater than found in CP-5. Consequently, a short operating cycle of 5 or 6 days, in which the fuel may be burned out to as much as 40% of its original loading, is contemplated. Amusingly enough, this cycle relaxes some of the limitations normally encountered with fuel cladding materials since short-term integrity seems more easily attainable than long term.

Questions of stability of the system with respect to power fluctuations (these could, in principle, lead to an oscillating xenon component of reactivity) have been examined. It appears that they can be controlled with a relatively modest control rod system. In order to have shim control during the extensive burnout of fuel, burnable poison is also specified. Boron appears to have good properties as far as large-scale smoothing out of reactivity is concerned, and cadmium (small quantities of which can be added to magnesium) has, at these fluxes, a burnout life comparable to the xenon build-up lifetime, thus offering a means for compensating for this quite appreciable effect.

In order to get some idea of what experimental facilities are desirable in such a reactor, appreciable time has been spent in discussions with potential users. Results of this survey have formed the main body of justification of the project and have guided the designer.

A few sidelights of the system contemplated are listed in order to illustrate how the purely quantitative aspects of the design flux may become qualitative ones. Thus, for a half hour after shutdown, delayed gamma-ray heating will produce thermal powers of several megawatts, making it virtually impossible to unload the system soon after shutdown except by transferring the fuel continuously through heavy water to another heavy water pot where it may be allowed to age. This aging fuel with its high gamma flux could be disassembled into several photoneutron sources, each having a strength of approximately 10^{12} neutrons per sec. Such sources could quite conceivably be used to supply thermal columns in which the availability of neutrons would be independent of the operation of a reactor. After further aging in such locations for about one week, the fuel elements could still be used as sources of extremely high flux gamma-irradiations while cooling for processing. Another illustration of the magnitude of the problem comes from the recognition that the flux at the 13-foot diameter tank wall is still in the neighborhood of 10^{14} neutrons per cm per sec.

ALPR

The design of the ALPR (Argonne Low Power Reactor) is a project which was undertaken at the request of the Army Reactors Branch of the AEC. It is a small boiling reactor power plant designed as a prototype of power plants suitable for operation in remote arctic regions. The plant will have a nominal capacity of 200 kw net electrical output plus a space-heating capacity equivalent to 400 kw.

The major equipment consists of a boiling light-water reactor operating at a 3-Mw power level, a condensing turbine-generator, and an air-cooled condenser. The design was guided especially by the so-called "Package Concept," which requires that all parts can be grouped into a minimum number of packages each of a size and weight practical for air transport.

The plant (Fig. 37) is to be housed in a three-story steel tank. The lower level of this tank will contain the reactor and its shielding material, which consists of gravel of local origin. The second level, the operating floor, will hold the turbine-generator and associated equipment. The third level will house the condenser and special equipment necessary to recirculate and maintain the proper temperature of the cooling air in view of the severe climatic conditions.

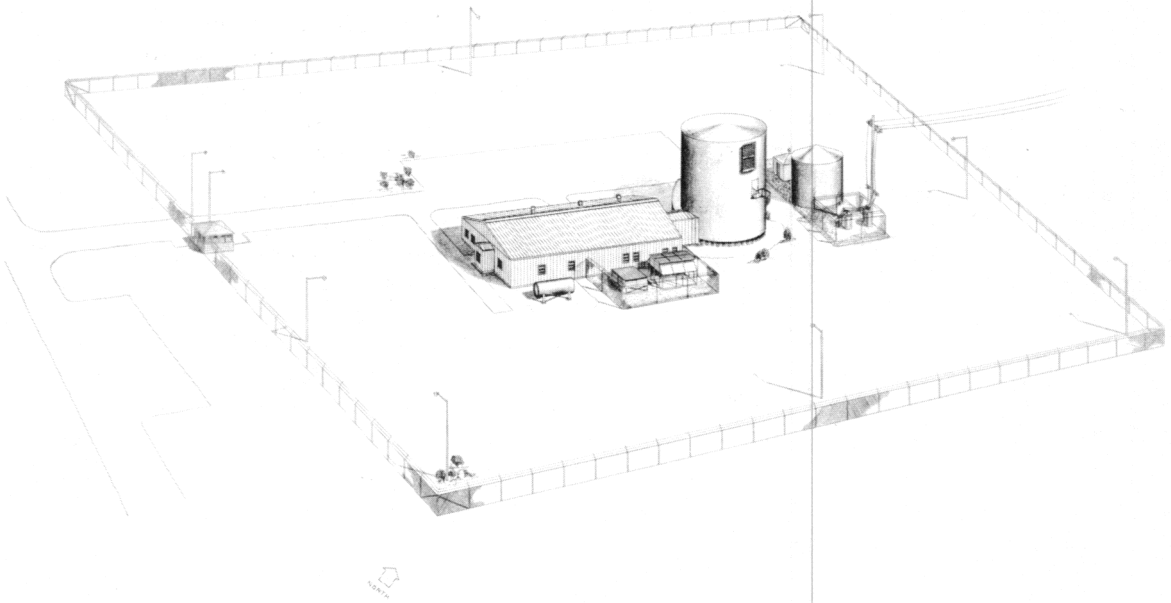

Fig. 37 A conception of the site planned for operation of ALPR

The building is supported in a manner simulating wood pile construction which may be used in case of future installations in the Tundra Region.

The prototype plant will be built at the National Reactor Testing Station in Idaho. Pioneer Service and Engineering Company is supplying the Architect-Engineering service for this project. Construction is expected to start in the middle of 1957. Various supporting facilities will be installed in connection with the prototype plant, particularly in regard to its use for testing purposes and for training of personnel.

BASIC PHYSICS INVESTIGATIONS

Fission Energetics

A knowledge of the prompt gamma rays accompanying fission is fundamental to a complete understanding of the fission process. Furthermore, since prompt emission constitutes a significant portion of the radiation emitted from a critical assembly, it is necessary to know the number and energy of the quanta in order to design the optimum shielding for such facilities.

Measurements of the fission energetics of Pu^{241}, Pu^{242}, Cm^{244}, and Cf^{252} have recently been completed. (It may be noted that the spontaneous fission of Cf^{252} has been shown, both theoretically and experimentally, to be similar to the neutron-induced fission of U^{235}. This gives an opportunity to study the fission phenomenon without complicating backgrounds.) Systematic trends have been noted on proceeding to isotopes with higher values of Z^2/A which are in qualitative agreement with the statistical theory of fission (see Fig. 38). It may be deduced that the energetics of fission are governed largely by Coulomb-surface forces. Quantitative agreement, however, is lacking.

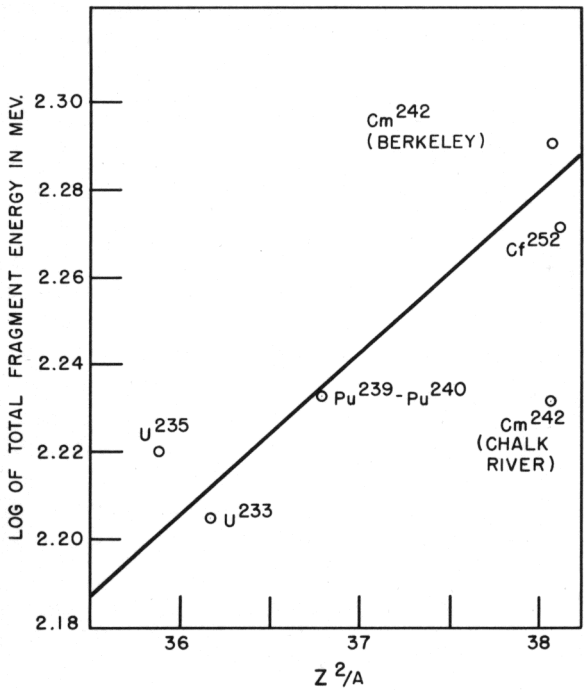

Fig. 38 Total fragment energies from the fission of even-even nuclei

A careful measurement of the photon spectrum accompanying fission has been made. Photons with a total energy of 8 Mev, considerably greater than had previously been measured or expected, are released at fission.

Calibration experiments have been performed to determine the fission yield of cesium-137 in the fast fission of various reactor fuels. Fast neutron fission yields of 6.87 per cent for uranium-235 and 7.45 per cent for plutonium-239 have been established. These yields are appreciably higher than those for thermal neutron fission of the same nuclides.

Neutron Lifetimes

An important characteristic of every reactor is the rate of increase of the power when the reactivity reaches prompt criticality. The period which is associated with this process is important in evaluating the safety of a reactor.

The measurement of the prompt reactor period cannot be done directly because of the hazard involved in bringing a reactor to prompt criticality. The determination must therefore follow an indirect route. The experiment which is known under the trade name of the "Rossi alpha" experiment is an example of such an approach.

During the Rossi alpha measurement the reactor is held at delayed criticality. This means that the neutron economy of the reactor is balanced only when the neutron bonus arising from the delayed neutrons following fission is taken into account. The prompt neutron excess appearing immediately upon fission does not suffice to balance the loss from neutron absorption or neutron leakage across the reactor boundaries. A reactor which is in this delayed critical condition will remain steadily at a given power level. The time scale on which the fission process occurs is extremely short compared with the time scale on which the appearance of the delayed neutrons is measured. Thus, within the very short interval in which a fission process occurs and the resulting neutron multiplies in another fission or disappears in an absorption or leakage process, the delayed neutron associated with the fission plays no part, and the pile acts as if it were instantaneously subcritical. The measurement of the time decay of the neutron population engendered by some ancestral neutron will give immediately the information from which the prompt pile period may be calculated. Since the pile is, for such an experiment, never brought above delayed criticality, the prompt period measurement may be carried out with no hazard involved.

In the actual measurement the abundance of the instantaneous neutron population is assumed to be proportional to the probability of detecting a neutron at a given point in the reactor. The decay of the instantaneous counting rate is measured as a function of time after the initial fission event occurred in the reactor. The procedure is a statistical one and care must be taken to emphasize the significant counts above the random noise generated in the reactor.

The measurement of the prompt e-folding time of a number of assemblies has resulted in a value of 0.6×10^{-6} sec for a mockup of the EBR. This implies that a neutron spends, on the average, 4.3×10^{-8} sec between birth by fission and death by absorption or leakage.

The Doppler Temperature Effect

The Doppler reactivity coefficient has been measured for uranium-238 and uranium-235 for a reactor of the EBR-I type. The Doppler temperature effect is a well-known phenomenon which arises from the broadening of neutron resonance levels due to thermal motion of the uranium nucleus. The measurement of this effect is important in the design of reactors since it may make a large contribution to the prompt temperature coefficient of a reactor. The Doppler reactivity coefficient may be calculated for thermal reactors; however, there is considerable uncertainty in the estimates for a fast reactor. This is a result of the uncertainties in the parameters of the resonance levels and their distributions in the region of a few hundred kiloelectron volts. The uncertainty in the theoretical estimates made desirable an experimental integral measurement of the Doppler effect to determine its magnitude and sign.

Fully enriched and natural uranium elements of helical shape were thermally cycled over a temperature range of about 120°C in an EBR-I mockup in the ZPR-III fast critical facility (described in the last Annual Report). The small changes in reactivity obtained by the thermal cycling of these elements were measured using a resonant amplifier tuned to the thermocycling frequency. It was necessary to use pile oscillation techniques in order to measure the small changes of neutron flux which resulted. Analysis of the data indicated that the Doppler reactivity coefficient for uranium-235 for an EBR-I type assembly is no greater than $1.2 \times 10^{-6} \Delta k/k$ per °C at 20°C. This value is considerably less than had been given by the early estimates from theoretical considerations.

Reactor Physics Constants Center

In 1956 a Reactor Physics Constants Center was formed for the purpose of identifying and publishing those constants which could be used in reactor physics calculations to determine the design and performance of neutron systems (both reactors and integral experiments). The initial work has been the collection of data concerned with thermal diffusion. In the course of this investigation it became apparent that no reasonably small number of constants could be used to characterize thermal diffusion except by previous specification of the thermal neutron spectrum of a system in suitable simple form.

The Constants Center stands ready to provide critical analysis of fundamental experiments whose performance significantly improves the nature of our understanding of reactor processes. To this end it has contracted to do the analytical and theoretical work connected with a tripartite program (United Kingdom-United States-Canada) to determine the spatial and spectral scattering law for neutrons at thermal and nearly thermal energies in moderators.

Finally, in fulfillment of its stated purpose of publishing standard information, the Constants Center will collect and publish as reasonable a compendium of the constants outlined in its prospectus as can be obtained within the limits of its own manpower. While it is expected that such a compendium will undergo drastic revision, it is hoped that it will at least serve the purpose of stimulating those workers in the field who have

good data to communicate them in properly analyzed form to the Center so that succeeding editions may become increasingly reliable.

SUPPORTING RESEARCH AND DEVELOPMENT

Heat Transfer Studies

During 1956 heat transfer work with water was devoted to the analysis of data from two 600-psi experimental systems to provide design data for boiling reactors and to further the understanding of the fundamentals of natural circulation boiling. As a result of these tests, a method has been developed for calculating the relationship between the volume fraction of steam in the core of a boiling reactor and the steam rate from the core.

An evaluation of available information on heat transfer, supplemented by studies of flow friction carried on at the Laboratory, has shown that a matrix of crossed wires is a promising geometry for an arrangement of fuel elements. On the basis of heat transfer power obtained per pumping power expended, a staggered crossed-wire matrix is preferred to an in-line arrangement and shows significant advantage over plate-type elements. For certain reactor applications, the optimum heat transfer design results in a one-pass core arrangement which also meets the nuclear dimensional requirements of about equal height and diameter.

Control Rod Drive Development

The control rod drive developed for the Experimental Boiling Water Reactor uses an external lead screw and nut type that drives a reciprocating extension rod through a linear or axial pressure breakdown seal. This unit met all the requirements for positionability, speed regulation, scram speed, position indication, reliability, and serviceability. It is adaptable for strokes up to six feet and pressures up to 1200 psi. For the EBWR, nine such mechanisms, designed for operation at 600 psi pressure with a four-foot stroke, were produced in the Argonne shops, tested individually, and installed and operated satisfactorily on the reactor.

Alternate drives developed for the EBWR were of the hydraulic and electromagnetic jack types. The hydraulic drive was based on the rotameter principle, wherein the control rod is attached to a piston which moves in a cylinder with tapered bore. Water flows upward continuously past the piston and the pressure differential across the piston develops the thrust required to support the control rod. Good positionability and position indication are achieved. However, the external hydraulic control system required was complicated and of questionable reliability.

In the control rod drive mechanism utilizing an electromagnetic jack, the rod is moved stepwise upward or downward, or held in a given position, by magnetic forces set up by a series of coils surrounding a tube containing an extension of the rod. Motion is achieved by energizing and de-energizing the various coils in a given sequence. The rod may be scrammed by cutting off all power to the coils. This drive has shown great promise in full-scale tests. A satisfactory method of position indication is under development.

The Plutonium Metallurgy Research Laboratory

The only existing, large, plutonium handling facility that has used successfully a closed, inert atmosphere with leak-tight gloveboxes is the Plutonium Metallurgy Research Laboratory at Argonne. It has been designed to handle any highly intense alpha-particle emitter which may be pyrophoric.

Operation of this facility for more than a year has demonstrated the feasibility of this approach and has emphasized several real advantages, especially in safety. No plutonium contamination has escaped from the boxes, so that personnel have never been exposed to high air counts, which is, to our knowledge, an unmatched record for work in this field.

The main purpose of this Laboratory is to develop and study fuel-element alloys containing plutonium or other alpha emitters. The Laboratory is fairly complete and diversified. It is equipped to study phase diagrams and has facilities for melting and casting, as well as for thermal analysis, dilatometry and metallography. Equipment is available to study workability (rolling, pressing, extruding), machinability, heat treatability, and corrosion characteristics. It is also equipped to study tensile and hardness properties, expansion characteristics, and thermal and electrical conductivity. In addition, the Laboratory has been called upon to make numerous test pieces for exponential, critical, and irradiation experiments.

The design of this research laboratory was governed by several restricting factors. The available room was only 27 feet by 30 feet. Special facilities that require low air counts were to be located in adjacent rooms. Argonne is located near populous areas, requiring careful control of the amount of contamination in waste gases. Since this was to be a research facility, it seemed desirable to study the advantages and disadvantages of an inert atmosphere from the points of view of maintenance and cost, the influence on metallurgical research, and aspects of safety. Also, it was desired to study various approaches to glovebox and accessory construction as well as to operating techniques, so that the experience gained could be applied to the design of a much larger facility for fabricating fuel elements.

Stainless steel gloveboxes with specially designed gasket flanges for windows and interbox connections were developed to achieve the desired tightness with respect to leakage of helium (Fig. 39). Space limitations precluded the use of a transfer corridor; to transfer objects through the system they must be passed from glove to glove. Transfer doors to the room are provided at strategic points in the system to permit replacement of even the largest equipment by special plastic-pouch transfer techniques.

The inert atmosphere of helium is slowly circulated in a closed system through copper plumbing to a regenerative-type adsorption purification system and then back to the boxes. Pressure in the boxes is maintained at values slightly less than atmospheric by a quickly acting vacuum-pressure system. In addition, a safety exhaust system automatically acts in the event that a leak develops in the system or that the controls do not function properly. Groups of gloveboxes can be isolated from each other so that leaks in one part of the system need not cause shutdown of the entire system.

A large-scale facility for developing the technology of fabricating plutonium is under construction at Argonne and is expected to be completed in 1957. It has been designed on the basis of the same principles which have been demonstrated in the operation of the Plutonium Metallurgy Research Laboratory.

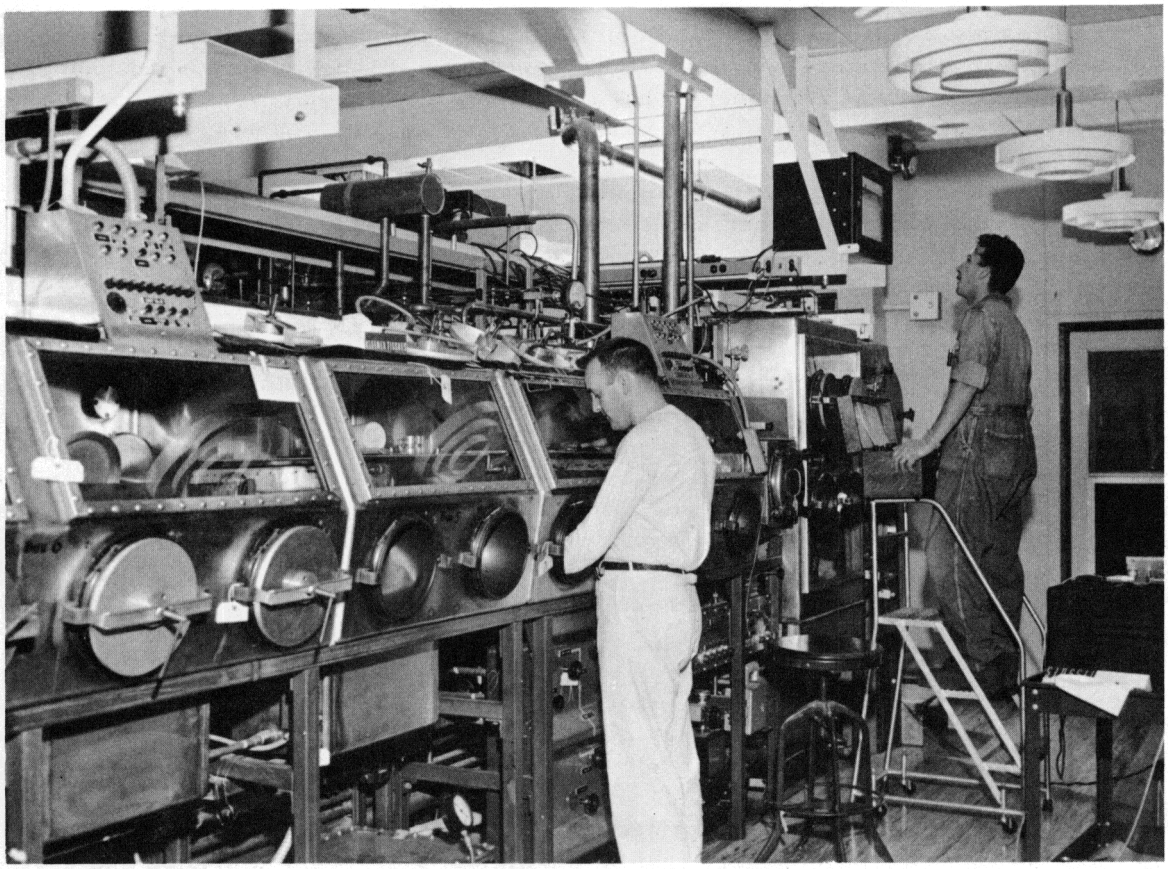

Fig. 39 A portion of the plutonium metallurgy research laboratory

Multi-Crucible Furnace

Melts of the refractory group of metals must be made in vacuum to prevent atmospheric contamination of the metal. Studies of alloy systems often require the making of numerous small melts which are exactly similar except for one variable, such as small changes in the proportion of one element. A multi-crucible arc melting furnace (Fig. 40) has been constructed which permits casting seven small size melts in a single loading. By the use of the multiple furnace, the repetitive work is much reduced, since many melts can be made with but a single evacuation.

Studies of Dispersion and Coalescence

An understanding of the fundamentals of the processes of dispersion and coalescence in immiscible liquid systems will aid in the design of equipment for solvent-extraction processes. Two methods of measuring the interfacial area in such immiscible liquids have been developed. The first, a photographic technique, is used as a basic standard. This method is accurate but tedious and time consuming. A more rapid method of measuring interfacial area indirectly by obtaining a measure of the transmittance of light through a known path length of emulsion has been worked out.

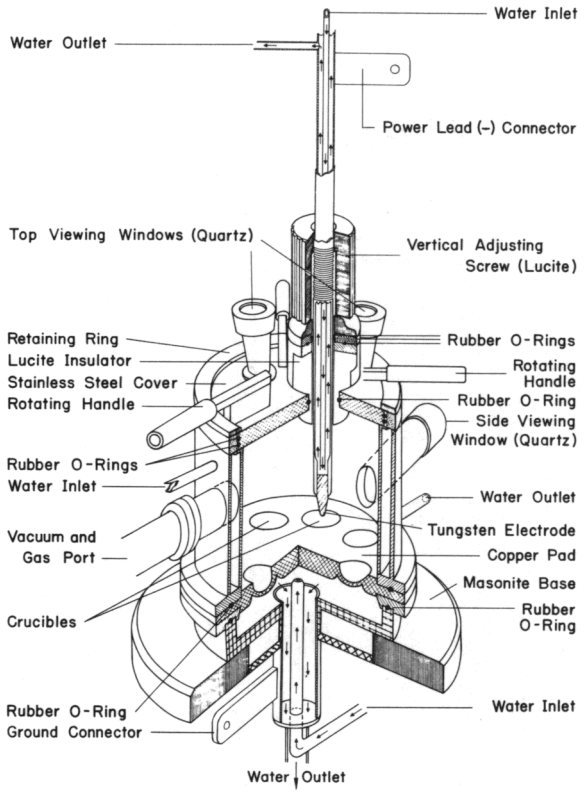

Fig. 40 Multi-crucible arc melting furnace

The correlation of interfacial area with energy input and physical properties gives a measure of the interfacial area as a function of the Weber number, which is a measure of the ratio of turbulent forces to surface forces.

Metal Oxidation and Ignition

The increased use of nuclear reactors with the accompanying handling of reactive metals such as uranium, thorium, zirconium and plutonium makes it imperative to understand the factors which influence their pyrophoric properties. In order to clarify these factors, a study of the oxidation characteristics of these metals has been undertaken. Experiments with uranium have shown that at an oxygen pressure of 200 mm and at temperatures ranging from 150° to 325°C, the oxidation occurs in two stages - a slow, but constant, rate which is followed by a more rapid one; both rates are dependent upon the temperature. The dependence of the reaction upon pressure has been studied from 20 to 800 mm and from 150° to 250°C. Comparison of the rates during the more rapid stage shows essentially negligible pressure dependence at 150°C; at 200°C there is a small effect; at 250°C the effect is more pronounced. Preliminary tests on the oxidation of zirconium have been made.

Fluidization Processes

As reported in the last Annual Report, the unit operation of fluidization is being studied in connection with the fluidization pilot plant for continuous calcination of uranyl nitrate to uranium trioxide, hydrogen reduction of uranium trioxide to uranium dioxide and hydrofluorination of uranium dioxide to uranium tetrafluoride (green salt). Studies have also been made on the fundamental characteristics of fluidized solids. A shielded and remotely operated pilot plant has been designed and is under construction for demonstrating the use of a fluidized bed method to continuously calcine radioactive waste solutions.

The contemplated green salt process has been previously described. Runs have been made in bench-scale equipment with six different ore concentrates, one foreign and five domestic, to test the processes of reduction by hydrogen and of hydrofluorination. A satisfactory conversion to crude green salt was obtained in both batch and continuous fluidized-bed runs.

Small-scale equipment has been developed and tested for all steps of the green salt process. These data have been extended to a pilot-scale green salt plant which has been constructed and is now undergoing "shakedown" runs. This equipment is shown in Fig. 41 and in the schematic diagram in Fig. 42. Uranium trioxide from the existing denitration reactor is fed to the top of the 4-stage stainless steel reduction column.

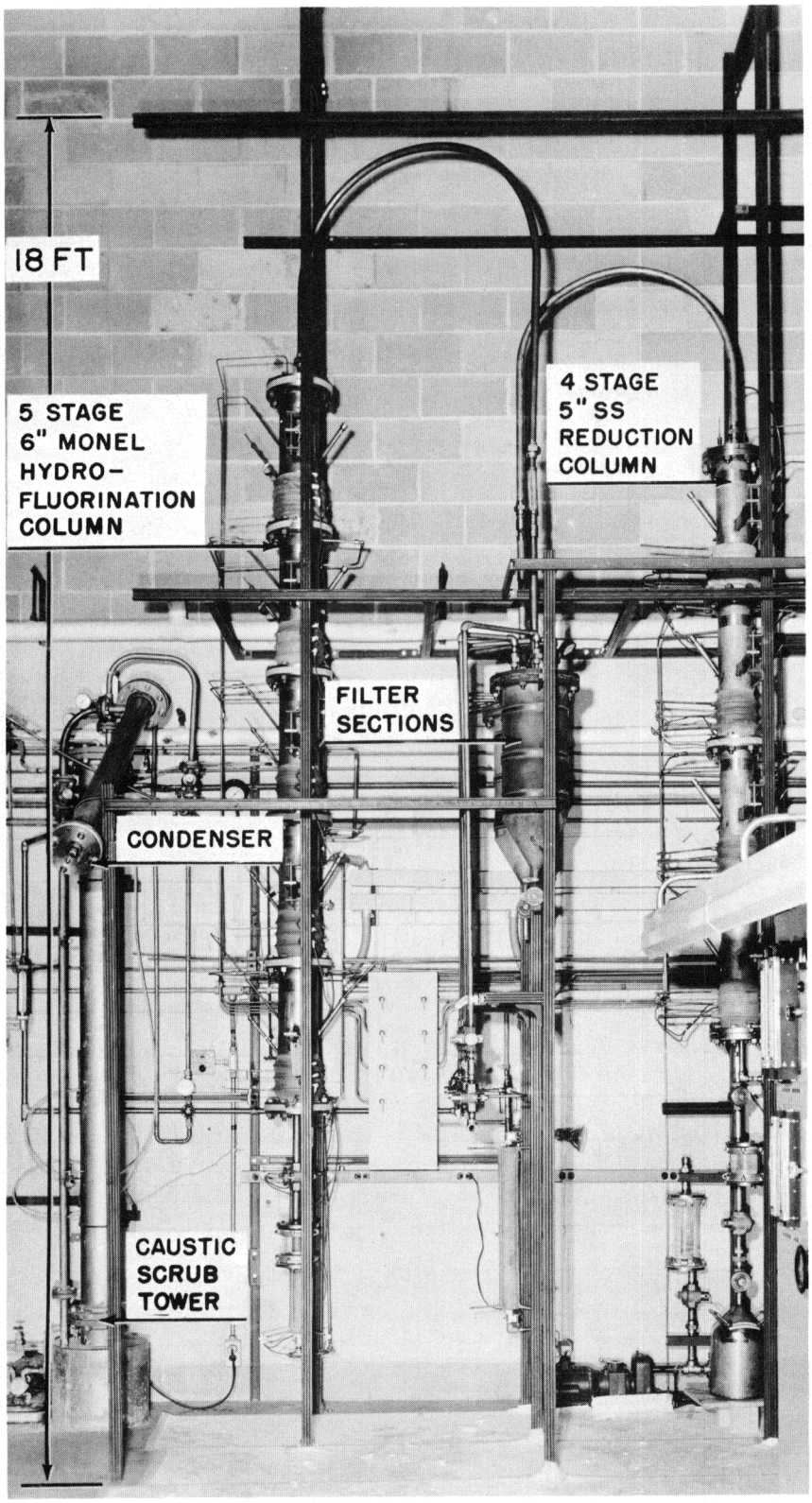

Fig. 41 Multi-stage fluidized bed pilot plant for production of green salt (UF_4)

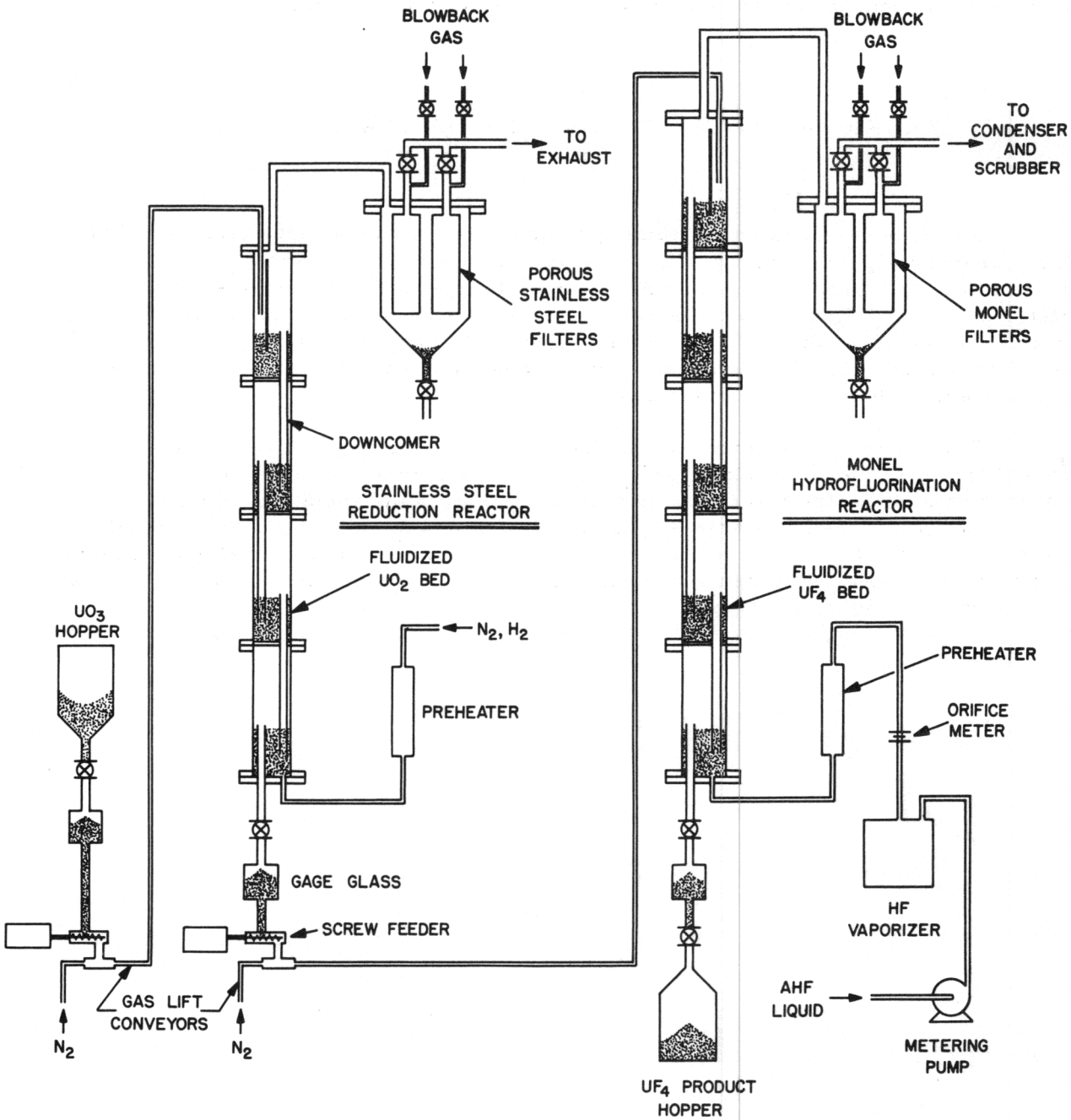

Fig. 42 Schematic diagram of fluidized-bed

Multistage operation permits each stage to be operated at a different temperature and thus permits a higher efficiency through a closer approach to countercurrent operation. The product overflows into a standpipe from which it is fed by a screw feeder to a gas lift, transporting it to the top of the 5-stage Monel hydrofluorination reactor. The green salt is recovered at the bottom of the hydrofluorination column.

THE ARGONNE HIGH-LEVEL GAMMA-IRRADIATION FACILITY

The Laboratory is now operating a High-Level Gamma-Irradiation Facility for research purposes. This facility is available to Argonne personnel and also to outside research organizations. Fission products in spent fuel elements from the Materials Testing Reactor provide the source of gamma rays. A gamma flux of one to two million roentgens per hour is maintained. A canal-type facility makes use of water as a shield for radiation protection, as a coolant for fuel elements and as a transparent medium for observing experiments.

The general arrangement of the facility is shown in Fig. 43. An irradiation rack, containing the radioactive fuel elements, is located on the floor of a canal and covered with sufficient water to protect personnel from the radiation. Materials to be irradiated are sealed in water-tight, thin-walled aluminum urns. The original rack was designed with spaces for 12 urns, $4\frac{1}{8}$ inches in diameter and 28 inches high. A new rack has been designed and constructed which accommodates an urn 20 inches in diameter and 30 inches high.

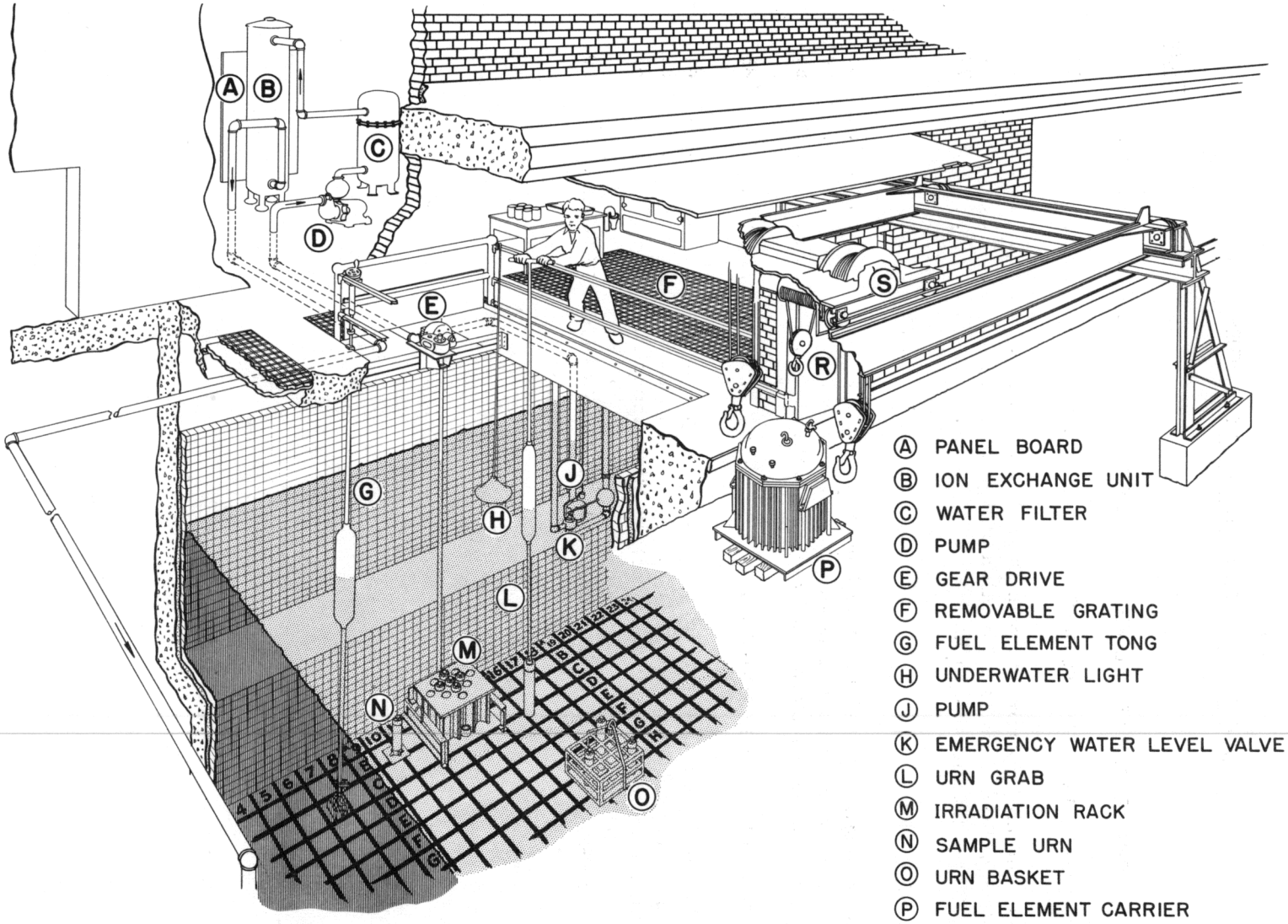

Fig. 43 The Argonne high-level gamma-irradiation facility

PART III

BIOLOGICAL AND MEDICAL SCIENCES

	Page
CONTROL OF DISEASE IN ANIMAL EXPERIMENTS	71
TOXICITY AND METABOLISM STUDIES	72
Radiostrontium Experiments with Dogs	72
Retention of Strontium as a Function of Age	77
Heavy Water Intoxication in Rats	77
BASIC BIOCHEMISTRY	80
Transmethylation and Methionine Metabolism	80
Nucleic Acid and Protein Metabolism	82
Complexes between Metals and Organic Anions	84
INSTRUMENTATION AND TECHNIQUES	85
Liquid Scintillation Counting	85
Multiple Tracer Techniques	87
Fine Structure Studies with the Electron Microscope	88
CANCER AS A SPECIAL CASE OF A GENERAL DEGENERATION PROCESS	90

CONTROL OF DISEASE IN ANIMAL EXPERIMENTS

The primary concern of the Division of Biological and Medical Research is the study of the effects of radiations on living things. It should be apparent that radiation exposures must be standardized if meaningful and reproducible data are to be obtained. It is perhaps not so obvious, however, that the other materials taking part in the experiment -- the living materials -- must also be standardized. This is particularly true where small changes must be evaluated, as in low-dose experiments.

The number of variables in living material is, of course, incalculable; however, several important sources of variation in biological experiments can be controlled. Individual differences can be minimized by using inbred strains which are almost completely homogeneous genetically. Other obvious differences -- age, sex, and weight or size of animals -- are usually taken into account in planning experiments. Because the environment has been recognized as an important source of variation in the responses of experimental animals, animal quarters are usually designed to provide constant temperatures, humidities, and lighting. Similarly, to minimize variations in nutritional status, standardized diets are used.

Until recently, another important source of variation, disease, has received less attention. Ideally, animals should be purchased only from disease-free colonies. A few such colonies have been established on an experimental basis. At present, however, disease-free animals are not commercially available. It is therefore reasonably safe to assume that all experimental animals harbor some sort of infection or infestation unless extraordinary precautions are taken. Many apparently healthy animals carry latent infections which may become overt when the animals are subjected to the stress of experimental procedures such as irradiation. In addition, experimental animals may, and frequently do, differ from group to group or even from cage to cage with respect to the specific disease or diseases present.

The use of large populations of randomly selected animals and the statistical treatment of the resultant data tends to minimize the variations caused by disease. However, not only are such procedures both expensive and time-consuming, but it is only necessary to consider a few examples to understand why they are also inadequate. The injection of a radioisotope into an animal may cause certain physiological or pathological changes; a disease may cause similar changes. Unless the confusing or nullifying effects of disease have been eliminated, the cause of the lesions found in an experimental animal at necropsy cannot be known with certainty. Perhaps more important is the effect of disease on the long-term radiation and cancer studies conducted at this Laboratory. For example, suppose that the administration of an isotope is followed in 12 to 18 months by the development of bone tumors. If a respiratory infection kills the experimental animals before they are one year old, the results of the experiment with respect to incidence of tumor development will be lost -- representing often a considerable loss of time and money.

The problem of disease control in the Bio-Med animal colony was approached by studying the disease conditions one by one, beginning with the most serious, with the aim of finding a specific means of control (prevention or cure) for each. Since it appeared that the most serious immediate problem was ectoparasitic skin conditions among the mice used in long-term experiments, this problem was studied first. The affected animals included thousands of mice injected with Sr^{90} or other isotopes, or exposed to external radiation, and maintained for the duration of their lives in order to

study survival or late effects such as tumor development. The mice displayed sparse, coarse, grayish-white hair, whitish skin, and large areas of self-inflicted lacerations. This condition interfered with the evaluation of radiation effects and quite possibly shortened the life span.

Because the literature contained very little reliable information on external parasites of laboratory animals, mice were obtained from several commercial sources and examined carefully to determine the incidence of infestation, the species, and the specific pathology attributable to each. Five species of mites were identified, including one species not previously reported in this country and three species not hitherto found on laboratory mice. The relative effectivenesses of the commercially available acaricides and insecticides were then determined in controlled experiments. Preliminary screening experiments indicated that only one, Aramite,* was capable of killing the ectoparasites without injuring the host. More tests established that three weekly treatments with Aramite resulted in the complete disappearance of the mites and in the healing of the associated lesions (see Fig. 44). It was established in further experiments that Aramite as used was non-toxic and that it did not increase the lethality of X irradiation. This control procedure is now used routinely in the Bio-Med animal colony, and many other institutions and commercial supply houses have already adopted it.

The treatment was also tested here to determine its effectiveness in the control of dog mange, a problem of some importance to pet owners and dog breeders if not to most biological laboratories. Advanced follicular mange (mites living in hair follicles) until now has been considered incurable. The mouse experiments had indicated that Aramite was effective against the mite Psorergates simplex (see Fig. 45), which causes follicular mange of mice. Therefore the agent was used to treat four dogs with severe cases of mange, at least two of which were infested with the follicular mite Demodex canis. All four cases were cured; four months later no mites can be demonstrated, there are no active lesions, the hair has a normal appearance, and has resumed normal growth except in badly scarred areas (see Fig. 46).

These results represent only the first step in a long-range program. They are important because a specific disease condition has been eliminated, and also because we now have the opportunity to demonstrate the value of disease control in biological experimentation.

TOXICITY AND METABOLISM STUDIES

Radiostrontium Experiments with Dogs

Our interest in the effects of radiostrontium on dogs is prompted, of course, by the major importance of Sr^{90} in the fallout spectrum. This element is deposited in the skeleton, and, as with other bone-seeking radioelements such as radium, the ultimate effect of appropriate doses acting over a long period of time is the induction of bone tumors. In order to determine the lower limit of the range of carcinogenic doses of radiostrontium, we must resort to experimental animals. The information gained from such experiments, coupled with similar radium studies, can be used as a basis for extrapolation to man. This is true because a great deal is known about the radium poisoning of humans; radium was used therapeutically 20 to 30 years ago and many

*2-(p-tert-butylphenoxy) isopropyl-2-chloroethyl sulphite. (Naugatuck Chemical Company)

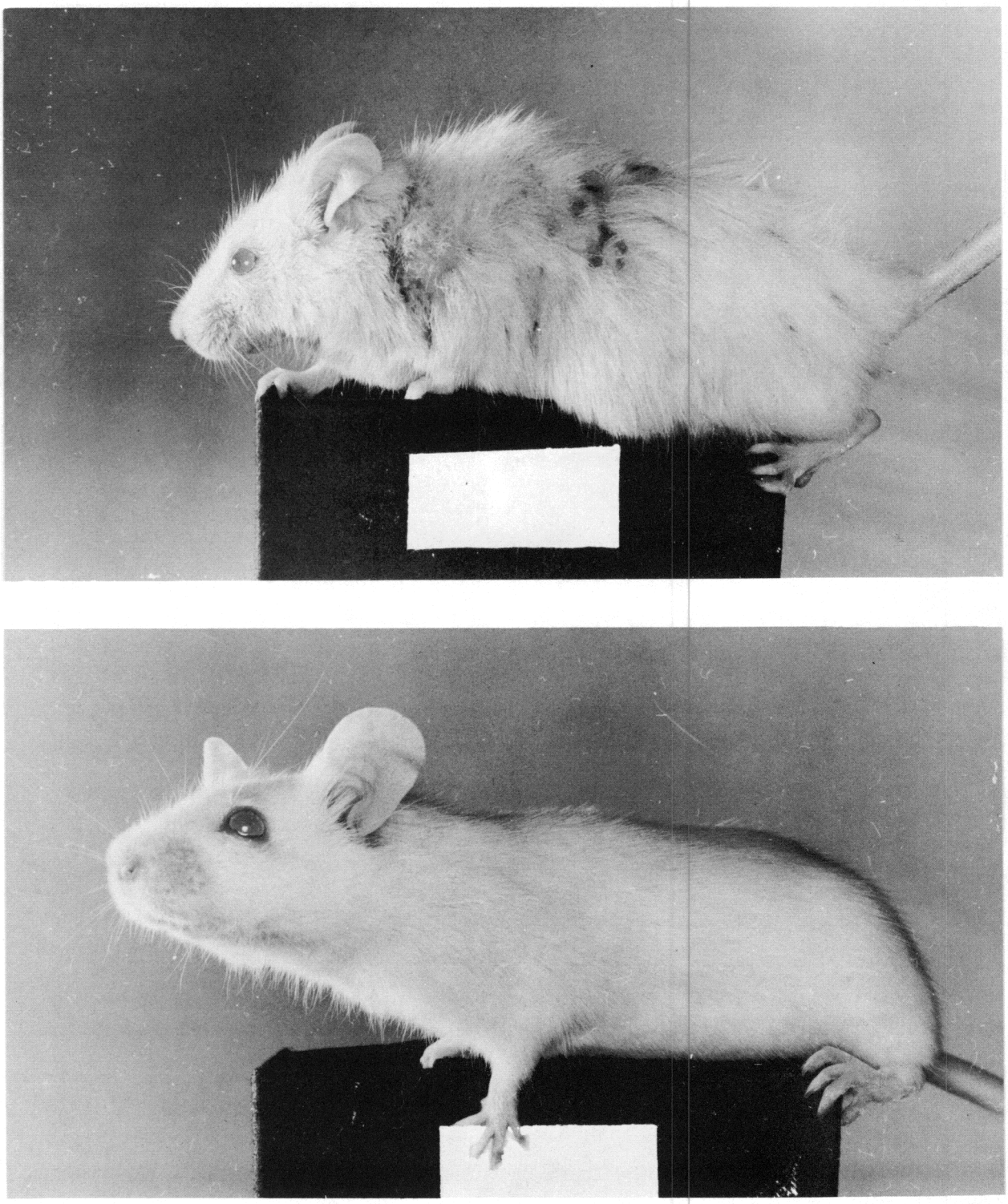

Fig. 44. Upper: untreated 18-month-old female mouse (CF No. 1 strain); lower: treated mouse of same age, sex, and strain.

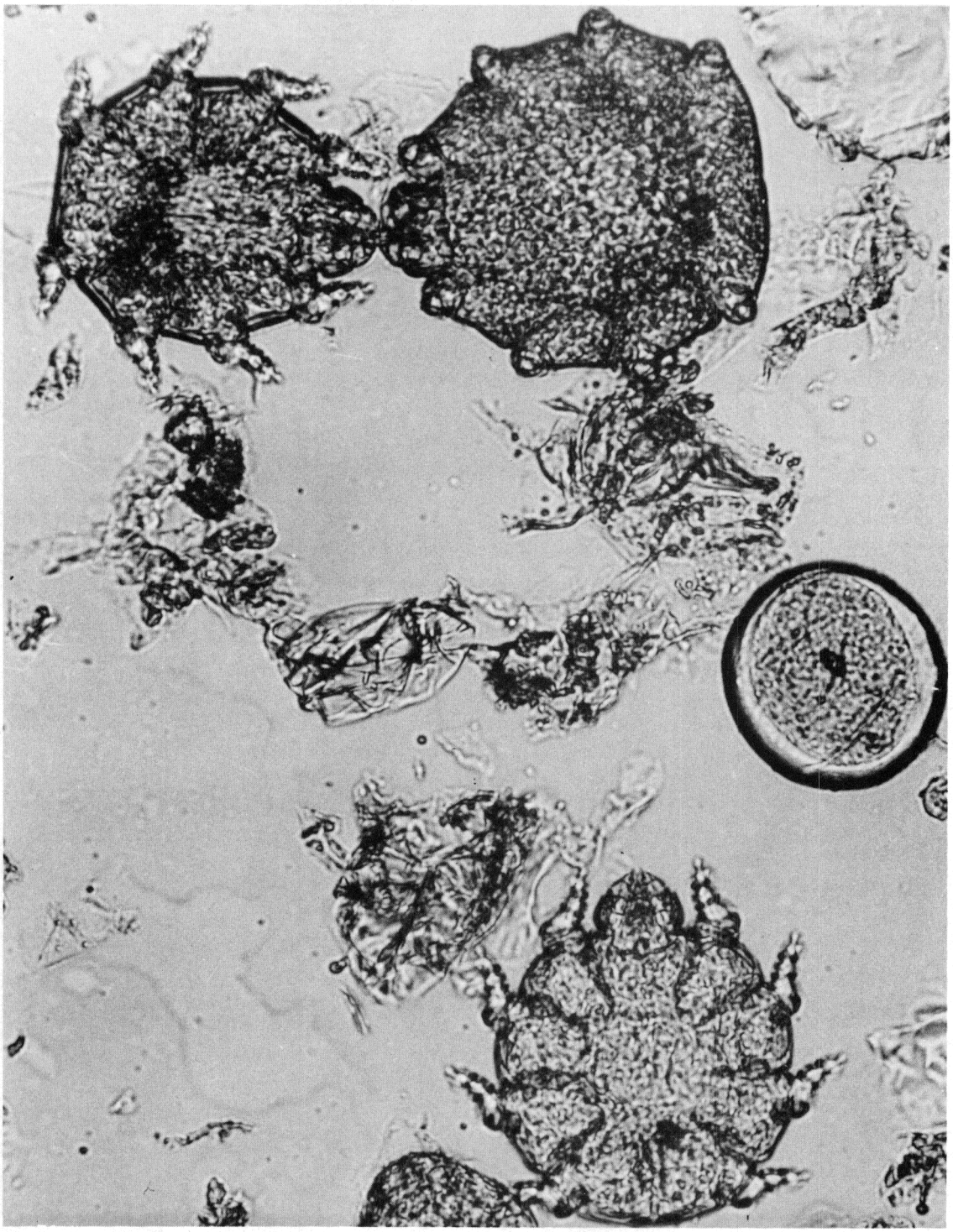

Fig. 45. Mite family (Psorergates).

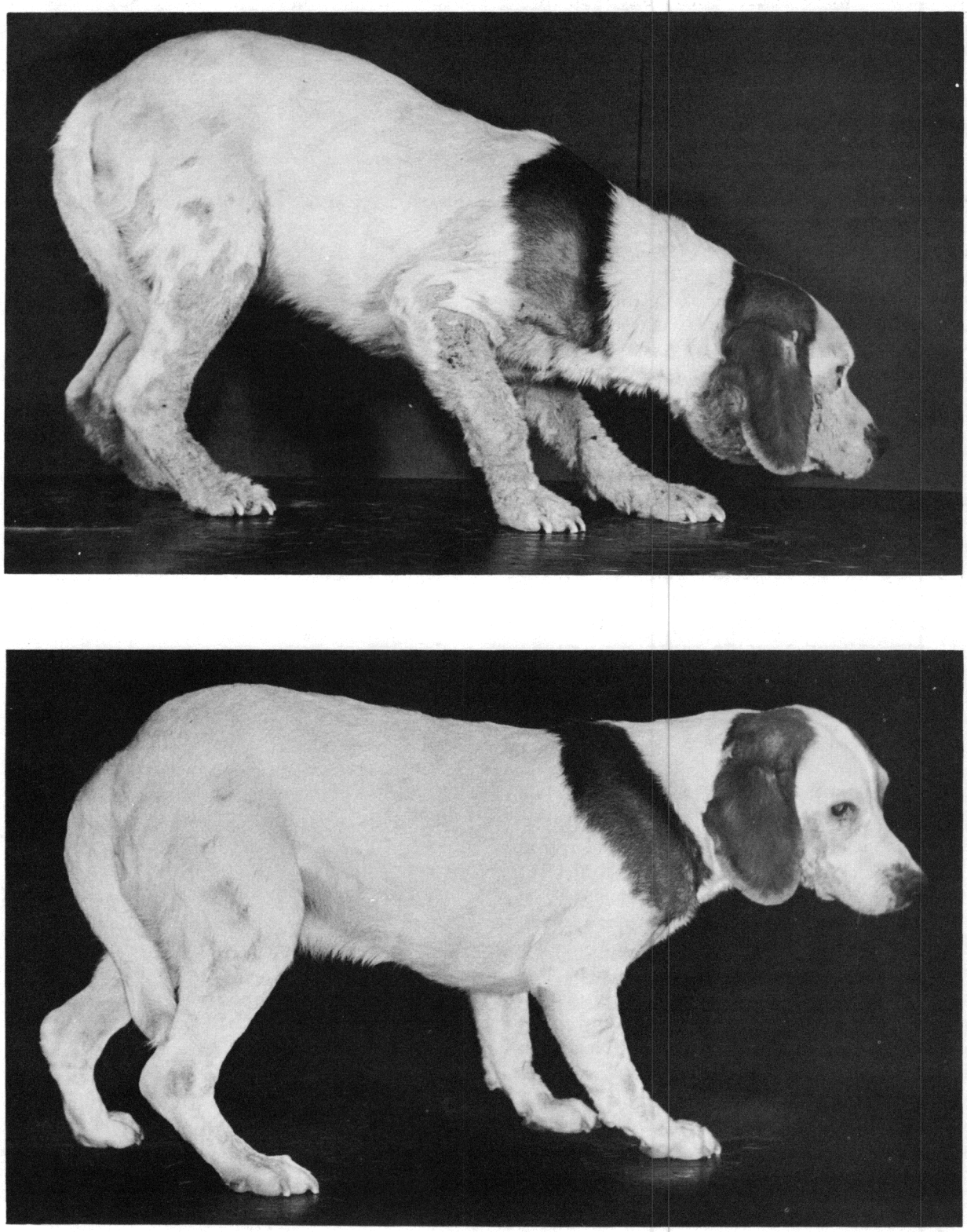

Fig. 46. Upper: untreated dog with follicular mange;
lower: same dog 4 months after initiation of treatment.

individuals were accidentally exposed in the radium dial industry. Detailed observations in the skeletal changes that have occurred in these people have been made already, and many are still under study. New cases are constantly being added to this known exposed population. The results of some radiostrontium studies on mice suggest marked increases in the incidence of bone tumors. The dog studies extend these data to another species that has the advantage of larger size and longer life.

The strontium dog experiments were initiated in 1945 by C. Ladd Prosser and Marguerite Swift at the Metallurgical Laboratory of the University of Chicago. A number of mongrel dogs and a few beagles were given injections of radiostrontium that consisted primarly of Sr^{89} (51-day half-life), with a small but, at the time, unknown amount of Sr^{90} (27.7-year half-life). The doses ranged from 1 to 0.1 mc/kg of body weight, that is, from acutely lethal doses to those causing no observable effects during the next few years. The results of the acute and subacute studies were reported by Swift and Prosser in 1947. The ten treated and two control dogs that survived this phase of the experiment were taken over by the Experimental Pathology Group of the Biological and Medical Research Division of Argonne National Laboratory for continuing study throughout their normal lives. As of December, 1956, four of the treated dogs (dose range 0.3 to 0.1 mc/kg) and both controls are still living. In 1947 three more dogs, 5-month-old mongrel littermates, were injected with 0.01 mc of Sr^{90} per kg for the study of the long-term effects of very low doses of this isotope. In 1953 and 1954 seven adult dogs were given Sr^{90} in a dose of 0.15 mc/kg and one was given 0.25 mc/kg. It was thought that this might represent an intermediate dose, small enough to permit survival beyond the acute and subacute stages, but large enough to produce recognizable skeletal damage within a few years. The latter supposition proved to be correct, but the former only partially; the dog that received 0.25 mc/kg and one that received 0.15 mc/kg died of acute irradiation disease.

With the aid of the Radiological Physics Division the current body burdens of all of the living dogs have been determined by measuring the Bremsstrahlung produced by the beta emanation of the Y^{90} daughter of Sr^{90}. The dogs of the original group injected with $Sr^{89,90}$ were found to contain from 3 to 25 μc each. From these data the original contamination by Sr^{90} was estimated to be 1-10%, which agrees with the contamination assumed to be present at the time of injection. The dogs injected in 1947 at 5 months of age retained an average of 21% of the dose of Sr^{90}, whereas the adults injected in 1953-1954 retained about 11%.

Three of the ten dogs injected with $Sr^{89,90}$ and one of the six dogs injected with Sr^{90} that survived the acute period have died with tumors involving bone. In each instance the radiographic appearance of their skeletons was essentially normal until the tumor appeared. This is strikingly different from the situation observed in plutonium poisoning of dogs and radium poisoning of man, where marked skeletal pathology develops before tumors appear. This course of events is apparently characteristic of strontium, for the development of bone tumors in otherwise normal-appearing bone is being observed also in cats injected with Sr^{90}. Some benign changes in the jaw, such as tooth decay, bone absorption, and receding gum line, have been seen throughout the dose range and appear to be associated with the absence of dental care. Those dogs that received adequate care from early life show only minimal changes of this kind.

These experiments, although still incomplete, already have been the source of important information on radiostrontium toxicity. Among other things, they have

demonstrated that the carcinogenetic dose levels for the dog fall within the range established for the mouse, and that the latent period from the deposition of a radioactive material in the skeleton to tumor formation can be as long in the dog as it is in man. Perhaps of greatest value has been the absence of change attributable to radiation among the three dogs that received 0.01 mc/kg of Sr^{90} almost ten years ago and had body burdens of from 14 to 19 μc nine years later.

Retention of Strontium as a Function of Age

Many workers have noted an apparent relationship between the retention of bone-seeking radioisotopes and the age of the animals at the time of injection. However, the relevant data are widely scattered in the literature and represent many unrelated experiments. The availability of cyclotron-produced Sr^{85}, which possesses a half-life of 65 days and which decays entirely by electron capture followed by emission of a 0.513-Mev gamma ray, provides the tool for a rather simplified study of the relationship.

The experimental animals were 67 male Sprague-Dawley rats, aged 4 to 428 days, each of which was given an intravenous injection of 3 μc of carrier-free Sr^{85}. Gamma activity was measured in the living animals at intervals in a pressurized gamma ionization chamber (Fig. 47); this instrument is provided with a sample well large enough to accommodate the largest rats while affording nearly 100% geometry, and is sensitive to 0.004 μc of Sr^{85}. Individual readings were corrected for variances in size and weight of the animals as well as for natural decay of the injected Sr^{85}. Averaged values for convenient age intervals were obtained from the specific retention curves and are plotted in Fig. 48.

Since the bone-seeking elements are taken up at growth sites and retained in the inorganic portion of bone, one might expect retention to be greatest in young growing animals. It is of interest that retention was relatively low in rats that were less than 40 days old at the time of injection. However, this seems reasonable when one considers that even though the initial uptake may be high in the younger animals, the rapid rate of remodeling shortly after injection means that the Sr^{85} that has been taken up in bone becomes available for excretion. The maximum retention occurred in rats that were 40 to 80 days old at injection; this is consistent with the fact that at this age the initial uptake is still relatively high while remodeling at disposition sites is decreasing. Beyond the age of 80 days at time of injection, retention decreased as expected, principally as a consequence of decreased initial uptake.

The fact that retention in the different groups varied as much as fourfold indicates that in studies with bone-seeking isotopes, an experimenter must specify the age or metabolic state of the animals at the time of injection in order to compare his studies with those of others. Further, the results show that statements concerning hazardous levels must take into account a range of biological factors which may not have been included in the experimental work on which they were based.

Heavy Water Intoxication in Rats

It was shown 20 years ago in a study on mice that heavy water had deleterious effects. Since larger quantities of heavy water are now available, it seemed of interest to investigate its action, particularly the biochemical effects, in the rat. The experiments reported here were performed through cooperative efforts of the Division of Biological and Medical Research and the Chemistry Division. The objects of the study were to describe the biochemical changes produced by D_2O and, if possible, to find the site of the primary injury.

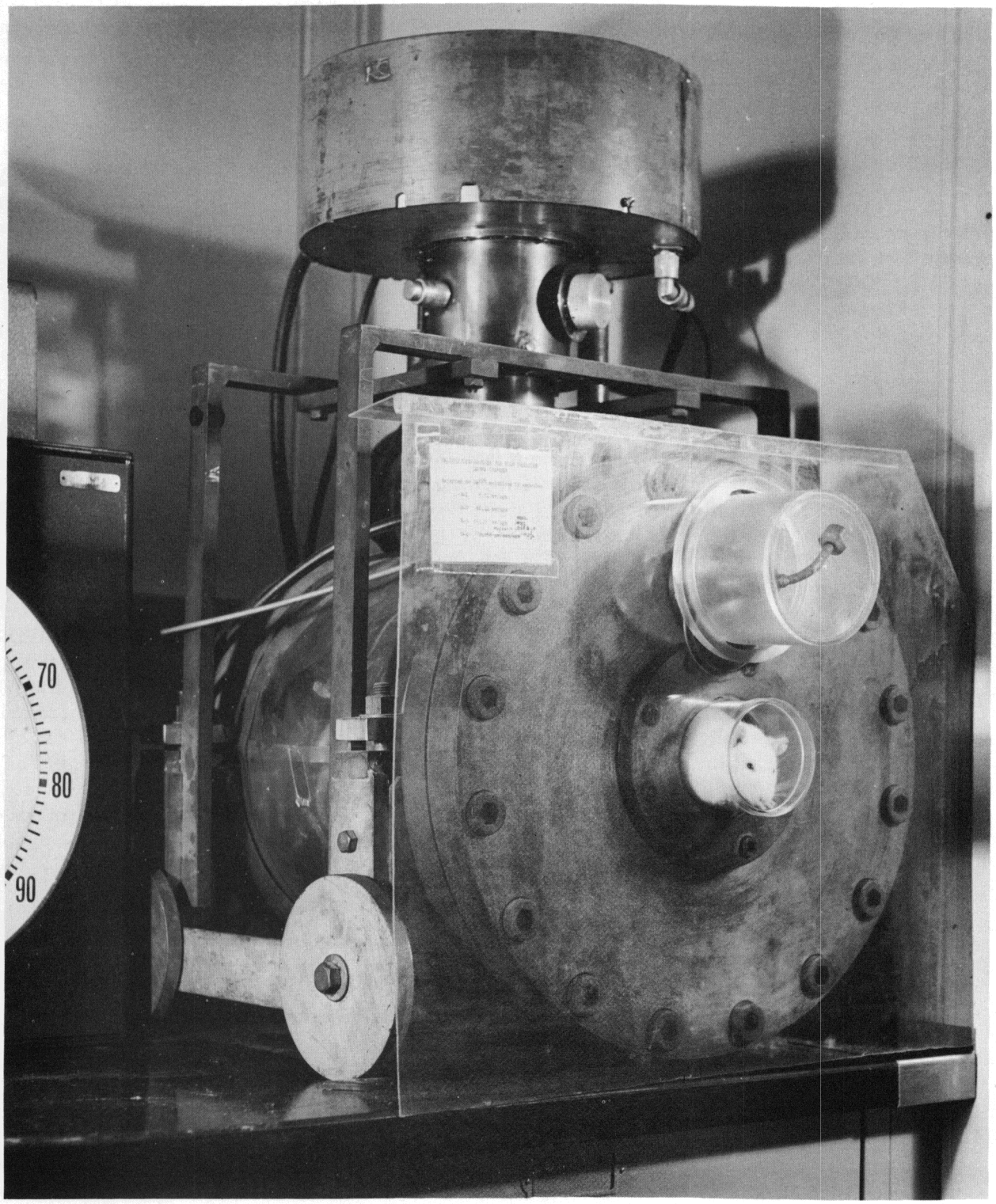

Fig. 47. Young rat in ionization chamber. The cylinder is partially withdrawn from the well so that the rat can be seen. The card at the upper left corner of the transparent shield contains calibration data. The edge of the recording instrument is seen at extreme left.

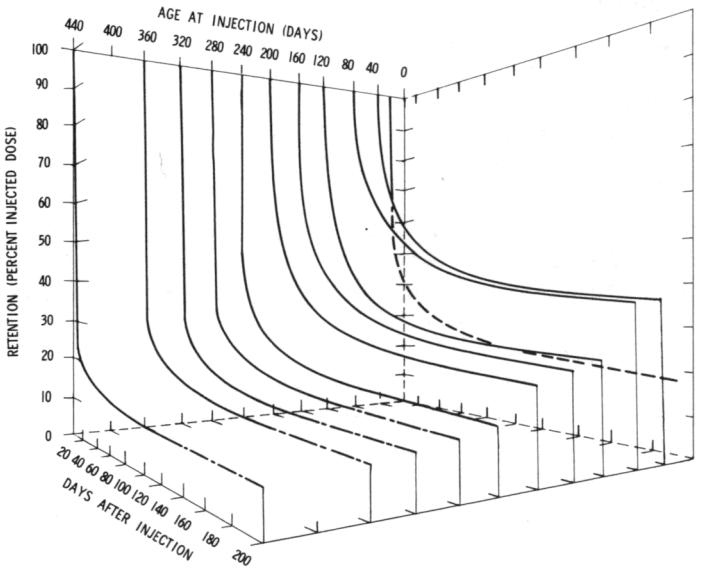

Fig. 48. Retention of Sr^{85} in rats as a function of age at time of injection. The broken lines on the "visible" portion of the surface represent curves for which data are not yet available; they are extrapolated from existing data.

In the first series of experiments, three rats were deprived of water for 24 hours, then given triply distilled D_2O as drinking water for 2 days, and mixtures containing 30-50 atom per cent thereafter. The plasma concentration* of D_2O rose to about 17 atom per cent within 2 days and continued to rise steadily but more slowly to about 30 atom per cent at 40 days. All three rats were manifestly ill by the end of 3 weeks, but no deaths occurred until after 40 days. In the second series, when 100% D_2O was given for 4 days, and a mixture containing 50 atom per cent thereafter, the plasma levels rose more rapidly, reaching 30 atom per cent at 20-25 days. Here also the deaths tended to occur as the concentration of D_2O reached 30 atom per cent.

The same general trend was observed in the two series; increases in plasma levels of non-protein nitrogen, urea, inorganic phosphate, and lactic acid; and decreases in plasma glucose, plasma protein, and body weight. Taken together, these changes indicate serious disturbances in carbohydrate and protein metabolism. Damage to kidney tubules was found at autopsy; this appeared to be a possible cause of death, but the metabolic disturbances indicated that the liver was also affected seriously. All rats showed marked hyperirritability, suggesting changes in the central nervous system; on the other hand, these symptoms might well have resulted from the uremia or the hypoglycemia.

Another finding of considerable interest was marked increase in the average weight of the adrenal gland. Adrenal hypertrophy is a characteristic response to stress presumably mediated through the pituitary gland. Following stimulation by ACTH, the hormone of the pituitary gland, adrenal function is increased and larger amounts of adrenocortical hormones are liberated. The adrenal hormones operate to correct changes in internal environment resulting from the stress, or help to adapt the animal to the new condition. Adrenal hypertrophy occurs when the stimulation by ACTH is maintained over prolonged periods. Thus the finding suggested that heavy water might act as a non-specific stress, and that the changes in the bodies of the rats might reflect a partial temporary adaptation to heavy water.

*Equivalent to that of all body water, since D_2O is distributed throughout body water. The deuterium also exchanges with hydrogen except when the latter is bonded to carbon.

The hypothesis could be tested rather easily; if it were true, D_2O should be much more toxic to hypophysectomized (pituitary glands removed surgically) rats, since the physiological stimulus to the adrenals would be missing. The necessary experiments were performed, and the results were quite clearcut. Although the D_2O was given only in 50% concentration and the levels in body water never exceeded 25 atom per cent, survival time was shorter than that of unoperated rats; the first hypophysectomized rat died at 6 days and none lived longer than 13 days. Increases in plasma levels of non-protein nitrogen and decreases in plasma glucose were equal to, or greater than, those seen in unoperated rats with plasma levels of D_2O of 30 atom per cent. There was no adrenal hypertrophy. D_2O was clearly more toxic in hypophysectomized rats, where the adaptation mediated through the pituitary could not occur.

In further experiments, attempts were made to locate precisely the sensitive sites in protein and carbohydrate metabolism. Assays of various tissues of D_2O-poisoned animals for several representative enzyme activities revealed slight decreases in several of them. However, since the liver itself increased in weight, total activities remained almost the same. The effect probably represents a non-specific response; it is seen also in livers which have been stimulated to grow by surgical removal of a part of the liver tissue. There were increases in two enzymes, arginase and uricase, but these changes may well have been adaptive, reflecting or paralleling the increases in non-protein nitrogen. None of the changes found can be implicated definitely as a primary cause of injury, but it is possible that a sensitive system may exist among the many that were not tested.

The results of the study permit only general conclusions as to the mode of action of heavy water. D_2O operates like a non-specific stress, to which the animals can adapt only partially and temporarily. Serious damage to the kidneys and liver was clearly indicated, and injury to the central nervous system was suggested but not established. Gluconeogenesis, the net synthesis of glucose from protein, was seemingly implicated as a disturbance in metabolic function, but the precise biochemical site was not found.

BASIC BIOCHEMISTRY

Transmethylation and Methionine Metabolism

A general project of the Biochemistry Group is concerned with the metabolism of the amino acid methionine. This compound is of interest because of the variety of reactions into which it may enter: it surpasses most of the other amino acids in versatility because of the presence in its molecule of a mobile methyl group and a sulfur atom in addition to the groups necessary for peptide bond formation. Thus, we observe its incorporation into proteins; next, it may serve as precursor of numerous sulfur compounds essential for cellular metabolism, for example, cysteine and glutathione; the methylthio group may be severed as an entity under the influence of methionase; and as a special feature, methionine is found in a central position in almost all schemes of transmethylation processes. The biochemical investigations at this Laboratory deal mainly with transmethylation, specifically with problems of the formation of new methyl groups and the biosynthesis of the methionine molecule.

Transmethylation -- the shifting of methyl groups from one compound to another -- is one of the outstanding examples of biochemical group transfer. It is involved in the formation of a variety of important metabolites. It may be recalled that in vivo experiments with tracer techniques have firmly established methionine as a source of methyl groups in many transmethylations. Attempts to carry out in vitro experiments with methionine, however, have shown that it does not react as a methyl donor directly; it has been shown elsewhere that methionine must first be activated by conversion into S-adenosylmethionine by an enzymatic process utilizing adenosine triphosphate (ATP):

$$\text{Methionine} + \text{ATP} \rightleftharpoons \text{S-Adenosylmethionine} + 3\ \text{Inorganic Phosphate} \quad (1)$$

$$\text{S-Adenosylmethionine} + \text{Methyl Acceptor} \rightarrow \text{S-Adenosylhomocysteine} + \text{Methyl Compound.} \quad (2)$$

In order to make a detailed study of transmethylations, it is necessary to procure pure S-adenosylmethionine in quantity. Because the conventional method using liver enzyme and adenosine triphosphate (equation 1) is cumbersome and expensive, a new procedure was developed here which used metabolizing yeast as a tool of biosynthesis. The addition of methionine to yeast leads to a depletion of the reserves of ATP (equation 1); this results in the stimulation of ATP production (up to 10-fold increase) by the cells, and corresponding amounts of S-adenosylmethionine are accumulated. This procedure for synthesis, together with simple methods of extraction and chromatographic purification, have now removed the compound from the list of rare biochemicals.

Further progress in the field of transmethylation was also facilitated by a new and simple analytical procedure employing chromatography. It is based on the unusually strong retention of S-adenosylmethionine by cation exchange resins; S-adenosylhomocysteine passes through the column with comparative ease. Decreased concentrations of the former compound and concomitant increases of the latter serve as an accurate measure of any transmethylation represented by equation 2.

One study dealt with the specificity of the enzymes catalyzing the formation of S-adenosylmethionine. Uridine-, cytidine-, and guanosinetriphosphates cannot serve as substitutes for adenosine triphosphate (equation 1), nor can tissue enzymes utilize D-methionine instead of L-methionine. In contrast, yeast uses either D- or L-methionine; S-adenosyl-D-methionine obtained in this fashion offers interesting prospects for studies on the stereospecificity of transmethylating enzymes.

Noteworthy among methionine analogues is ethionine, in which the methyl of methionine is replaced by an ethyl group. There is a voluminous literature on its effects as an antimetabolite of methionine, but in no instance has it been shown which of the metabolic routes of methionine suffered interference from ethionine. Progress toward an interpretation has been made here in a study which showed that ethionine can replace methionine in the formation of the S-adenosylthionium compound: S-adenosylethionine which was isolated from yeast which had been exposed to ethionine. Of special interest is the discovery of in vitro transethylation with this compound.

The availability of S-adenosylmethionine in chromatographically pure form and in quantity has facilitated the mapping of its stability and of other chemical properties. The compound was found to be very stable toward acid at low temperature. Hydrolysis by heating in slightly acid neutral solution leads to the formation of methylthioadenosine and homoserine. Alkali at room temperature rapidly splits off the adenine moiety. This sensitivity of the adenine ribose linkage is not observed with adenosine or methylthioadenosine; the presence and proximity of the thionium type of linkage in

S-adenosylmethionine appears to be responsible for this liability. The other fragment remaining after alkali treatment is S-ribosylmethionine, a novel compound whose properties and biological significance are under study.

Enzymatic studies with S-adenosylmethionine as a methyl donor promise to corroborate many of the transmethylations which had been formulated earlier on the basis of in vivo studies. In some instances, however, evidence is accumulating that a more complex mechanism is involved. For example, N-dimethylglycine and N-dimethylaminoethanol had been surmised to be methyl acceptors in the final steps of the formation of betaine and choline, respectively. Experiments with S-adenosylmethionine and tissue and yeast enzymes have failed to establish these compounds as methyl acceptors, which suggests revision of the existing concepts and continued search for details of the reaction mechanism.

Other work has led to the discovery of new transmethylation reactions in which homocysteine is the acceptor:

$$\text{S-Adenosylmethionine} + \text{Homocysteine} \longrightarrow \text{S-Adenosylhomocysteine} + \text{Methionine}. \qquad (3)$$

This process may be of great significance in the biosynthesis of methionine, because the neogenesis of methyl groups most likely takes place by reduction of a one-carbon unit (as yet unidentified) after its linkage to the sulfur atom of S-adenosylhomocysteine. The methyl groups formed in this way are then transferred to homocysteine (equation 3) and provide the methionine for protein synthesis.

In higher plants another thionium compound, S-methylmethionine, was found some years ago. It was suspected of participation in methyl transfer but this concept has only recently been verified in this Laboratory.

$$\text{S-Methylmethionine} + \text{Homocysteine} \longrightarrow 2\ \text{Methionine}. \qquad (4)$$

It remains to be seen whether S-methylmethionine is the principal methyl donor in higher plants, a role which seems to be restricted to S-adenosylmethionine in animals.

The biosynthesis of methionine, the origin of the methyl group, and the participation of vitamin-related co-factors in methionine metabolism are among the most intriguing problems of present-day biochemistry. It appears that further significant advances are imminent.

Nucleic Acid and Protein Metabolism

Although the metabolism of nucleic acids and proteins has been investigated extensively, it has not been possible to make satisfactory estimates of their rates of synthesis and degradation. The reason is that the conventional methods for studying these parameters in biological systems cannot be applied successfully to the compounds in question.

One general method is based on the rise in radioactivity of the specified compound (A) in the animal after giving a single dose of a precursor (B) which is labeled in a position known to enter molecule A. The incorporation of the label from B into molecule A usually involves many reactions, but only the final one (or more) producing A, and the one in which A is degraded, are of interest here. In order to calculate their velocities, it is necessary to know the amounts of the respective precursors and

degradation products as well as the changes in their specific activities with time. Because the precursor pools contributing to nucleic acids and protein are largely unknown, it has not been possible to use this method for absolute measurements, although it has been used to compare turnover (renewal rate) under a variety of conditions.

A second general method involves feeding the labeled compound for a more prolonged period, until isotopic equilibrium is attained, and then observing the fall in radioactivity after administration of the labeled precursor is stopped. In order to calculate the rates of the specified reactions under these conditions, it is necessary to measure the extent to which isotope is incorporated into molecule A from breakdown products of A itself, or from other labeled body constituents. This has not hitherto been possible.

A new approach has been developed over the past two years at Argonne by which the difficulties may be by-passed. In most of the experiments, the tracer has been $C^{14}O_2$, administered continuously to rats as $CaC^{14}O_3$ incorporated in the diet, by feeding at hourly intervals for periods of one hour to 12 days. Under this schedule of administration, the specific activity of intracellular CO_2 (equivalent to that of urea, and measured as such) rises immediately, remains at a constant level as long as label is being administered, and then drops abruptly to a negligible value. Then, knowing the specific activity of this "metabolic" CO_2, it is possible to determine the rate at which it is incorporated into the compound under study. The effect of feedback (reutilization of fragments) remains, but it may be corrected with the knowledge of the specific activities of the component parts at isotopic equilibrium, obtained in other experiments.

Nucleic acid metabolism. It was shown that metabolic CO_2 enters the C-6 position of the purines without dilution, and that glycine enters the C-4, C-5, and N-7 positions without dilution. The rate at which metabolic CO_2 was incorporated into purines in deoxyribose nucleic acid (DNA) in livers of young growing rats was about 6-9% per day, approximately the same as, but never more than, the growth rate of liver itself in these animals. This has led us to conclude that the rates of cell death and DNA degradation are insignificant compared with those of synthesis, and also to conclude, with others, that mitotic cell division is accompanied by the synthesis of only one cell complement of DNA. The rate of formation of DNA-purines in the livers of adult animals indicates that slightly less than 1% of the DNA is replaced daily, a figure consistent with values calculated from measurements of mitotic activity (0.15-1% per day). It is suggested that intracellular turnover of DNA may be considered to represent turnover of cells. In adult rat liver, the average lifespan of the DNA molecule is estimated to be at least 150 days; however, there are several different types of liver cells which differ in their lifespan.

The velocities of individual reactions in nucleic acid metabolism were also calculated. Each day, in the liver of the young growing rat (70 g), 4.9 μmoles of purine are synthesized and 2.4 μmoles are degraded; 5.4 μmoles of purine are incorporated into ribose nucleic acid (RNA) and 3.3 μmoles are released; and 0.36 μmole of purine is incorporated into DNA.

In similar experiments performed with $Na_2HP^{32}O_4$ as the tracer, reaction rates for RNA were determined from the specific activities of acid-soluble phosphate (a metabolic pool, analogous to metabolic CO_2 in the C^{14} experiments) and RNA-phosphate. However, it was necessary to measure directly the activity of the acid-soluble phosphate at frequent intervals because, unlike the metabolic CO_2, it represents a relatively large amount, comparable to the RNA-phosphate, and can be transported easily from one part of the body to another. The acid-soluble phosphorus data were expressed in

terms of an equation, and the predicted specific activities of the RNA were calculated on the assumption that some component of the acid-soluble phosphorus fraction was the precursor of the RNA-phosphate. The similarity of the predicted and observed values showed that the assumption was justified. Calculations of reaction rates were then made similar to those in the C^{14} experiments.

In the young growing animal, the turnover rate for RNA is not given by the ratio of rate of formation to average amount present, since there is synthesis for growth as well as for turnover; instead it is given by the ratio of rate of RNA degradation to average amount present. The true rate of turnover or renewal was calculated from the C^{14} experiments to be 11% (on basis of adenine data), and 15% (on basis of guanine data), and from the P^{32} experiments to be 11% and 15%. The two methods clearly give comparable results. It was concluded that both the RNA and DNA molecules are renewed as units, that is, that there is little or no exchange of component parts once the macromolecule is formed.

Protein. The first experiment in the measurement of turnover of liver proteins was concerned with the parameters of arginine metabolism. The guanidine carbon of arginine is derived entirely from CO_2 and is renewed by the reactions of the Krebs-Hensleit urea cycle at a rate several orders of magnitude greater than the reactions of protein degradation; thus the specific activity of this group in free arginine can be readily observed by the measurement of urea. The carboxyl group reaches a specific activity of about 10% of the urea value and is formed at a rate similar to its rate of formation from protein. Since there is negligible feedback of guanidine carbon into the protein, the calculation of the rate of incorporation of arginine into protein is facilitated. Knowledge of this value then makes it possible to compute the rate of formation of the carbon chain of arginine and the feedback of the carbon chain into protein. The average value for the half-life of liver protein obtained from 4 animals is 3.02 ± 0.27 days. This is in agreement with previous results from this Laboratory which showed that the liver protein had been essentially removed after an exposure for 14 days to $C^{14}O_2$. The rate of synthesis of the carbon chain of arginine is about the same. From this, it is possible to show that about 50% of the arginine derived from protein is reincorporated into the protein of the liver.

Complexes Between Metals and Organic Anions

The formation of complexes between metals and certain groups of organic ions has been studied for some time. Information from such studies is applied in three types of problems. Firstly, difference in the affinities of metal ions for a given organic anion may serve as the basis for separation or analysis of the metals. Secondly, affinity between organic anions and metals may provide a means of removing toxic or radioactive elements from the body. Thirdly, such knowledge is fundamental to an understanding of the mechanism by which enzyme systems are activated or inhibited by metals.

The biological application constitutes a much more complicated problem: the complexing reaction does not take place in a defined medium or under well-defined conditions, but, instead, occurs in that complex physical and chemical environment that is summed up in the term "physiological conditions." To be an effective therapeutic agent for metal poisoning, the organic ion must first be non-toxic and stable enough not to be metabolized immediately by the body. It must also have physical and chemical properties permitting it to be absorbed and brought into contact with the metal. Then it must be capable of forming a stable, relatively non-toxic complex with the metal under "physiological conditions;" it must bind the metal ion preferentially, with relatively little binding with "bulk" cations such as Ca^{++}. The complex must be either soluble

and readily excreted, or insoluble and deposited in a relatively inert form in the tissues. Although the formation constant is by no means the sole basis of therapeutic usefulness, it offers a means of selection of the more promising complexing agents from a large number of possibilities.

Formation constants (k_f) for a number of complexes have been determined by methods involving ion exchange, solvent extraction, or pH titration (Table 1). Concurrently, a screening method using pH titration has been devised for the preliminary testing of chelating agents for removing toxic metals and radioelements from the body. One compound, diethylenetriaminepentaacetic acid (DTPA), was selected in an earlier stage of the work for preclinical testing. In mice acutely poisoned with Mn^{++}, it has proved to be more effective than its better-known analog, ethylenediaminetetraacetic acid (EDTA), which has already found some use in the therapy of metal poisoning.

The organic anions surveyed have included not only synthetic chelating agents, but also a group of compounds that occur naturally in the body as metabolic intermediates and that have complexing properties (acetic, citric, fumaric, lactic, pyruvic acids and others listed in the table). Some of these, e.g., citrate, are known to be involved in the binding and transportation of metals in the body. This area of the problem is the subject of continuing study.

INSTRUMENTATION AND TECHNIQUES

Liquid Scintillation Counting

The use of liquid scintillation counting for the detection of low energy β-emitting isotopes such as C^{14} or tritium permits the measurement of samples with very low specific activities. The method provides relatively high efficiency of detection through intimate contact of the detector with the sample; at the same time, in many cases, it permits simpler method of sample preparation than do gas-filled counters. In our Laboratory measurements made with a fast-coincidence liquid scintillation counter (Tri-Carb Counter, Model 314, Packard Instrument Company, La Grange, Illinois) gave efficiencies of 75% for C^{14}, 25% for tritium-labeled hydrocarbons and approximately 5% for tritiated water.

The liquid scintillation method consists of dissolving the labeled material in a liquid phosphor, such as 2,5-diphenylosazole or terphenyl-diosane, and measuring the scintillation pulses with a photomultiplier tube.

The preparation of samples for assay is relatively simple, consisting merely of dissolving the labeled compound in the liquid phosphor. For many organic materials (e.g., sterols and fatty acids) this may be done by employing a liquid phosphor with an aromatic solvent. For assay of tritiated water or water-soluble materials, satisfactory measurements can usually be obtained using either a terphenyl-diosane solution phosphor, or a liquid phosphor consisting of 2,5-diphenylosazole or terphenyl, with an aromatic solvent and a material such as ethyl alcohol which is miscible with both water and the aromatic solvent. Since resolution of energies is possible, it is feasible with proper instrumentation to determine simultaneously tritium and C^{14} in mixtures by proper adjustment of the energy gates. Our attention has so far been given mainly to developing and perfecting more promising methods of assay appreciable to biological problems.

Table 1

FORMATION CONSTANTS OF COMPLEXES BETWEEN METALS AND ORGANIC ANIONS

(Ionic strength (μ) = 0.16, temperature = 25°C.)

Parent acid	Mn^{++}	Co^{++}	Zn^{++}	$(UO_2)^{++}$
Acetic	0.61*	0.91* 0.55 (μ=0.50, pH=4.52)* 1.10+		2.38 (k_1)* 6.38 (k_3)*
Aconitic (cis)	2.47*			
(trans)	2.27*			
Azelaic	1.03*			
γ-Carboxypimelic	1.91*			
Citraconic	1.77*			
Citric	3.54* 3.54+	(4.6)(k_1)* (3.0)(k_2)* (1.0)(k_3)*	(4.7) (k_1)* 4.75 (k_1)+ (3.0) (k_2)* (1.0) (k_3)*	8.50 (k_1)±
Diethylbarbituric	(0.1)*,**			
Fumaric	0.99*			
Glutaric	1.13*			
Glycine ($^-OOC-CH_2-NH_3^+$)				1.45 (k_1)±
Glycolic	0.99*	1.64* 1.62+		2.78 (k_1)* 2.75 (k_1)+ 1.30 (k_2)* 1.52 (k_2)+
3-Indolylacetic	(0.52)*			
Isocitric	2.55*			
α-Ketoglutaric	(1.24)*			
Lactic	1.19*			
Maleic	1.68*			
Malic	2.24*			
Malonic	2.30* 2.66+	2.85* 2.85+		
Oxalic $(C_2O_4)^{--}$	2.93*	(3.8)*	(3.8)*	5.26 (k_1)* 4.81 (k_2)*
(HC_2O_4)				3.38 (k_1')* 2.57 (k_2')*
(C_2O_4)				1.53 (k_1'', μ=1)* 1.30 (k_2'', μ=2)*
Pimelic	1.08*			
Pyruvic	(0.50)*			
Salicylic	(<1.35)*			
Serine				0.87 (k_f)±
Succinic	1.26*			
Sulfosalicylic	(1.35)*			
Tetraglycinate $(GGGG)^-$		3.04(k_1)* 5.47(k_1 k_2)*		

*k_f values obtained by ion-exchange method. **Values in parentheses are provisional.
+Values obtained by pH-titration method. ±Values obtained by solvent-extraction method.

It has been found that some materials which are insoluble in the scintillators can be suspended by grinding with absolute ethanol. When the resultant paste is added to the toluene scintillator, the dispersion is sufficiently fine that no sedimentation occurs during the counting period. Furthermore, the diameters of the particles are so small that with C^{14} no self-absorption of the beta rays occurs.

Another technique which has been investigated is the possibility of counting tissues directly. Various tissues containing C^{14} and tritium have been homogenized, suspended, and counted. The results are encouraging, although certain questions such as pulse-height shifting and possible quenching effects need to be answered.

One important precaution that must be observed is that highly purified materials must be used in preparation of the liquid phosphors. Trace impurities can shift the positions of the emission bands of the scintillation light as well as quench it. Because of the high sensitivity of fluorescence to trace amounts of certain materials it is necessary to determine whether the compound to be assayed impairs the scintillation characteristics of the phosphor.

Some interesting possibilities have presented themselves. Since we can now detect as little as 10^{-10} curie of tritium, we may now be able to use it as a tracer for organic molecules. With biochemical methods, it should be possible to prepare labeled molecules of complex or even unknown structures, with the specific activity high enough for detection even after great dilution in the organism. With the short half-life (12.4 yr) and the high isotopic purity that is attainable, it may be possible to work in the range of dilutions as high as a million-million fold. Furthermore, the low radiation energy of tritium minimizes health hazards, since its radiation (0.0189 Mev) is completely absorbed in less than 10^{-3} centimeter of liquids or solids.

Multiple Tracer Techniques

A method for measuring quantitatively the amounts of various radioelements present in a radioactive mixture has been developed and used successfully in blood volume studies and in ascertaining the affinity of various chelating agents for metal ions.

The method utilizes a NaI(Tl) well-type scintillation counter with its associated electronic equipment including a single-channel pulse-height analyzer. Since gamma-emitting isotopes most readily lend themselves to analysis in a mixture, they were given primary consideration. Nuclear gamma rays are emitted with certain discrete energies characteristic of the nucleus from which they arise. Both Cr^{51} and Mn^{54} emit gamma rays of definite energies (see Fig. 49) and the fact that these energies are not the same allows for their simultaneous measurement. Absorption of gamma rays by the NaI crystal occurs in several ways, depending upon the energies involved; however, part of the absorption process results in a pulse whose energy is directly proportional to the energy of the absorbed photon. Note in Fig. 49 that the primary peaks or photopeaks which correspond to total absorption are discrete and well separated. By setting the pulse-height analyzer so that only the area under one peak is being counted it is possible to count Mn^{54} alone, even though Cr^{51} is present in the sample. Similarly, Cr^{51} may be counted at its appropriate setting, although in this case correction must be made for those counts from Mn^{54} which also appear in this region of the spectrum. Such correction is done empirically. By using Cr^{51} and Mn^{54} sources of known activity it is possible to quantitate the amount of activity from each isotope appearing in a mixture. As many as three gamma-emitting isotopes have been measured simultaneously by this method with an accuracy of 3% or better, and there is no reason why

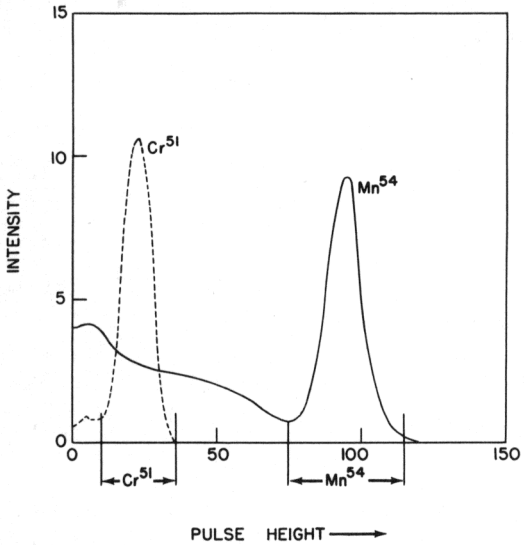

Fig. 49. Gamma-ray spectra of Cr^{51} and Mn^{54}.

mixtures containing more radioelements might not be handled by this method. Such a technique is not limited to biological or medical use, but may find application to such things as the assay of thorium or uranium ores, the study of mixing and extraction in chemical processes, and the processing of reactor fuel elements, to name only a few.

Fine Structure Studies with the Electron Microscope

In the past two decades the electron microscope has progressed from a physicist's dream to a precision research instrument applicable to metallurgy, chemistry, physics, biology, and medicine. Commercially manufactured microscopes are now available which have resolving power very near the theoretical limit. As a consequence, the visualization of molecular architecture in biological materials is now within the realm of possibility. Practical observation of molecular relationships is no longer dependent on improvement of the microscope but on improvements of technique in the utilization and application of the instrument to a given research problem.

Improvements in technique for cutting very thin sections of living cells have been achieved rapidly, and methods of preservation and preparation of living material are reliable enough to insure accurate observation and interpretation of structures close to the limit of the microscope resolving power. A considerable emphasis has been placed on the utilization of this powerful tool in the biological and medical research programs at Argonne.

The fine structure of cilia

Certain problems of transport and locomotion in biological systems require the presence of subcellular structures capable of doing mechanical work, that is, of moving materials, or, in unicellular forms of life, of moving the organism itself. Several basic methods are known to exist by which this may be accomplished. Of these, one of the most widely occurring, in plants as well as in animals, is ciliary movement. For example, cilia serve to move mucus and foreign materials from the human respiratory tract to the nasal cavity, to transport the human ovum from the ovary to the uterus, and to transport the sperm to the egg or ovum. They also represent the sole means of locomotion in many unicellular organisms.

A cilium can be defined as a hair-like structure which protrudes from the free edge of a cell and which serves to transport materials past the cell, or which protrudes from the edge of a free cell and serves to move the cell about. The length of a typical cilium is about one-thousandth of an inch and the diameter is much smaller - about one one-hundredth of the length. A cell may have one cilium or up to several hundred that beat synchronously in whip-like or cork-screw-like fashion.

Cilia were first seen by the world's first microscopist, van Leeuwenhoek, in the middle of the seventeenth century, but only in the last five years have the structural details of a cilium been observed. Numerous studies of a variety of materials, here and at other laboratories, have demonstrated that a basic and rigorously uniform pattern exists in cilia wherever they are found, in the flagella of small animals, and in the tails of sperm cells. This pattern is always characterized by eleven fibrils, two in the center of a ring formed by the other nine, and by a membrane which surrounds all of the fibrils. Furthermore, the nine fibrils, which are arranged in a ring, show a figure-eight structure when cross-sectioned. Fig. 50 illustrates this basic pattern. Now that the structure of cilia is better understood, we are directing our attention to two other phases of the problem: first, the way in which these structural parts produce a whip-like or cork-screw-type beat, and, secondly, the mechanism that makes the cilia beat synchronously and that changes the direction of the ciliary beat. Evidence obtained so far suggests that the nine fibrils contract in a very precise sequence to produce the characteristic movement. Synchronization and control of direction of the beat may be effected by nerve-like impulses of an electrical nature, conducted over fibers joining the base of one cilium with others.

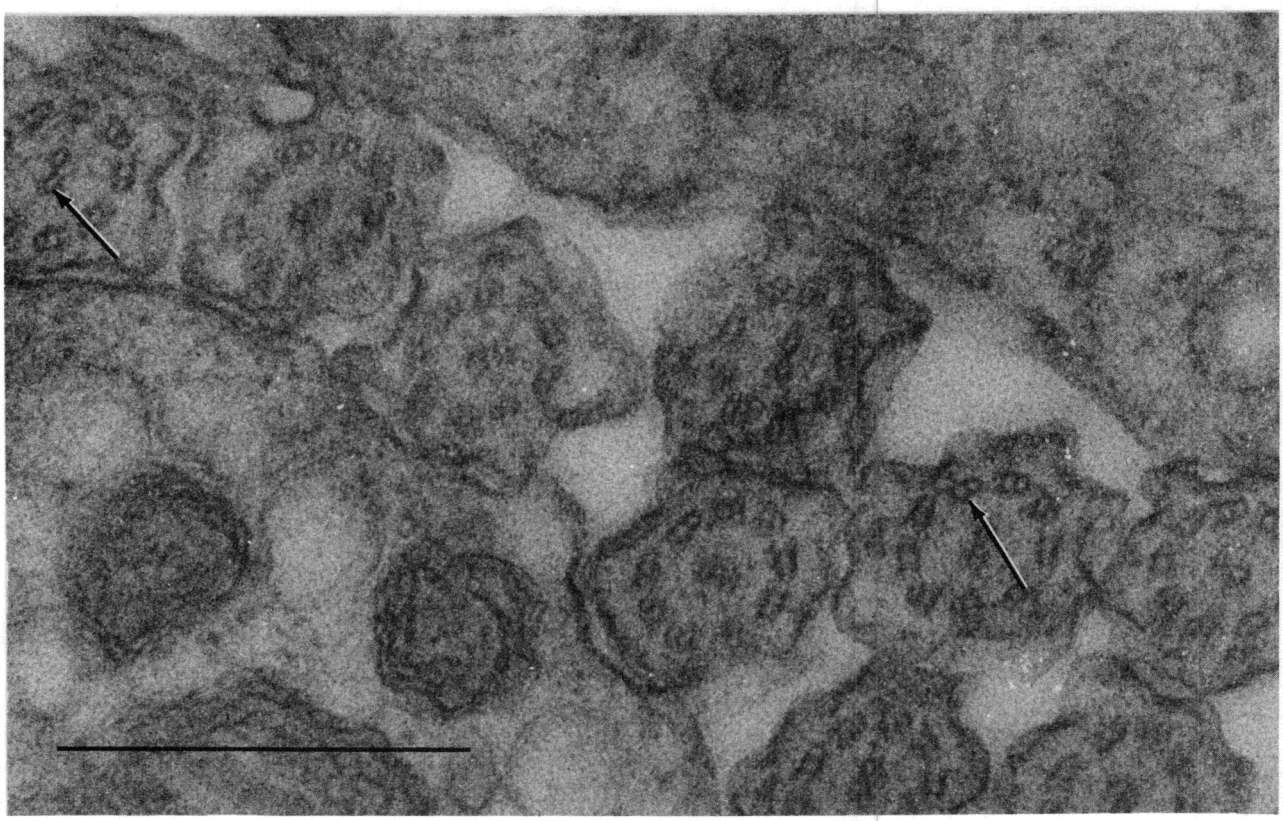

Fig. 50. Cross sections through nine sperm tails from the snail, Helix. The basic ciliary pattern of two central fibrils (upper arrow) surrounded by a ring of nine, figure-eight fibrils (lower arrow). A thin membrane is also seen enclosing all of the fibrils. The line at the left indicates a distance of one-half of one micron.

Fine structure of the chromosome

Biologists have many times found it possible to overcome technical difficulties in their research problems by seeking out the right experimental animal. While in most cases the desired structure or process may be impossible to reach with the methods available, one may find occasionally a species in which the problem is, so to speak, naturally isolated in a form that is unusual but convenient for study. This sort of consideration was responsible for the selection of the African insect Steatococcus tuberculatus for a study of chromosome structure. The insect has only two meiotic chromosomes which, in the spermatozoon, are housed end to end in a long cylindrical sheath. By cross-sectioning these spermatozoa, one may obtain cross sections of single chromosomes.

Electron micrographs show that these chromosomes consist of about 64 chromosome microfibrils, 30 A in diameter and of indefinite length. The units were observed in side view as well as in cross section. In these chromosomes there was no indication of transverse structures or of a central "master thread." Thus the cytogenetic implications are that the chromosome is made up of multiple, roughly parallel, microfibrillar threads, each one possibly as long as the chromosome. Presumably a group of threads acts as a single unit in the determination of heredity and, for instance, the response to irradiation, but the transverse forces regulating these all-or-none reactions are not yet understood.

Fine structure of the inorganic portion of bone

Investigators have not arrived at any agreement with respect to the chemical or physical configuration of the mineral portion of bone. As a result, we do not have a clear understanding of the chemical and physical aspects of metabolism of the "bone-seeking" radioelements, since it is in the mineral portion of bone that retention occurs. The tolerance levels of these radioelements are referred to radium; hence it is most important to have a clear understanding of radium metabolism. The recent interest in Sr^{90} also has emphasized the need for more knowledge of the mineral portion of bone.

Recent methods of ultra-thin sectioning, using the diamond knife, permit the preparation of undecalcified bone for electron microscopy. This removes one great obstacle to the study of fine details of bone structure. This Laboratory has produced electron micrographs of thin sections of undecalcified dog and human cortical bone, which show rather clearly needle-shaped crystals 40-60 A wide and, on the average, 600-700 A long (see Fig. 51). The shape and size of these crystals are important considerations, since the initial uptake of these elements into bone is considered to be a surface reaction. The structure was observed to be the same whether sections were prepared from untreated bone or from bone embedded in methacrylate.

CANCER AS A SPECIAL CASE OF A GENERAL DEGENERATIVE PROCESS

In many cancer studies at this Laboratory and elsewhere, attempts have been made to discover the underlying mechanism by which tumors come into existence. While a great many of these have been directed toward describing the process of carcinogenesis in biological terms, the statistical approach has also been productive. A recent study at Argonne, using analysis of vital statistics, indicates that cancer has some characteristics in common with the degenerative diseases.

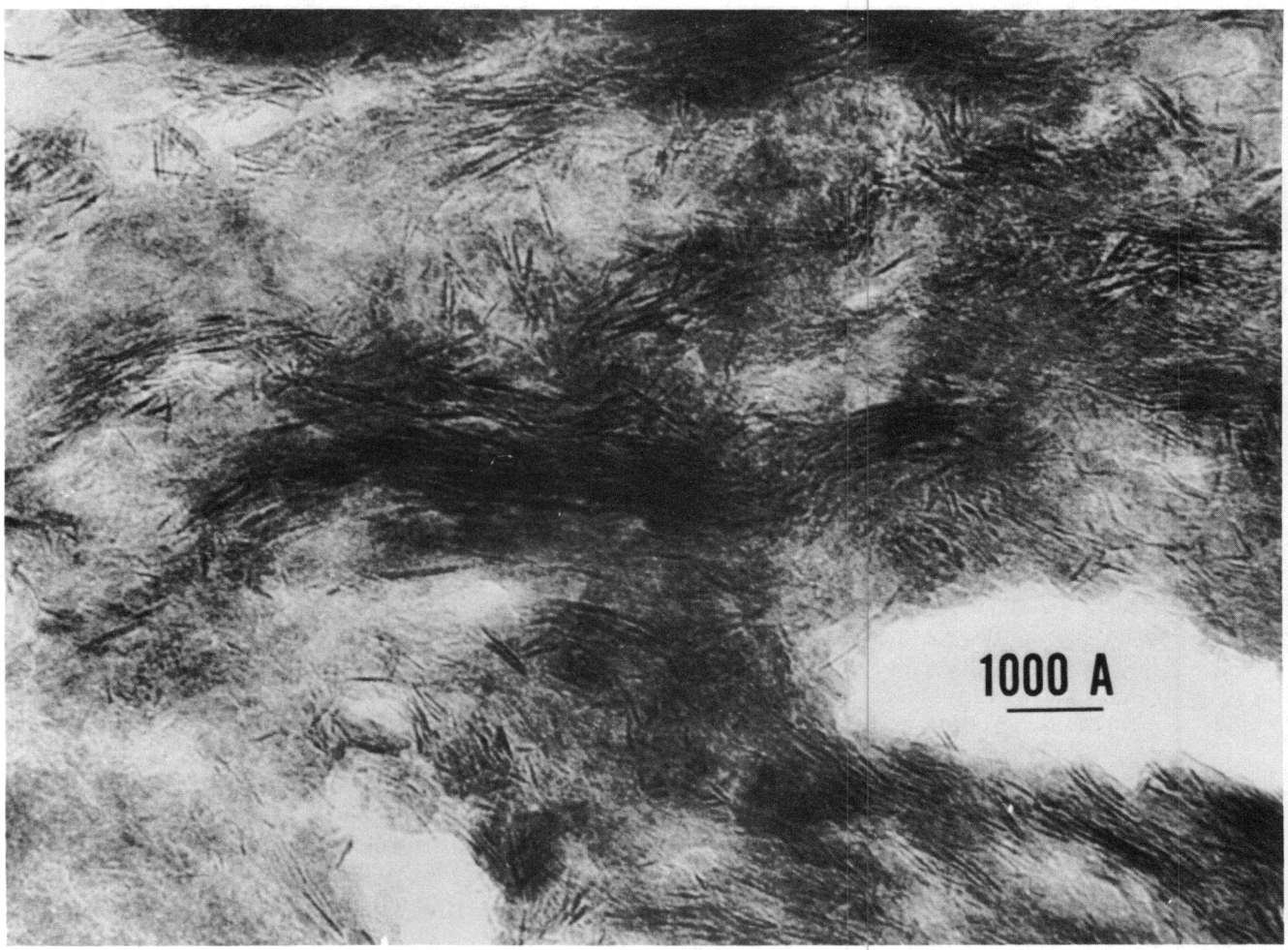

Fig. 51. Bone crystals.

The study was suggested by observations elsewhere that when the logarithm of death rate from cancer (either total or of a specific site) was plotted against the logarithm of age at death, the result was usually a straight line. The slope of the line indicated a sixth power relationship, a fact that has been used to support several theories of carcinogenesis. Another interesting possibility -- that the same linear relationship might be present in other causes of death -- was recognized and investigated in the present study.

The question was first examined by analyzing the United States death rates for the years 1949-1951. Plots were made on the same log-log basis for several broad groups of causes of death. Five groups -- circulatory system, malignant neoplasms, nervous system and sense organs, respiratory system, and genito-urinary system -- showed the sixth power relationship to a marked degree for age 30 and older, with departures from linearity being restricted to groups under 30. The sum of these groups gave an almost perfect linear relationship from age 30 and older (Fig. 52). These five groups represent the overwhelming majority of the chronic degenerative causes of death, while the remaining three -- infective and parasitic diseases, diseases of the digestive system, and accidents -- which did not show the linear relationship, represent the acute causes of death.

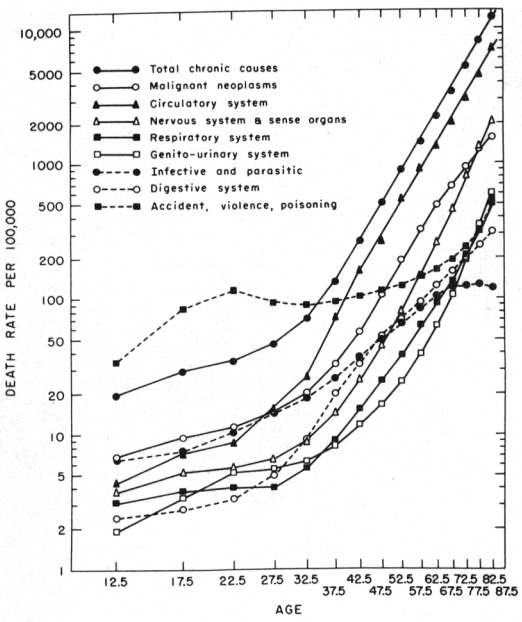

Fig. 52. Log-log plots showing the relationship of death rate to age in United States white males (1949-1951) for broad groups of causes of death. Solid lines, chronic causes; dotted lines, acute causes.

In order to find out whether the same situation obtained in other countries, a slightly different method had to be used. In the absence of reliable statistics for most of the countries of the world as to death rates for various specific causes, life table data, which are available in most cases, were used. The value used was q_x, the proportion of persons alive at the beginning of the year of the specified age, who die during that year of all causes. The countries tested were United States, Canada, Israel (Jewish population), India, Union of South Africa (Asian population), Brazil, Japan, Portugal, Belgian Congo (African population), Costa Rica, El Salvador, Argentina, Ceylon, Finland, France and Norway. Similar sixth power relationships were exhibited by all. Deviations from linearity at younger ages were always in the direction of the actual figures being higher than the extrapolated values.

On the basis of the demonstrated log-log sixth power linear plot of the chronic degenerative diseases, and the nonlinearity of the acute causes of death, an attempt was made to determine the relationship of acute causes to chronic degenerative causes in the total death rate. Life table values for United States white males for three periods, 1900-1902, 1929-1931, and 1949-1951, were plotted against age on the log-log basis. The usual departure from linearity at earlier ages were marked in the 1900-1902 period, less so in the 1929-1931 period, and still less in the 1949-1951 period, but all three curves tended to merge into a common straight sixth power line at age 40 and older (Fig. 53). This merging of the three plots at age 40 and older demonstrates a well-known fact, that chronic degenerative diseases become most important as causes of death at the older ages; the values show essentially no change over the period from 1900-1951. On the other hand, at the earlier ages, the acute causes constitute almost 100% of the total death rate, and chronic degenerative diseases represent only a minor fraction. Even though it is apparent that acute causes have been decreasing steadily over the 50-year period from 1900-1951, their presence is evident as departures from the straight line in the plots, with highest values at 1900-1902 and lowest at 1949-1951. On the assumption that the 1949-1951 values represented the least effect of acute causes of death on the overall figures, the equation for the straight line for the 40 and older group was calculated, giving values for the degenerative causes of death. These were then subtracted from the total values of q_x for other countries, and the resulting values were assumed to represent the acute causes of death.

These acute causes of death (q_x's) were found to plot out as simple exponential increases with age, with common slopes for the countries tested, but with intercepts which represent in a general way the levels of public health and medical care of the countries. Plots for four of the countries are shown in Fig. 54A. When the sum of the five major groups of degenerative diseases were similarly subtracted from the total causes of death in United States of white males 1949-1951, leaving a residue representing the acute causes of death, a similar exponential increase with age was apparent (Fig. 54B).

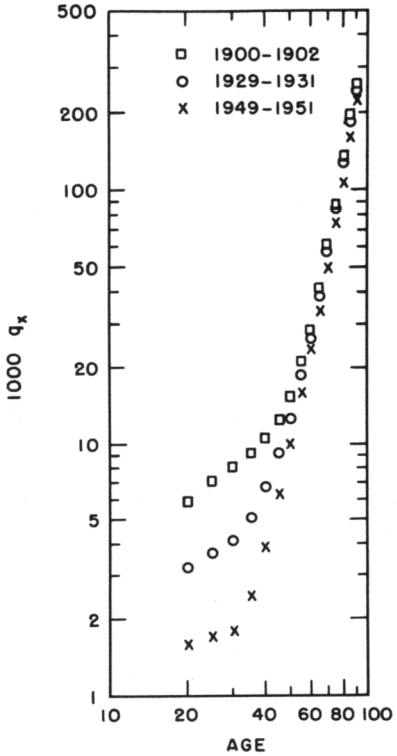

Fig. 53. Log-log plot of 1000 q_x vs. age for United States white males for 1900-1902, 1929-1931, and 1949-1951. Lines are omitted in order to show more clearly the good fit of the three sets of points on the straight portion of the curve.

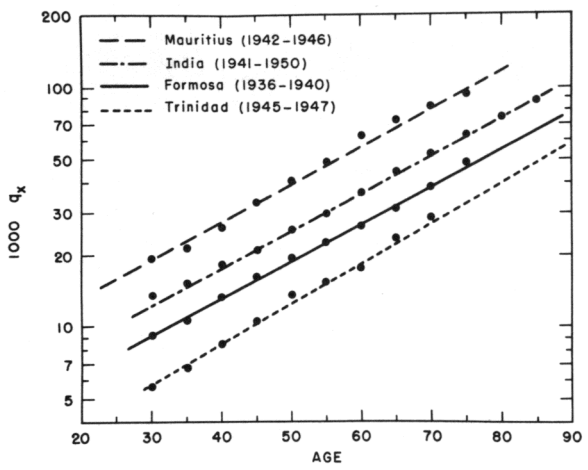

Fig. 54A. Typical semi-log plots of acute portions of 1000 q_x (total minus chronic), for four of the countries tested.

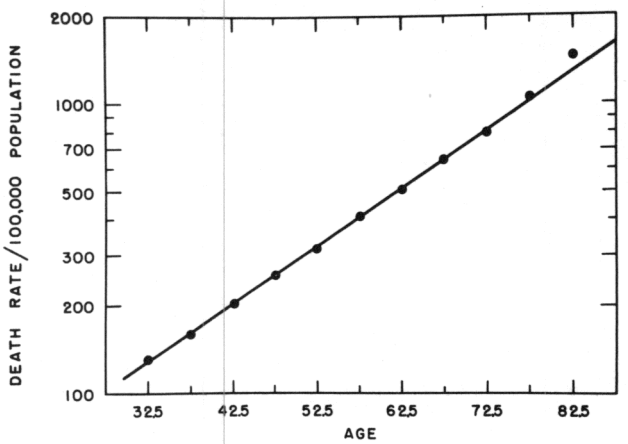

Fig. 54B. Semi-log plot of death rate per 100,000 population from acute causes of death (total minus chronic), for United States white males, 1949-1951.

It therefore appears that the death process in man can be separated broadly into chronic degenerative causes and acute causes, with death from the degenerative causes increasing as the sixth power of age and death from the acute causes increasing in simple exponential fashion.

Total and specific causes of death have previously been fitted by the Gompertzian or semi-log plot. However, it would appear from this work that the degenerative causes increase with age at a much higher rate than predicted by the Gompertzian, and are therefore better fitted by the log-log plot. On the other hand, the acute causes of death clearly are fitted by the Gompertzian function.

The presence of the sixth power relationship in a large number of different situations suggests a general underlying principle. Since we have no knowledge whatever of what this principle is in biological terms, we can only speculate that it could be a very general organizational scheme which provides about five redundant elements within each essential unit. An element might be a molecule, a cell or organelle (internal structural and functional unit of a cell), a group of cells, or a whole organ. The essential units might be separate or overlapping. Carcinogenesis may be a special case of this general degenerative process.

PART IV

LABORATORY SERVICES AND ADMINISTRATION

	Page
INTRODUCTION	96
LABORATORY ORGANIZATION	96
MANAGEMENT POLICIES AND PRACTICES	97
RESEARCH AND DEVELOPMENT COSTS	98
Personnel Data	98
Average Cost Per Scientific Staff Man Year	99
Services and Administration	99
LABORATORY FACILITIES AND EQUIPMENT	100

LABORATORY SERVICES AND ADMINISTRATION

INTRODUCTION

The management activities during 1956 of particular interest are those related to an expansion of the scientific staff and to the formulation and execution of plans for additional facilities. This section provides current information on the organization, management policies, research and development costs and facilities with particular note of these two specific activities.

LABORATORY ORGANIZATION

The organization chart on page 103 provides a graphic summary of the Laboratory's scientific, service and administrative functions and of the numbers of personnel assigned. It is not intended that this chart indicate lines of authority or organizational structure. However, each organizational unit has been listed with numbers of personnel as of December 31, 1956, except that some minor adjustments were made to present more accurate functional data.

There were two significant changes in the organization of the Laboratory during 1956. The Particle Accelerator Division was organized in April and the Applied Mathematics Division was organized in November. These new divisions previously operated as groups within the Physics Division. The Particle Accelerator Division has principal responsibility for the technical aspects of the development, design and construction of a 12.5-Bev Proton Accelerator, estimated to cost $ 27 million and scheduled for completion in 1962. The assignment of division status to a specific project, while contrary to usual Laboratory practice, is believed desirable in view of the size and duration of the project and the reasonable certainty of a continuing program of high energy accelerator development. The Applied Mathematics Division provides computation services to the Laboratory, including computer programming and operation, development of computational methods and consultation. At the present time, facilities include one digital computer (AVIDAC), one analog computer (REAC), and the usual assortment of desk calculators and other minor equipment. The immediate plans are for a sizeable increase in staff and extensive replacements and additions of equipment. This change in organization results from the increasing need for such services by a larger and more diverse portion of the scientific staff.

Three new permanent committees were established during 1956. These actions were principally a formalization of past practice and were considered necessary to improve communications within the Laboratory. The three new committees are: The Laboratory Policy Committee, whose principal responsibility is to review and make recommendations relative to the suitability of present administrative and service activities; the Reactor Development Program Committee, which periodically reviews all aspects of the reactor program with the intent of reaching Laboratory-wide agreement and understanding as to the immediate and long-term future course of the program; and the Administrative Committee, which serves as a means of keeping the members of the

central administrative groups informed with respect to a wide variety of matters which may not be communicated in the day-to-day activities of these personnel.

MANAGEMENT POLICIES AND PRACTICES

During the year ending December 31, 1956 there were many problems to be faced by the Laboratory management, and there were a number of changes and formalizations of policies, all with the objective of providing the most satisfactory conditions for research and development activities. There were changes in travel policies, changes in personnel administration, issuance, or substantial revision of management manuals in such areas as security, property management, radiation safety and procurement. Most attention, however, was given to the more basic problems of development and maintenance of staff and providing the staff with adequate facilities.

The need for more attention to staff development and maintenance resulted from significant additional program commitments particularly in reactor development and high energy accelerator development, as well as from the increasing demand by private industry for scientists and engineers with training and experience in nuclear energy. In general the program is directed towards more publicity of the Laboratory's programs and accomplishments, particularly by means which will reach prospective employees and towards training of young scientists. The publicity approach has included 1) considerable advertising in professional journals, 2) distribution of brochures on facilities, program and environment through the present staff and through academic institutions, 3) direct contacts by the Laboratory's senior staff with the academic staff of universities, 4) exhibits and films of significant accomplishments, and 5) general extension of relations with public news media. Training programs include lecture and laboratory courses for present staff and technicians; one-year post-doctoral appointments in the physical and biological sciences administered by the National Research Council; two-year appointments, including ten months of full-time attendance at lecture and laboratory courses for recent M.S. or Ph.D. graduates interested in reactor technology; summer employment programs for university faculty, graduate students and undergraduates, and one or two-year assignments at the Laboratory for employees of private companies. While some of these activities are relatively new and results are difficult to measure in any short period of time, the indications provide considerable encouragement. The Laboratory management believes that the program meets the scientific personnel shortage problem in a way that is beneficial to the national economy as well as to the Laboratory itself.

RESEARCH AND DEVELOPMENT COSTS

(A comparison of operations in the year ending June 30, 1956 with the previous year and year ending June 30, 1957 estimates)

Personnel Data

	Average Employment FY 1955	Average Employment FY 1956	Employment at 12/31/56	Estimated Employment FY 1957
Scientific Staff	509	560	643	680
Other Research and Development	386	442	517	533
Shop Services - Direct Program	394	423	475	479
Technical Services	139	143	161	165
General Services	276	269	262	260
Buildings, Grounds and Utilities	284	287	314	312
Security	171	160	159	160
Administration	155	151	151	161
Total Non-Scientists	1,805	1,875	2,039	2,070
Total Laboratory	2,314	2,435	2,682	2,750

Ratios of Non-Scientist to Scientist

Other Research and Development	0.76	0.79	0.80	0.78
Shop Services - Direct Program	0.77	0.75	0.74	0.70
Technical Services	0.27	0.25	0.25	0.24
General Services	0.54	0.48	0.41	0.38
Buildings, Grounds and Utilities	0.56	0.51	0.49	0.46
Security	0.34	0.29	0.25	0.24
Administration	0.30	0.27	0.23	0.24
	3.54	3.34	3.17	3.04

Because of increased activities the average employment of scientific staff in FY 1956 was 10% above the FY 1955 level; employment of other personnel increased less than 4% in the same period. Current estimates for FY 1957 indicate that a further expansion of 21% can be made in the scientific staff with only a 10% increase in other personnel. The ratios of the non-scientific to scientific population indicate that these FY 1957 estimates are realistic. It should also be noted from the above data that the direct research service activities remain relatively constant with staff effort, but that all other services are reduced. In fact some reduction in absolute numbers was possible for general services, security and administration, even with the 10% staff increase.

The staff increase from FY 1955 to FY 1956 and from FY 1956 to FY 1957 are distributed equally between the reactor programs and the research programs. The reactor situation is one of general expansion, whereas the expansion in the research program is for the most part related to development and design of a 12.5-BEV proton accelerator.

Average Cost Per Scientific Staff Man Year*

(In Thousands of Dollars)

	Actual		Estimated
	FY 1955	FY 1956	FY 1957
Research and Development (including Shop Services - Direct Program)	$21.3	$22.6	$25.9
Technical Services	2.0	2.0	1.9
General Services	3.3	3.0	2.5
Buildings Grounds and Utilities	4.7	4.8	4.4
Security	1.9	1.7	1.5
Administration	2.2	2.1	2.0
General Expense	1.0	1.0	.8
Total Indirect Costs	$15.1	$14.6	$13.1
Total Costs	$36.4	$37.2	$39.0

*Excludes cost of Specific Reactor Construction (BORAX, EBWR and ALPR)

The increases in direct costs in the above table result principally from increases in wage rates; however, the estimates for FY 1957 do include several major experimental projects and extensive mock-up work, particularly for the reactor programs. Furthermore, if wage rates had remained at FY 1955 levels, the total indirect cost per scientist would be less than $14,000 in FY 1956 and about $12,300 in FY 1957. The following table provides functional details of the indirect costs.

Services and Administration

(In Thousands of Dollars)

	FY 1955		FY 1956		Estimated FY 1957	
	Man Years	Cost	Man Years	Cost	Man Years	Cost
Industrial Hygiene and Safety	78	$ 511	80	$ 575	93	$ 665
Health	14	103	15	106	15	110
Technical Information	36	342	37	353	45	445
Special Materials	25	168	26	180	27	189
Buildings, Grounds and Utilities, Operations and Maintenance	284	2,344	287	2,642	312	2,928
Security	171	966	160	948	160	976
General Administration	50	463	49	495	50	509
Accounting	71	448	68	454	72	514
Materials Handling	133	853	123	844	114	840
Communications	27	239	30	244	28	255
Fire Protection	39	249	38	262	38	277
Personnel	34	203	34	226	39	327
Procurement	29	173	29	184	30	193
Food Services	34	32	34	17	35	33
General Expense		501		561		569
	1,025	$7,595	1,010	$8,091	1,058	$8,830
At FY 1955 - Labor Rates		$7,595		$7,747		$7,997

LABORATORY FACILITIES AND EQUIPMENT

The acquisition cost of completed facilities and equipment on hand at the Laboratory at December 31, 1956 was as follows:

		(In Thousands of Dollars)
Buildings		
Research and Development		$42,931
All Other Buildings		7,347
		$50,278
Utilities, Roads and Land Improvements		15,550
Total Facilities		$65,828
Equipment		
Laboratory	$9,591	
Reactors and Accelerators	3,283	
Shop	2,747	
Office	1,358	
Motor Vehicles	437	
Heavy Mobile	324	
All Others	1,992	
Total Equipment		$19,732
Total Facilities and Equipment		$85,560

The following major items were completed during the year ending December 31, 1956.

	(In Thousands of Dollars)
Experimental Boiling Water Reactor Building	$ 1,000
Ventilation Improvements - Chemistry Building	466
Addition to Reactor Engineering Building	304
Liquid Metals Mock-up Building	290
Bent Crystal Spectrometer	219
Ventilation Improvements - Physics Building	165
Metallurgy Laboratory for International School	164
Convert Quonset to Accelerator Development Space	149
Universal Counting Circuits	113

The following major facilities, equipment, and experimental projects were under construction at December 31, 1956.

	Estimated Cost (In Thousands of Dollars)
Experimental Fuel Fabrication Facility	$4,000
Argonne Low Power Reactor	1,300
Chemical Engineering Hot Laboratory	867
High Speed Digital Computer ("George")	300
3.5-Mev Van de Graaff and Building	284
Thorium Oxide Critical and Exponential	273
10' 90° High Resolution Mass Spectrometer	264
Modifications to Experimental Breeder Reactor I	225
Neutron Velocity Selector	145
60" Scattering Chamber	114
Welding Shop	106

In addition to the above, design work is in progress for the following major facilities and equipment. Funds are available except as noted.

	Estimated Cost (In Thousands of Dollars)
Experimental Breeder Reactor II	$22,800 (1)
Boiling Test Facility (ARBOR)	8,500
Shielded Rooms for High Gamma Emitting Pu	1,800
Zero Power Reactor Facility	1,500
Transient Guest Facility	533
Ventilation Improvements - West Area Buildings	476
Analog Computer	325 (2)
High Energy Pulsed Electron Accelerator	275 (2)
Shielded Room for Metallurgy	161
Shielded Room for Cyclotron Service	148
2 - 12" 60° Mass Spectrometers	140 (2)

(1) Revised estimate - additional appropriation to be requested.

(2) Cannot be procured until additional funds are allocated.

It is planned to start construction of the following additional projects prior to June 30, 1959.

	Estimated Cost (In Thousands of Dollars)
12.5-Bev Proton Accelerator	$27,000
Alpha Metallurgy Building	12,000
Utility Additions	7,500
Irradiation Test Reactor (10MW)	5,500
Administration and Service Building	5,000
Reactor Engineering Building	2,200
10-Mev Van de Graaff and Building	2,000
Chemical Engineering Laboratories	1,120
Remote Control Building	875
Cafeteria	850
Plant Maintenance Building	750
Computer Facility	720
Electronics Building	710
Industrial Hygiene and Safety Building	480
Research Reactor Improvements (2 MW to 4 MW)	380
Site Access Roads	250
10-Curie Gamma Facility (Biology)	125
Gamma Analysis Facility (Chemical Engineering)	100
Chemistry Hot Laboratory	(1)
Research Reactor (250 MW)	(1)

(1) No estimates made.

FUNCTIONAL ORGANIZATION CHART

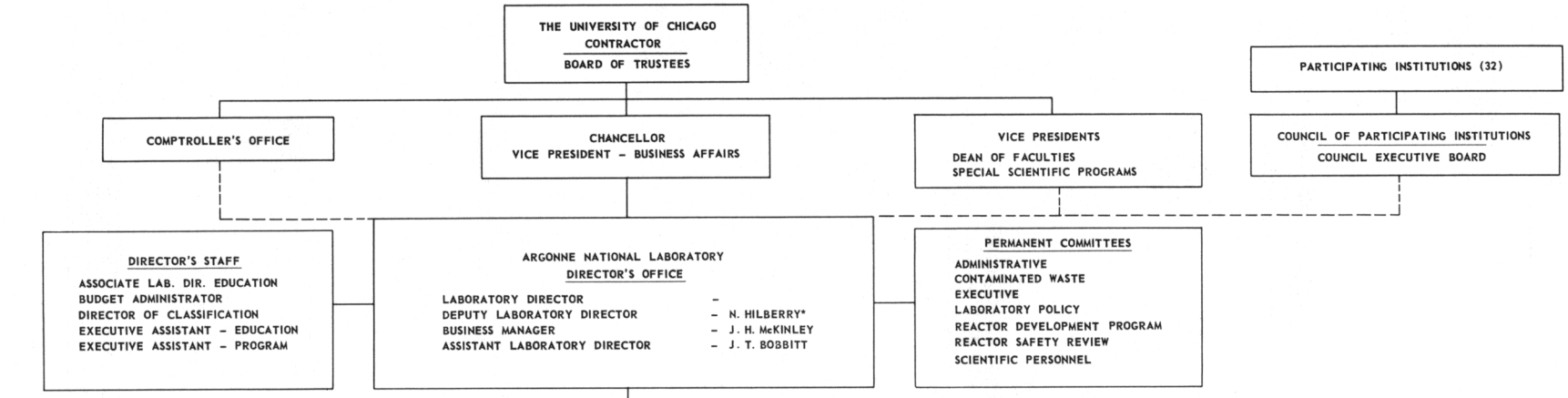

GENERAL SERVICES & ADMINISTRATION

	NUMBER OF EMPLOYEES	
	MANAGERIAL & PROFESSIONAL	OTHER
ACCOUNTING	21	51
BUSINESS MANAGER'S OFFICE	11	7
BUILDINGS, GROUNDS & UTILITIES	60	254
COMMUNICATIONS	4	24
FIRE PROTECTION	9	29
FOOD SERVICES	8	28
HEALTH SERVICES	8	7
LABORATORY DIRECTOR'S OFFICE	8	7
MATERIALS HANDLING	15	101
PERSONNEL	13	15
PURCHASING	14	15
SECURITY	29	130
OTHER	6	12
TOTALS	206	680

SCIENTIFIC PROGRAMS & SERVICE

	DIRECTOR	NUMBER OF EMPLOYEES	
		SCIENTIST	OTHER
APPLIED MATHEMATICS	D. A. FLANDERS	22	6
BIOLOGY & MEDICINE	A. M. BRUES	68	75
CHEMICAL ENGINEERING	S. LAWROSKI	60	74
CHEMISTRY	W. M. MANNING	113	51
IDAHO (REACTOR ENGINEERING)	M. NOVICK	16	23
INTERNATIONAL SCHOOL	R. G. TAECKER	13	11
METALLURGY	F. G. FOOTE	52	66
PARTICLE ACCELERATOR	J. J. LIVINGOOD	20	15
PHYSICS	L. A. TURNER	58	27
RADIOLOGICAL PHYSICS	J. E. ROSE	16	10
REACTOR ENGINEERING	A. H. BARNES	143	103
REACTOR OPERATIONS	W. H. McCORKLE	6	20
REMOTE CONTROL	R. C. GOERTZ	15	19
TEMPORARY POSITIONS	--	29	16
OTHER SCIENTIFIC	--	12	1
TOTALS		643	517

TECHNICAL SERVICES & SHOPS

	NUMBER OF EMPLOYEES	
	MANAGERIAL & PROFESSIONAL	OTHER
CENTRAL SHOPS (MECHANICAL)	32	262
ELECTRONICS	15	33
GRAPHIC ARTS	5	35
INDUSTRIAL HYGIENE & SAFETY	28	62
PLANT ENGINEERING & INSTALLATION	13	54
REACTOR DRAFTING	1	25
SPECIAL MATERIALS	12	14
TECHNICAL INFORMATION	15	30
TOTALS	121	515

*APPOINTED LABORATORY DIRECTOR FEBRUARY 20, 1957

DECEMBER 31, 1956

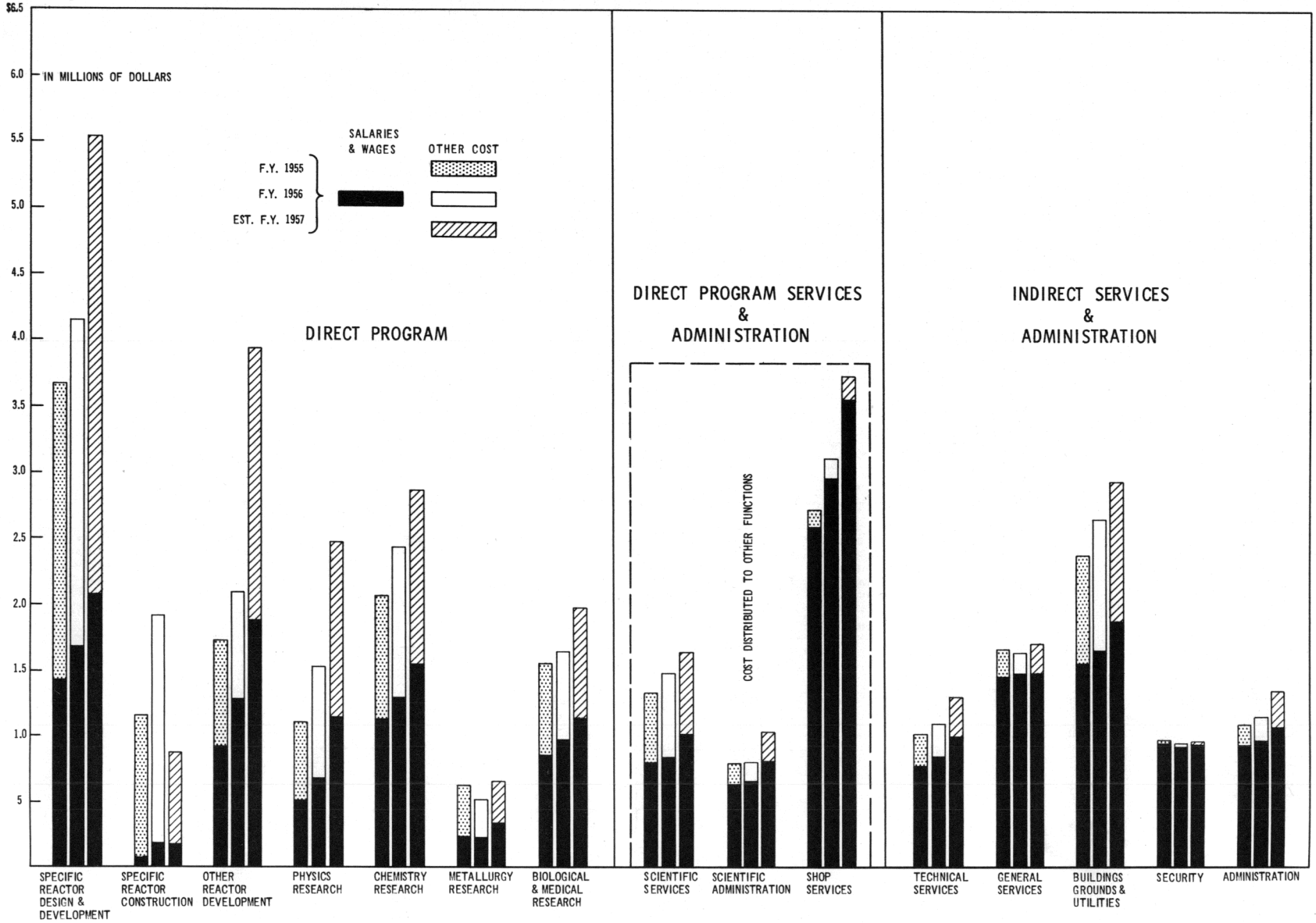

LABORATORY COST (IN MILLIONS)

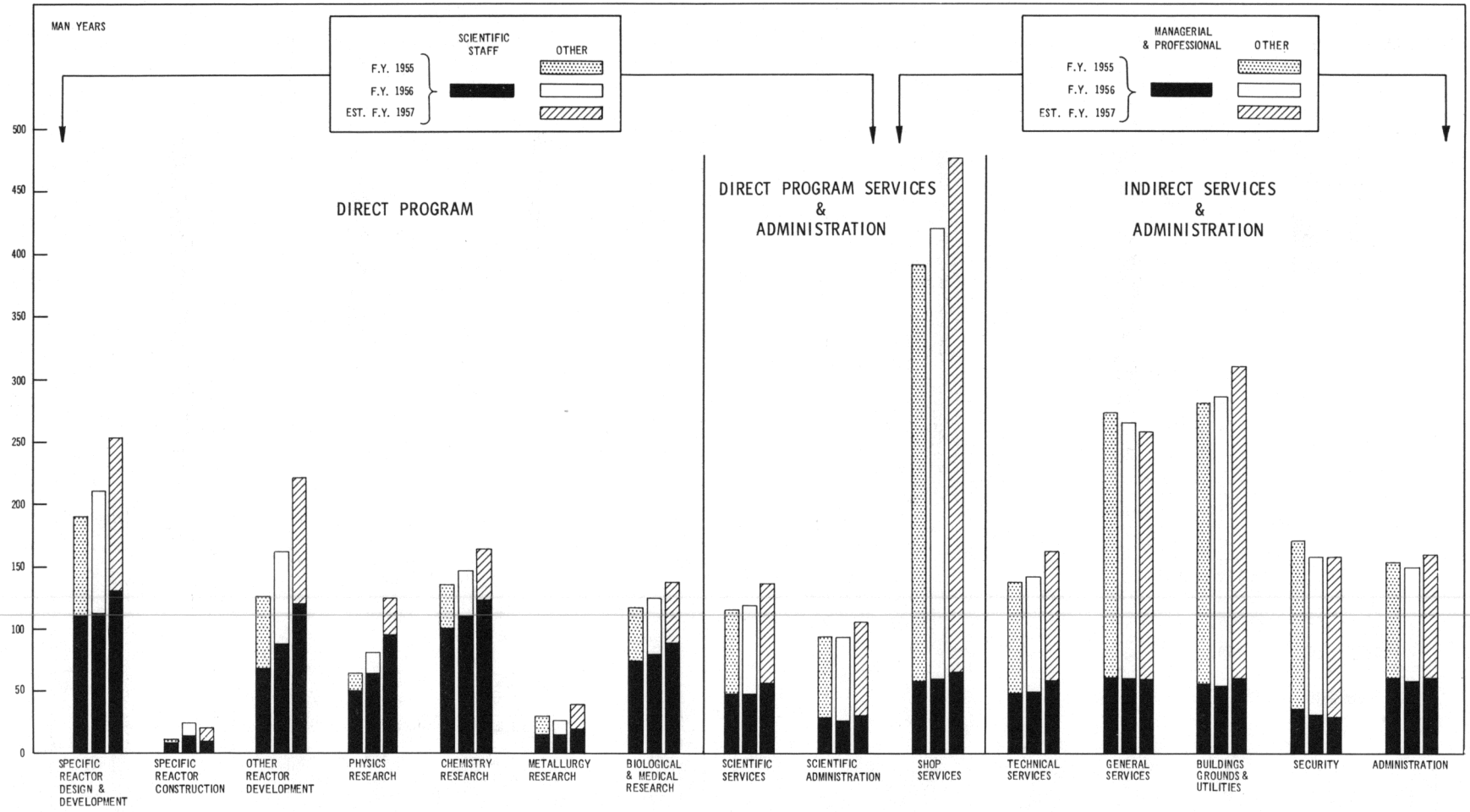

LABORATORY MAN YEARS

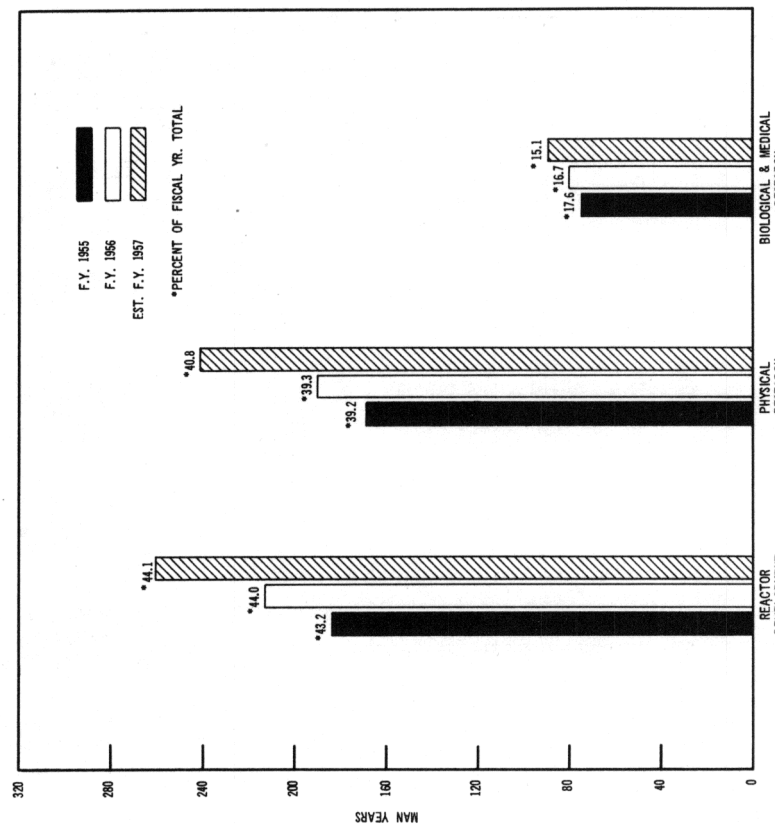

RESEARCH AND DEVELOPMENT PROGRAM SCIENTIFIC MAN YEAR SUMMARY

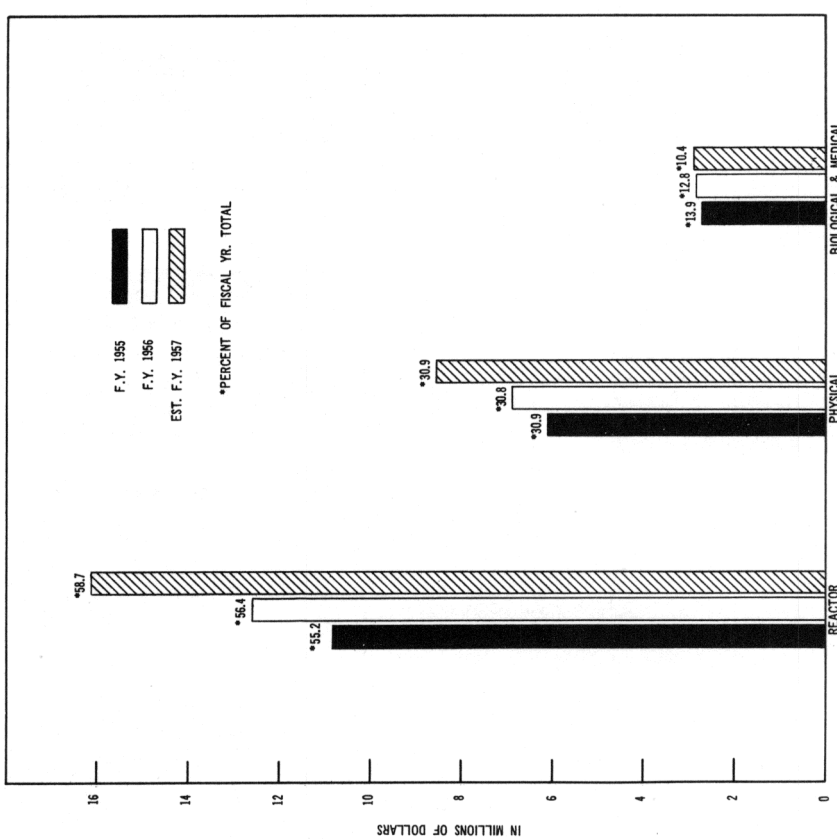

RESEARCH AND DEVELOPMENT PROGRAM COST SUMMARY

APPENDIX

SCIENTIFIC PUBLICATIONS OF THE STAFF OF ARGONNE NATIONAL LABORATORY SINCE THE PREVIOUS ANNUAL REPORT

Abraham, B. M., Osborne, D. W., and Weinstock, B.
Calorimetric Measurement of the Heat of Vaporization of Liquid He^3
Bull. Am. Phys. Soc. 1 349 (November 23, 1956)

Abraham, B. M. (See Osborne, D. W.)

Ackermann, R. J. and Thorn, R. J.
Gaseous Oxides of Aluminum, Tungsten and Tantalum
J. Am. Chem. Soc. 78 4169 (1956)

Ackermann, R. J., Thorn, R. J. and Gilles, P. W.
Vapor Pressure of Thoria
J. Am. Chem. Soc. 78 1767 (1956)

Ackermann, R. J. (See Winslow, G. H.)

Adams, R. M., and Katz, J. J.
A New Variable Thickness Infrared Cell and the Infrared Spectra of HF, DF, H_2O, and D_2O
J. Opt. Soc. 46 895-898 (1956)

Adams, R. M. (See Freedman, M. S.)

Ader, M. (See Feder, H. M.)
(See Kaplan, L.)

Anderson, E. (See Beams, H. W.)

Andre, C. G., Huizenga, J. R., Mech, J. F., Ramler, W. J., Rauh, E. G. and Rocklin, S. R.
Proton Cross Sections of Bi^{209}
Phys. Rev. 101 645-651 (1956)

Bankoff, S. G.
The Contortional Energy Requirement in the Spreading of Large Drops
J. Phys. Chem. 60 952 (1956)

Barnes, R. F. (See Diamond, H.)
(See Friedman, A. M.)
(See Mech, J. F.)

Barton, A. D.
Glycogen Particles in Rat Liver Homogenates
Fed. Proc. 15 10 (March 1956)

Barton, A. D. (See Laird, A. K.)

Baumgardner, J. B. (See Lynch, F. J.)

Beams, H. W., Tahmisian, T. N., Devine, R. L., and Anderson, E.
Electron Microscope Studies on the Dictyosomes and Acroblasts in the Male Germ Cells of the Cricket
J. Biophys. Biochem. Cytol. 2 (4) 123-128 (July 1956)

Beams, H. W., Tahmisian, T. N., Anderson, E., and Devine, R. L.
Studies on the Structure of the Nuclear Membrane in the Larval Gonads of Heliothis obsoleta
Proc. Soc. Exptl. Biol. Med. 91 473-475 (1956)

Berlman, I. B. and Marinelli, L. D.
"Twin" Scintillation Fast Neutron Detector
Rev. Sci. Instr. 27 858-859 (1956)

Bernstein, E. Katz, Stearner, S. P. and Brues, A. M.
Liver Function in the Chick Following X-Irradiation
Am. J. Physiol. 186 543-548 (1956)

Bevilacqua, F.
Electrical-Discharge Saw Cuts "Hot" Metal
Am. Machinist 100 125-129 (November 19, 1956)

Bingle, J. (See Fischer, J.)

Bollinger, L. M., Coté, R. E., Hubert, P., LeBlanc, J. M. and Thomas, G. E.
Energy Dependence of ν for Pu^{239}
Bull. Am. Phys. Soc. 1 165 (April 26, 1956)

Bollinger, L. M., and Palmer, R. R.
Neutron Cross-Section Measurements of Antimony, Gallium, Cadmium, and Mercury
Phys. Rev. 102 228 (1956)

Bollinger, L. M. (See Coté, R. E.)
(See Dahlberg, D. A.)
(See Saplakoglu, A.)

Bowe, J. C.
Drift Velocity and Average Energy of Electrons in Noble Gases
Bull. Am. Phys. Soc. 1 342 (November 23, 1956)

Brar, S. S., and Marinelli, L. D.
Ionization in Heavy Gases of Low Z
Rad. Res. 5 471 (1956)

Brues, A. M.
Modes of Radiation Injury
Chemistry 29 (1) 21-30 (September 1955)

Brues, A. M.
Radiation as a Carcinogenic Agent
Rad. Res. 3 272-280 (1955)

Brues, A. M. (See Bernstein, E. Katz)
(See Stearner, S. P.)
(See Stroud, A. N.)

Brunson, G. S., Pettitt, E. N., McCurdy, R. D.
Delayed Neutron Yields in Pu, U^{233}, U^{238}, and Th Relative to Yield in U^{235}
Nuclear Science and Engineering 1 174-184 (1956)

Buck, W. L. (See Swank, R. K.)

Burgy, M. T., Allison, S. K., and Littlejohn, C. S.
Stopping Powers of Various Gases for Helium and Lithium Ions
Bull. Am. Phys. Soc., 1 342 (November 23, 1956)

Burson, S. B. (See Martin, D. W.)

Butler, J. W.
Sampling Random Numbers
Proc. Symposium on Monte Carlo Methods, Univ. Florida, March 16, 1954
Ed. H. A. Mayer, New York: John Wiley & Sons, 1956. pp. 249-264

Campos, F. D. (See Sidhu, S. S.)

Casson, H.
Inelastic Scattering of 14-Mev Neutrons Measured by Time-of-Flight
Bull. Am. Phys. Soc. Series II., Vol. 1 56 (January 30, 1956)

Cerutti, B. C., Lichtenberger, H. V., Okrent, D., Rice, R. E., and Thalgott, F. W.
ZPR-III, Argonne's Fast Critical Facility
Nuclear Science and Engineering 1 126-134 (1956)

Chatterley, D. M. (See Stroud, A. N.)

Chavin, W.
Thyroid Distribution and Function in the Goldfish Carassium auratus L. as Determined by the Uptake of Tracer Doses of Radioiodine
Anat. Rec. 124 272 (1956)

Chellew, N. (See Feder, H. M.)

Childs, W. J., and Goodman, L. S.
Spin and Magnetic Moment of the 1.7-Hr. Metastable State of In^{113}
Bull. Am. Phys. Soc. 1 342 (November 1956)

Christian, E. J. (See Stearner, S. P.)

Chupka, W., Berkowitz, J., and Inghram, M. G.
Molecular Species Evaporating from ZrO_2 and $Zr-ZrO_2$ Mixtures
Bull. Am. Phys. Soc. 1 202 (April 26, 1956)

Chupka, W. A., Berkowitz, J., and Kistiakowsky, G. B.
Mass Spectrometric Study of the Kinetics of Nitrogen Afterglow
J. Chem. Phys., 25 457 (1956)

Chupka, W. A., Inghram, M. G., and Porter, R. F.
The Dissociation Energy of Gaseous LaO
J. Chem. Phys. 24 792-795 (1956)

Chupka, W. A. (See Inghram, M. G.)
(See Stanton, H. E.)

Cimbleris, Borisas (SNSE)
Pneumatic Local-Type Oscillator
Bull. Am. Phys. Soc. Series II, Vol. 1 68 (January 30, 1956)

Claassen, H. H., Weinstock, B., and Malm, J. G.
Raman Spectrum of UF_6
J. Chem. Phys. 25 426-427 (1956)

Claassen, H. H. (See Malm, J. G.)

Clark, J. W. (See Jordan, D. L.)
(See Vogel, H. H., Jr.)

Cohen, D., Amis, E. S., Sullivan, J. C., and Hindman, J. C.
Kinetics of the Reaction Between Neptunium (IV) and Neptunium (VI) in Mixed Solvents
J. Phys. Chem. 60 701-702 (1956)

Cohen, D., Sullivan, J. C., Amis, E. S., and Hindman, J. C.
Isotopic Exchange Reactions of Neptunium in Solution. IV. The Effect of Variation of Dielectric Constant on the Rate of the Np(V)-Np(VI) Exchange
J. Am. Chem. Soc. 78 1543-1545 (1956)

Cohen, D. (See Sullivan, J. C.)

Cook, J. M. (See Hall, J. F.)

Coté, R. E., and Bollinger, L. M.
Interference between Fission Resonances
Bull. Am. Phys. Soc. 1 328 (November 23, 1956)

Coté, R. E., Bollinger, L. M., LeBlanc, J. M., and Thomas, G. E.
Neutron Cross-Section Measurements on Plutonium
Bull. Am. Phys. Soc. 1 187 (April 26, 1956)

Coté, R. E. (See Bollinger, L. M.)
(See Saplakoglu, A.)

Crespi, H., Uphaus, R., and Katz, J. J.
The Ultracentrifugal Behavior of Some Proteins in Nonaqueous Solvents
J. Phys. Chem. 60 1190 (1956)

Crosbie, E. A., and Hamermesh, M.
Clebsch-Gordon Coefficients for the Symmetric Groups
Bull. Am. Phys. Soc. 1 209 (April 26, 1956)

Dahlberg, D. A., and Bollinger, L. M.
Neutron Cross Sections of Zinc
Phys. Rev. 104 1006-1008 (1956)

Daniels, E. W.
Recovery from Lethal X-Radiation Injury in Amoebae Following Injection of Centrifugal Portions of Nonirradiated Cells
Rad. Res. 5 604 (1956)

Daniels, E. W.
X-Irradiation of the Giant Amoeba Pelomyxa illinoisensis
J. Exptl. Zool. 130 183-198 (1955)

Davidson, W. C., and Goldberger, M. L.
Comparison of Spin-Flip Dispersion Relations and Pion Nucleon Scattering Data
Phys. Rev. 104 1119-1121 (1956)

Day, P. P.
K-Capture Branch in Tm^{170}
Phys. Rev. 102 1572-1574 (1956)

Day, P. O. (See Primak, W.)

Delbecq, C. J., Smaller, B., and Yuster, P. H.
Paramagnetic Resonance Investigation of Irradiated KCl Crystals Containing U-Centers
Phys. Rev. 104 599-604 (1956)

Delbecq, C. J. and Yuster, P. H.
Proposed Mechanism for the Conversion of U-Centers to F-Centers below 90°K
Phys. Rev. 104 605-606 (1956)

Delbecq, C. J., Yuster, P. H., and Smaller, B.
Optical Investigation of Irradiated KCl Crystals Containing U-Centers
Bull. Am. Phys. Soc. 1 125 (March 15, 1956)

Delbecq, C. (See Smaller, B.)

De Palma, R. E. (See Schlenk, F.)

Devine, R. L. (See Beams, H. W.)
(See Tahmisian, T. N.)

Diamond, H., and Barnes, R. F.
The Alpha Half-Life of Pu^{244}
Phys. Rev. 101 1064-1066 (1956)

Diamond, H. (See Fields, R. P.)
(See Mech, J. F.)

Dietrich, J. R.
The Physics of Advanced Reactors
Brit. J. Appl. Phys. Suppl. 5 S9 - S23 (1956)

Draley, J. E., and Greenberg, S.
Application of Material in Low Temperature Water and Organic Liquid-Cooled Reactors
IND Special Report Series No. 2 (February 2, 1956), American Institute of Mining and Metallurgical Engineers.

Draley, J. E., and Ruther, W. E.
Aqueous Corrosion of Aluminum. Part 1. Behavior of 1100 Alloy
Corrosion 12 31-38 (September 1956)

Draley, J. E., and Ruther, W. E.
Aqueous Corrosion of Aluminum. Part 2. Methods of Protection above 200°C
Corrosion 12 (10) 20-30 (October 1956)

Ducoff, H. S.
Radiation-Induced Fission Block in Synchronized Cultures of Tetrahymena pyriformis W
Exptl. Cell Res. 11 218-219 (1956)

Dwight, A. E.
Allotropic Transformations in Ti, Zr, and U Alloys
J. Metals 8 162 (1956)

Eggler, C., and Huddleston, C. M.
Gaseous Scintillation Counting
Nucleonics 14(4) 34-36 (April 1956)

Eggler, C., and Huddleston, C. M.
Gaseous Scintillation Counting
Trans. Prof. Group Nucl. Sci. IRE NS-3(4) 36 (November 1956)

Eggler, C., Huddleston, C. M., Krohn, V. E., and Ringo, C. R.
Measurement of Neutron Spectra of the Experimental Breeder Reactor
Nuclear Sci. Eng. 1 391-408 (1956)

Ehret, C. F., and Monk. G. S.
Design and Performance of a Biological Spectrograph
Rad. Res., 5 88 (1956)

Ehret, C. F., and Powers, E. L.
Macronuclear and Nucleolar Development in Paramecium bursaria
Exper. Cell Res. 9 241-257 (1955)

Ehret, C. F. (See Powers, E. L.)

Eib, M. (See Gordon, S. A.)

Ekstein, H.
Scattering in Field Theory
Il Nuovo Cimento 4 1017-1058 (1956)

Ekstein, H., and Schiffman, T.
Free Vibrations of Isotropic Cubes and Nearly Cubic Parallelepipeds
J. Appl. Phys. 27 405-412 (1956)

Ekstein, H., and Tanaka, K.
Insensitivity of the Scattering Matrix
Phys. Rev. 104 259-263 (1956)

Ekstein, H. (See Tanaka, K.)

Engelkemeir, D.
Nonlinear Response of NaI(Tl) to Photons
Rev. Sci. Instr. 27 589-591 (1956)

Engelkemeir, D., Fields, P. R., Fried, S., Pyle, G. L., Stevens, C. M., Asprey, L. B. Browne, C. I., Smith, R., and Spence, R.
The New Isotopes Pu^{246} and Am^{246}
J. Inorganic and Nuclear Chem. 1 (6) 345-351 (1955)

Engelkemeir, D. W. (See Huizenga, J. R.)
(See Magnusson, L. B.)

Erickson, G. F., and Kaufmann, S. G.
Neutron-Sensitive Electron Multiplier Tubes
Rev. Sci. Instr. 27 107-108 (1956)

Erickson, G. F., Kaufmann, S. G., and Pahis, L. E.
Recent Neutron Detector Studies at Argonne National Laboratory
IRE Trans. of Prof. Group on Nuclear Sci. NS-3 (3) 8-10 (June 1956)

Evans, G. H., and Strain, H. H.
Separation of Certain Alkali Metal and Alkaline Earth Cations by Electrochromatography
Anal. Chem. 28 (10) 1560-1563 (1956)

Faris, J. P. (See Stewart, D. C.)

Feder, H. M., Chellew, N., and Ader, M.
Melt Refining of Uranium
Progress in Nuclear Chemistry Series III, Process Chemistry, ed. F. R. Bruce, J. M. Fletcher, H. H. Hyman, and J. J. Katz. London: Pergamon Press, Ltd., 1956. pp. 301-308.

Feinstein, R. N.
Interpretation of Some Enzyme Activity Increases After Whole Body X-Irradiation
Rad. Res. 4 217-219 (1956)

Feinstein, R. N., and Green, F. O.
An Activator of Desoxyribonuclease in Rat Plasma
Arch. Biochem. Biophys. 60 502-504 (1956)

Feinstein, R. N., and Green, F. O.
Control of Desoxyribonuclease Activity
Fed. Proc. 15 250 (March 1956)

Feldes, J. P. (See Zinn, W. H.)

Ferentz, M. and Raboy, S.
On the Consequences of the Possible Existence of the Hyperdeuteron
Il Nuovo Cimento 4 487-490 (1956)

Ferguson, D. E. (See Stoughton, R. W.)

Ferraro, J. R., Katzin, L. I., and Gibson, G.
Heats of Solution of the Thorium Nitrate in Water and in Certain Organic Solvents
J. Inorganic and Nuclear Chem. 2 118-124 (1956)

Ferraro, J. R. (See Katzin, L. I.)

Fields, P. R., Pyle, G. L., Inghram, M. G., Studier, M. H., and Manning, W. M.
Pile Neutron Cross Sections of the Heavier Plutonium Isotopes
Nuclear Science and Eng. 1 62-67 (1956)

Fields, P. R., Studier, M. H., Diamond, H., Mech. J. F., Inghram, M. G., Pyle, G. L., Stevens, C. M., Fried, S., and Manning, W. M.
Transplutonium Elements in Thermonuclear Test Debris
Phys. Rev. 102 180-182 (1956)

Fields, P. R. (See Engelkemeir, D.)
(See Friedman, A. M.)
(See Magnusson, L. B.)
(See Mech, J. F.)
(See Smith, A. B.)

Finkel, A. J., and Hathaway, E. A.
Medical Care of Wounds Contaminated with Radioactive Materials
J. Am. Med. Asso. 161 121-126 (May 12, 1956)

Finkel, M. P.
Relative Biological Effectiveness of Internal Emitters
Radiology 67 665-672 (1956)

Finkel, M. P., and Scribner, G. M.
Mouse Cages and Spontaneous Tumors
Brit. J. Cancer 9 (3) 464-472 (1955)

Firestone, R. F.
The Radiation Chemistry of Water Vapor. The Indirect Effect on Deuterium
J. Am. Chem. Soc. 78 3226-3227 (1956)

Fischer, J. and Bingle, J.
The Vapor Pressure of Bromine from 24 to 116°C
J. Am. Chem. Soc. 77 6511-12 (1955)

Fischer, J., Bingle, J., and Vogel, R. C.
Liquid Vapor Equilibria in the System Bromine-Bromine Trifluoride
J. Am. Chem. Soc. 78 902-904 (1956)

Fischer, J., Liimatainen, R. C. and Bingle, J.
The Condensed System Bromine Trifluoride-Antimony Pentafluoride
J. Am. Chem. Soc. 77 5848-49 (1955)

Fisher, E. S. (See Misch, R. D.)

Flynn, K. F., Glendenin, L. E., and Steinberg, E. P.
Search for Be^{10} as a Product of Ternary Fission
Phys. Rev. 101 1492 (1956)

Flynn, R. J.
Ectoparasites of Mice
Proc. Animal Care Panel 6 75-91 (1955)

Flynn, R. J., and Jaroslow, B. N.
Nidification of Mites in the Skin of Mice (Psorergates simplex Tyrrell, 1883: Myobiidae)
J. Parasitology 42 49-52 (February 1956)

Foote, F. G.
Physical Metallurgy of Uranium
Institute of Mining and Metallurgical Engineers (October 1955)

Foote, F. G. (See McLain, S.)

Fred, M., Meggers, W. F., and Tomkins, F. S.
Emission Spectrum of Actinium
Science, 124 940 (1956)

Fred, M. (See Manning, T. E.)

Freedman, M. S., Novey, T. B., Porter, F. T., and Wagner, F., Jr.
Correction of Phosphor Backscattering in Electron Scintillation Spectrometry
Rev. Sci. Instr. 27 716-719 (1956)

Freedman, M. S., Turkevich, A., Adams, R. M., Sugarman, N., Raynor, S., and Stang, L. G., Jr.
The Slow-Neutron Absorption Cross Section of 9.2-Hr Xe^{135} by the Method of Negative Activation
J. Inorganic Nuclear Chem. 2 271 (July 1956)

Freedman, M. S. (See Huizenga, J. R.)
(See Novey, T. B.)
(See Porter, F. T.)

Fricke, H., Leone, C. A., and Landmann, W.
Effect of γ Rays on the Serological Properties of Ovalbumin
Rad. Res. 5 478 (1956)

Fried, J. M., Rosenthal, M. W., and Schubert, J.
Induced Accumulation of Metabolites with Chelating Properties in Therapy of Experimental Metal Poisoning
Proc. Soc. Exptl. Biol. Med. 92 331-333 (1956)

Fried, S. M., Pyle, G. L., Stevens, C. M., and Huizenga, J. R.
Spontaneous Fission Half-Life of Cm^{246}
J. Inorganic Nuclear Chem. 2 415 (1956)

Fried, S. M. (See Engelkemeir, D.)
(See Fields, P. R.)

Friedman, A. M., Gindler, J. E., Barnes, R. F., Sjoblom, R., and Fields, P. R.
Properties of Fm^{252}
Phys. Rev. 102 585-586 (1956)

Friedman, A. M. (See Magnusson, L. B.)
(See Smith, A. B.)

Freund, G. A.
Organic Coolant-Moderators for Power Reactors
Nucleonics 14 (8) 62-64 (August 1956)

Fuchs, L. H. (See Hoekstra, H. R.)
(See Primak, W.)

Gilles, P. W. (See Ackermann, R. J.)

Gindler, J. E., Huizenga, J. R., and Schmitt, R. A.
Photofission and Photoneutron Emission in Thorium and Uranium
Phys. Rev. 104 425-433 (1956)

Gindler, J. E. (See Friedman, A. M.)
(See Huizenga, J. R.)

Glendenin, L. E. (See Flynn, K. F.)

Goertz, R. C. (See Kelman, L. R.)

Goleb, J. A.
The Quantitative Spectrographic Determination of Zirconium and Niobium in Uranium Metal
Anal. Chem. 28 965-967 (1956)

Goodman, L. S., and Wexler, S.
Nuclear Spin and Magnetic Moment of 54-Min In^{116m}
Bull. Am. Phys. Soc. 30 12 (December 28, 1955)

Goodman, L. S. (See Childs, W. J.)

Gordon, S. A.
The Biogenesis of Natural Auxins
Chemistry and Mode of Action of Plant Growth Substances. Proceedings of International Conf. on Growth Substances, held at Wye College, University of London, July 1955. (London: Butterworths Publications, 1956) pp. 65-75

Gordon, S. A.
Auxin Biosynthesis--A Cytoplasmic Locus of Radiation Damage Progress in Radiobiology-Proc. Intern. Conf. on Radiobiology, Cambridge, August 1955. (Edinburgh: Oliver and Boyd, 1956) pp. 44-47

Gordon, S. A., and Eib, M.
Auxin Transport in the Phototropic Response
Plant Physiol. 31 (Suppl.) 14 (August 26, 1956)

Gordon, S. A., and Moss, R. A.
The Activity of S-(Carboxymethyl)-Dimethyldithiocarbamate as an Auxin
Plant. Physiol. 31 (Suppl.) 27 (August 26, 1956)

Gordon, S. A. (See Paleg, L. G.)

Grahn, D., and Hamilton, K.
Acute Lethal Response of Four Inbred Mouse Strains to Single-Dose Whole-Body X-Irradiation
Rad. Res. 5 479 (October 1956)

Grahn, D., Sacher, G. A., and Walton, H., Jr.
Comparative Effectiveness of Several X-Ray Qualities for Acute Lethality in Mice and Rabbits
Rad. Res. 4 228-242 (March 1956)

Grahn, D. (See Lesher, S.)

Greenberg, E., and Westrum, E. F., Jr.
Heat Capacity and Thermodynamic Functions of Uranium Chloride from 6° - 350°K
J. Am. Chem. Soc. 78 4526 (1956)

Greenberg, E., and Westrum, E. F., Jr.
Heat Capacity and Thermodynamic Functions of Uranium (IV) Oxychloride and Uranium (IV) Oxybromide from 10° - 350°K
J. Am. Chem. Soc. 78 5144 (1956)

Greenberg, S. (See Draley, J. E.)

Grossweiner, L. I.
Metastable States of Photoexcited Ovalbumin and Constituents
J. Chem. Phys. 24 1255-1256 (1956)

Grossweiner, L. I., and Matheson, M. S.
Short-Lived Species from the Photolysis of Aqueous Alkali Halides and Halogen Solutions
J. Chem. Phys. 23 2443-2444 (1955)

Gruen, D.
Chromatography and Spectrophotometry of Fused Salts
Nature 178 1181 (1956)

Gruen, D. M., Conway, J. G., McLaughlin, R. D., and Cunningham, B. B.
The Fluorescence Spectrum of Am^{+3} in $LaCl_3$
J. Chem. Phys. 24 1115-1116 (1956)

Gruen, D. M., Malm, J. G., and Weinstock, B.
The Magnetic Susceptibility of Plutonium Hexafluoride
J. Chem. Phys. 24 905-906 (1956)

Gurian, J. M.
Note on Fitting the Multi-hit Survival Curve
Biometries 12 123-126 (June 1956)

Gustafson, P. F., and Marinelli, L. D.
Study of an Accidental Puncture Contaminated with Th^{227}
Rad. Res. 5 481 (October 1956)

Gustafson, P. F., and Marinelli, L. D.
A Th^{227} Accident
Radiol. 66 269 (1956)

Hall, J. F., and Cook, J. M.
Programming a Monte Carlo Problem
Proceedings of the Second Annual Computer Applications Symposium. Armour Research Foundation, October 24, 1955. pp. 94-104.

Hall, Vincent
Observations on the Organization, Development, and Ultramicroscopic Structure of the Capillaries of the Renal Glomerulus
Am. J. Path. 32 646 (May-June 1956)

Hall, V. C., Jr. (See Zinn, W. H.)

Hamermesh, B. (See Rose, D.)

Hamermesh, M. (See Crosbie, E. A.)
(See Sokoloff, J.)

Hamilton, K. (See Grahn, D.)

Hampson, D. C. (See Rodger, W. A.)

Hanna, S. S., Krone, R. W., and Everett, A.
Lifetime of the First Excited State in Na^{23}
Bull. Am. Phys. Soc., 1 329 (November 23, 1956)

Hanna, S. S., LaVia, E. C., and Gelinas, R. W.
Alpha Spectrum in the Li^7 (p, γ) Be^{8*} (2) He^4 Reaction
Phys. Rev., 103 143 (1956)

Hanna, S. S., and Shaforth, S. M.
Angular Correlation in the 2.86-Mev Cascade in B^{10}
Phys. Rev., 104 399 (1956)

Haroldsen, R. O. (See Zinn, W. H.)

Hart, E. J.
Radiation Chemistry of the Aqueous Formic Acid-Ferric Sulfate System
J. Am. Chem. Soc. 77 5786-88 (1955)

Hart, E. J., Ramler, W. J., and Rocklin, S. R.
Chemical Yields of Ionizing Particles in Aqueous Solutions: Effect of Energy of Protons and Deuterons
Rad. Res. 4 378-393 (May 1956)

Hart, E. J., and Walsh, P. D.
Radiation Chemistry of Aqueous Ferrous Sulfate-Cupric Sulfate Solutions. Effect of 4.3-Mev Alpha Rays
Rad. Res. 5 603 (November 1956)

Hathaway, E. A. (See Finkel, A. J.)

Haugsnes, J.
Total Neutron Cross Sections at 14 Mev
Bull. Am. Phys. Soc. 1 187 (April 26, 1956)

Hayden, R. J., and Wasserburg, G. J.
A^{40} -K^{40} Dating
Nuclear Processes in Geologic Settings. Natl. Res. Counc. Nucl. Sci. Series Rept. 19. Natl. Acad. Sci. Publication 400. Washington, D. C., July 31, 1956, pp. 131-4

Hayden, R. J., Wasserburg, G. J., and Jensen, K. J.
A^{40}/K^{40} Dating of Igneous Rocks and Sediments
Geochim. Cosmochim. Acta 10 (3) 153 (1956)

Hayden, R. J., Wetherill, G. W., Wasserburg, G. J., Aldrich, L. T., and Tilton, G. R.
Decay Constants of K^{40} as Determined by the Radiogenic Argon Content of Potassium Minerals
Phys. Rev. 103 987 (1956)

Heaton, L. (See Sidhu, S. S.)

Henderson, D. J. (See Mech, J. F.)

Hennig, G. R.
Properties of Graphite Compounds
Proceedings of the Conference on Carbon, Univ. of Buffalo, Buffalo, N. Y. June, 1956 pp. 103-112

Hennig, G. R., and Smaller, B.
Paramagnetic Resonance Absorption in Graphite
Proceedings of the Conference on Carbon, Univ. of Buffalo, Buffalo, N. Y., June 1956 pp. 113-115

Hennig, G. R. (See Knater, M. A.)
(See Montet, G. L.)

Hess, D. C., and Edwards, G.
Isolation and Isotopic Analysis of Lead in Meteorites and Rocks "Nuclear Processes in Geologic Settings." Natl. Res. Counc. Nucl. Sci. Series Rept. 19. Natl. Acad. Sci. Publication 400 (Washington, D. C., July 31, 1956) pp. 100-108

Hilberry, N.
Preparing for the Day You Build an Atomic Power Plant in Somebody's Back Yard
Elec. Light and Power 34 (25) 24 (December 1, 1956)

Hildebrandt, R. A. (See Kaplan, L.)

Hill, M. S. (See Straube, R. L.)

Hindman, J. C. (See Cohen, D.)
(See Sullivan, J. C.)

Hirsch, A. (See Mech, J. F.)

Hoekstra, H. R.
Oxygen Isotope Variations in Some Uranium Minerals
Nuclear Processes in Geologic Settings. Natl. Res. Counc. Nucl. Sci. Series Rept. 19. Natl. Acad. Sci. Publication 400. Washington, D.C., July 31, 1956, pp. 160-165

Hoekstra, H. R., and Fuchs, L. H.
Synthesis of Coffinite -- $USiO_4$
Science 123 105 (1956)

Holland, R. E., and Ehlert, R. C.
Time-of-Flight Measurements on Neutrons from the Reaction $Mn^{55}(p,n)$ Fe^{55}
Bull. Am. Phys. Soc. 1 327 (November 23, 1956)

Holt, B. D.
Determination of Micro Quantities of Hydrogen
Anal. Chem. 28 1153-1157 (1956)

Huddleston, C. M. (See Eggler, C.)

Huizenga, J. R., Herber, R. H., Sugihara, T. T., Coryell, C. D., and Bennet, W. E.
Probable Absence of K Capture in the Decay of Lead-205
Phys. Rev. 103 955 (1956)

Huizenga, J. R., Engelkemeir, D. W., Freedman, M. S., Porter, F. T., and Gindler, J. E.
Radiations of Np^{234}
Bull. Am. Phys. Soc. 1 171 (April 26, 1956)

Huizenga, J. R., Krohn, V. E., and Raboy, S.
Angular Correlation of Gamma Rays in Pb^{204m}
Bull. Am. Phys. Soc. Series II, Vol. 1 43 (Jan. 30, 1956)

Huizenga, J. R., Krohn, V. E., and Raboy, S.
Angular Correlation of Gamma Rays in Pb^{204m}
Phys. Rev. 102 1063-1065 (1956)

Huizenga, J. R., and Wing, J.
Long-Lived Lead-205
Phys. Rev. 102 926-927 (1956)

Huizenga, J. R. (See Andre, C. G.)
(See Fried, S. M.)
(See Gindler, J. E.)
(See Mech, J. F.)

Hutchison, D. A.
Secondary Ion-Radical Processes in Electron Beams at Low Pressures
Bull. Am. Phys. Soc. 1 228 (June 21, 1956)

Hutchison, D. A.
Critical Ionization Potentials Using a Parallel-Plate Energy Selector
J. Chem. Phys. 24 628-629 (1956)

Hyman, H. H., and Katz, J. J.
The Bromine Trifluoride Process for Metallic Uranium Fuel Elements
Progress in Nuclear Energy, Series III-Process Chemistry. London: Pergamon Press, 1956. p. 274

Hyman, H. H., Vogel, R. C., and Katz, J. J.
Fundamental Chemistry of Uranium Hexafluoride Distillation Processes for the Decontamination of Irradiated Reactor Fuels
Progress in Nuclear Energy, Series III-Process Chemistry. London: Pergamon Press, 1956. p. 261

Hyman, H. H. (See Lawroski, S.)

Inghram, M. G., Berkowitz, J., and Chupka, W. A.
Dissociation Energies of the TaO and TaO_2 Molecules
Bull. Am. Phys. Soc. 1 341 (November 23, 1956)

Inghram, M. G., Chupka, W. A., and Porter, R. F.
A Mass Spectrometric Study of Barium Oxide Vapor
J. Chem. Phys. 23 2159-2165 (1955)

Inghram, M. G., and Gomer, R.
Massenspektrometrische Untersuchungen der Feldemission Positiver Ionen
Ztschr. Naturforschung (Mattauch Number) 10a (11) 863-872 (1955)

Inghram, M. G., Porter, R. F., and Chupka, W. A.
Mass Spectrometric Study of Gaseous Species in the $B-B_2O_3$ System
J. Chem. Phys. 25 498-501 (1956)

Inghram, M. G. (See Chupka, W.)
(See Fields, P. R.)
(See Stanton, H. E.)

Inglis, D. R.
Nuclear Moments of Inertia from Nucleon Motion in a Rotating Well
Phys. Rev. 103 1786-1795 (1956)

Jaffey, A. H.
Long Term Variation in Composition and Neutron Yield in Pile Plutonium
Nuclear Sci. Eng. 1 (3) 204-215 (July 1956)

Jaroslow, B. N., and Taliaferro, W. H.
Restoration of Hemolysin-Producing Capacity in X-Irradiated Rabbits
Fed. Proc. 15 594 (1956)

Jaroslow, B. N., and Taliaferro, W. H.
The Restoration of Hemolysin-Forming Capacity in X-Irradiated Rabbits by Tissue and Yeast Preparations
J. Infec. Dis. 98 75-81 (1956)

Jaroslow, B. N. (See Flynn, R. J.)

Jensen, K. J. (See Hayden, R. J.)

Jesse, W. P., and Sadauskis, J.
The Ionization by Alpha Particles in Mixtures of Gases
Phys. Rev. 100 1755-1762 (1955)

Jesse, W. P., and Sadauskis, J.
Recoil Particles from Po^{210} and Their Ionization in Argon and Helium
Phys. Rev. 102 389-390 (1956)

Jordan, D. L., Clark, J. W., and Vogel, H. H., Jr.
The Additivity of γ Rays and Fission Neutrons in Producing Spleen Weight Reduction
Rad. Res. 4 77-85 (January 1956)

Jordan, D. L. (See Vogel, H. H., Jr.)

Kafalas, P., and Irvine, J. W., Jr.
Nuclear Excitation Functions and Thick Target Yields: (C+d)
Phys. Rev. 104 703-705 (1956)

Kanter, M. A., and Hennig, G. R.
Quenched-in Lattice Defects in Graphite
Bull. Am. Phys. Soc. 1 119 (March 15, 1956)

Kaplan, L., Hildebrandt, R. A., and Ader, M.
The Trinitratouranyl Ion in Organic Solvents
J. Inorganic and Nuclear Chem. 2 153-163 (1956)

Katz, E. J., and Powers, E. L.
Changes During Development of Plasma Amino Acids in X-Irradiated Chick Embryos
Rad. Res. 3 331 (November 1955)

Katz, J. J., and Kopple, K. D.
The Synthesis of Poly-α-amino Acids in Anhydrous Hydrogen Fluoride
J. Am. Chem. Soc., 78 6199 (1956)

Katz, J. J., and Maybury, R. H.
Protein Denaturation in Heavy Water
Nature, 177 629 (1956)

Katz, J. J. (See Adams, R. M.)
(See Crespi, H.)
(See Hyman, H. H.)
(See Koch, A. L.)
(See Sheft, I.)

Katzin, L. I.
Regularities in the Absorption Spectra of the Halides
J. Chem. Phys. 23 2055-2060 (1955)

Katzin, L. I., Ferraro, J. R., Wendlandt, W. W., and McBeth, R. L.
The Relations of Thorium Nitrate and Certain Organic Solvents. The Coordination Number of Th^{4+}
J. Am. Chem. Soc. 78 5139-5144 (1956)

Katzin, L. I., and Gebert, E.
The Iodide-Iodine-Triiodide Equilibrium and Ion Activity Coefficient Ratios
J. Am. Chem. Soc. 77 5814-19 (1955)

Katzin, L. I., and Spinrad, B. I.
A U^{233} Breeder -- U^{235} Converter Reactor
Nuclear Sci. Eng. 1 343-354 (1956)

Katzin, L. I., and Stoughton, R. W.
A Manganese Dioxide Procedure for Isolation and Concentration of Protactinium from Irradiated Thorium Compounds
J. Inorg. Nucl. Chem. 3 229 (1956)

Katzin, L. I. (See Ferraro, J. R.)

Kaufmann, S. G., Kirn, F. S., and Loewenstein, W. B.
Fission and Activating Ratios in the EBR
Nuclear Sci. Eng. 1 (3) 193-203 (July 1956)

Kaufmann, S. G. (See Erickson, G. F.)

Kelman, L. R., Wilkinson, W. D., Shuck, A. B., and Goertz, R. C.
Handling Alpha-Active Pyrophoric Materials. 1-What is the Best Approach?
Nucleonics 14 61-65 (March 1956)

Kelman, L. R., Goertz, R. C., Shuck, A. B., and Wilkinson, W. D.
Handling Alpha-Active Pyrophoric Materials. 2-Design and Construction of Glove Boxes
Nucleonics 14(4) 65-71 (April 1956)

Kelman, L. R., Goertz, R. C., Shuck, A. B., and Wilkinson, W. D.
Handling Alpha-Active Pyrophoric Materials. 3-Glovebox-Atmosphere Control
Nucleonics 14 (5) 77-82 (May 1956)

Kemp, N. E.
Electron Microscopy of Growing Oocytes of Rana pipiens
J. Biophus. Biochem. Cytol. 2 281-292 (1956)

Kirn, F. S. (See Kaufmann, S. G.)

Kittel, J. H.
Damaging Effects of Radiation on Solid Reactor Materials
Nucleonics 14 (9) 63-65 (September 1956)

Klein, P. D., Handa, D. T., and Swick, R. W.
The Fate of Ascorbic Acid in Early Radiation Damage
Proc. Soc. Exp. Biol. Med. 90 204-207 (1955)

Klein, P. D., Handa, D. T., and Swick, R. W.
The Fate of Ascorbic Acid in Early Radiation Damage
Rad. Res. 3 333 (November 1955)

Klein, P. D., and Swick, R. W.
DNA Synthesis in Spleens of Scorbutic Guinea Pigs
Fed. Proc. 15 290 (1956)

Klein, R. M., and Vogel, H. H., Jr.
Necessity of Indoleacetic Acid for the Duplication of Grown-Gall Tumor Cells
Plant Physiol. 31 17-21 (1956)

Koch, A. L.
The Enzymes of Nucleoside Metabolism in Escherichia coli
Fed. Proc. 15 290 (1956)

Koch, A. L.
The Kinetics of Glycine Incorporation by Escherichia coli
J. Biol. Chem. 217 931-946 (1955)

Koch, A. L.
The Metabolism of Methyl Purines by Escherichia coli. I. Tracer Studies
J. Biol. Chem. 219 181-188 (1956)

Koch, A. L., and Lamont, W. A.
Metabolism of Methyl Purines by Escherichia coli. II. Enzymatic Studies
J. Biol. Chem. 219 189 (1956)

Koch, A. L., Lamont, W. A., and Katz, J. J.
The Effect of Anhydrous Strong Acids on Ribonuclease and Lysozyme
Arch. Biochem. Biophys. 63 106-117 (July 1956)

Koch, A. L., and Levy, H. R.
Protein Turnover in Growing Cultures of E. coli
J. Biol. Chem. 217 947-958 (1955)

Koch, A. L. (See Swick, R. W.)

Koch, L. J.
Power Reactor Experiments: EBR-II
Nucleonics 14 (8) 43-44 (August 1956)

Krohn, V. E., Crouch, M. F., and Ringo, G. R.
Coherent Neutron Scattering Amplitudes of Krypton and Xenon, and the Electron-Neutron Interaction
Phys. Rev., 102, 1321 (1956)

Krohn, V. E., Novey, T. B., and Raboy, S.
Attenuation of Am^{241} α - γ Angular Correlations in Liquid Film Sources
Bull. Am. Phys. Soc. 1 330 (November 23, 1956)

Krohn, V. E. (See Eggler, C.)
(See Huizenga, J. R.)

Kubota, L. (See Wassermann, F.)

Kurath, D.
Gamma Transition Widths in the 1p-Shell
Bull. Am. Phys. Soc. 1 180 (April 26, 1956)

Kurath, D.
Intermediate Coupling in the 1p-Shell
Phys. Rev. 101 216-224 (1956)

Lach, E. J., and Perlow, G. J.
Small Vacuum Valve
Rev. Sci. Instr. 27 336-337 (1956)

Laird, A. K.
Intracellular Localization of Pancreatic Amylase
Fed. Proc. 15 521 (1956)

Laird, A. K., and Barton, A. D.
Consistent Biochemical Pattern in Malignant Tumors
Science 124 32-34 (1956)

Laird, A. K., Barton, A. D., and Nygaard, O.
Synthesis of Protein and Ribonucleic Acid in Rat Liver during Refeeding after Starvation
Exper. Cell. Res. 9 523-540 (1955)

Landmann, W. (See Fricke, H.)

Lane, R. O., and Monahan, J. E.
Differential Neutron Resonance Cross Sections of Be^9 and Na^{23}
Bull. Am. Phys. Soc. 1 187 (April 26, 1956)

Lane, R. O., and Monahan, J. E.
Differential Cross Section for Neutrons Scattered from the 585-Kev Resonance in S^{32}
Bull. Am. Phys. Soc. 1 346 (November 23, 1956)

Lawroski, S., and Hyman, H. H.
Survey of Separations Processes for Irradiated Fuels
Progress in Nuclear Energy, Series III-Process Chemistry. London: Pergamon Press, 1956. p. 43

Lee, L. L., and Mooring, F. P.
Low-Lying T = O Levels in P^{30}
Bull. Am. Phys. Soc. 1 281 (June 21, 1956)

Lee, L. L., Jr. (See Mooring, F. P.)

Leone, C. A.
Some Immunochemical Studies on Hemocyanin
Fed. Proc. 15 598 (March 1956)

Leone, C. A. (See Fricke, H.)

Lesher, S., Sacher, G. A., and Grahn, D.
Effects of Continuous Gamma Exposure in the Ranges 1.6 to 200 Kr/Day on Survival and Intestinal Histopathology in the Mouse
Rad. Res. 5 489 (October 1956)

Lesher, S. W. (See Nebel, B. R.)

Lewis, Y. S. (See Smith, D. E.)

Lichtenberger, H. V. (See Cerutti, B. C.)
(See Zinn, W. H.)

Liimatainen, R. C., and Mecham, W. J.
Removal of Halogens, Carbon Dioxide and Aerosols from Air in a Spray Tower
J. Air Pollution Control Assoc. 6 17-49 (May 1956)

Liimatainen, R. (See Fischer, J.)

Lindenbaum, A., and Lisco, H.
Autoradiographic Study of Localization of Aurintricarboxylic Acid in Experimental Beryllium Poisoning
Proc. Soc. Exptl. Biol. Med. 92 354-357 (1956)

Lindenbaum, A. (See Wassermann, F.)

Lisco, H. (See Lindenbaum, A.)

Loewenstein, W. B. (See Kaufmann, S. G.)

Looney, W. B.
Skeletal Roentgenographic Changes Following Radioelement Deposition
Am. J. Roentgenol. 75 559-572 (1956)

Lucas, H. F., Jr. (See Stehney, A. F.)

Lynch, F. J., and Baumgardner, J. B.
Alpha Air Proportional Counter
Rev. Sci. Instr. 26 1134-37 (1955)

Malm, J. G., Weinstock, B., and Claassen, H. H.
Infrared Spectra of NpF_6 and PuF_6
J. Chem. Phys. 23 2192-2193 (1955)

Malm, J. G. (See Claassen, H. H.)
(See Gruen, D. M.)
(See Weinstock, B.)

Manning, W. M. (See Fields, P. R.)

Magnusson, L. B., and Engelkemeir, D. W.
Intensities of X Rays and γ Rays in Am^{241} α Decay
Bull. Am. Phys. Soc. 1 171 (April 26, 1956)

Magnusson, L. B., Friedman, A. M., Engelkemeir, D., Fields, P. R., and Wagner, F., Jr.
Properties of Bk^{245}
Phys. Rev. 102 1097-1103 (1956)

Manning, T. E., Fred, M., and Tomkins, F. S.
Nuclear Moments of Am^{241} and Am^{243}
Phys. Rev. 102 1108 (1956)

Marinelli, L. D.
Radioactive Poisoning
Nuclear Power 1 (11) 92 (June 1956)

Marinelli, L. D. (See Berlman, I. B.)
(See Brar, S. S.)
(See Gustafson, P. F.)
(See Miller, C. E.)

Martens, F. H. (See Reardon, W. A.)

Martin, A. F. (See Sheft, I.)

Martin, D. W., Brice, M. K., Cork, J. M., and Burson, S. B.
The Decay of Radioactive Ce^{143} (33.4 hr)
Phys. Rev. 101 182-188 (1956)

Martin, D. W., Burson, S. B., and Cork, J. M.
Decay of Mo^{101}(14.6 Min)
Bull. Am. Phys. Soc. 1 329 (November 23, 1956)

Martin, D. W., Cork, J. M., and Burson, S. B.
The Decay of Ca^{49} and Sc^{49}
Phys. Rev. 102 457-458 (1956)

Mason, G. W. (See Peppard, D. F.)

Matheson, M. S. (See Grossweiner, L. I.)
(See Weeks, J. L.)

McBeth, R. L. (See Katzin, L. I.)

McCorkle, W. H.
Using Intermediate Experiments for Reactor Nuclear Design
Nucleonics 14 54-56 (March 1956)

McCurdy, R. D. (See Brunson, G. S.)

McGonnagle, W. J.
Ultrasonic Shear Wave Testing
Metal Progress 70 (4) 97-99 (October 1956)

McGonnagle, W. J.
Some Nondestructive Testing Methods for Testing Welds
Welding Journal 35 (11) 1110-1119 (1956)

McLain, S. and Foote, F. G.
Educational and Research Problems in Nuclear Metallurgy (with Special Reference to Fuel Elements)
J. Eng. Ed. 46 (9) 760-767 (1956)

McMahon, J. P. (See Schumann, R. W.)

Mech, J. F., Diamond, H., Studier, M. H., Fields, P. R., Hirsch, A., Stevens, C. M., Barnes, R. F., Henderson, D. J., and Huizenga, J. R.
The Alpha and Spontaneous Fission Half-Lives of $Plutonium^{242}$
Phys. Rev. 103 340-341 (1956)

Mech, J. F. (See Andre, C. G.)
(See Fields, P. R.)

Mecham, W. J. (See Liimatainen, R. C.)

Miller, C. E., and Marinelli, L. D.
An Analysis of the Background Radiation Detected by NaI Crystals
Rad. Res. 3 337 (November 1955)

Miller, C. E., and Marinelli, L. D.
A Preliminary Report on the Scintillation Spectrum of the Gamma Radiation Emitted by Human Beings
Rad. Res. 5 490 (October 1956)

Miller, C. E., and Marinelli, L. D.
The Gamma-Ray Spectrum of Normal Human Beings
Radiol. 66 104 (1956)

Miller, C. E., and Marinelli, L. D.
The Gamma-Ray Activity of Contemporary Man
Science 124 122-123 (1956)

Miller, C. E., Marinelli, L. D., Rowland, R. E., and Rose, J. E.
Reduction of NaI Background
Nucleonics 14(4) 40-43 (April 1956)

Miller, C. E., Marinelli, L. D., Rowland, R. E., and Rose, J. E.
An Analysis of the Background Radiation Detected by NaI
Trans. Prof. Group Nucl. Sci. IRE NS-3(4) 90 (November 1956)

Miller, D. (See Shor, A. J.)

Miller, M. (See Sacher, G. A.)

Minich, O. T. (See Nebel, B. R.)
(See Powers, E. L.)

Misch, R. D., and Fisher, E. S.
Variation of Anodic Film Growth With Grain Orientation in Zirconium
Acta Metallurgica 4 222 (1956)

Misch, R. D., and Fisher, E. S.
Anodic Film Growth on Hafnium in Nitric Acid
J. Electrochem. Soc. 103 153-156 (1956)

Monahan, J. E., Hausman, H., Mooring, F. P., and Raboy, S.
Inelastic Scattering of Neutrons by Na^{23}
Bull. Am. Phys. Soc. Series II, 1 56 (January 30, 1956)

Monahan, J. E. (See Lane, R. O.)

Montet, G. L., Hennig, G. R., and Kurs, A. F.
Tracer Studies on Radiation-Damaged Graphite
Nuclear Science and Eng. 1 33-52 (March 1956)

Mooring, F. P. and Lee, L. K., Jr.
Resonant Detection of Neutron Energy Groups
Bull. Am. Phys. Soc. 1 327 (November 23, 1956)

Mooring, F. P. (See Lee, L. L., Jr.)
(See Monahan, J. E.)

Moss, R. A. (See Gordon, S. A.)

Mueller, M. H.
The Phase Found in the U-Zr Alloys
Acta Cryst. 8 849-850 (1955)

Mueller, M. H.
Vacuum Seal for Thin Metal Windows
Rev. Sci. Instr. 27 411 (1956)

Mueller, M. H., Chernock, W. P., Singer, J., and Beck, P. A.
Correction Factor for the Quantitative Determination of Fiber Textures
J. Appl. Phys. 27 1170 (1956)

Munick, R. J.
Temperature Dependence of the Conduction Current from Plexiglas
Bull. Am. Phys. Soc. 1 302 (June 21, 1956)

Munick, R. J.
After Effects of Gamma Irradiation upon the Electrical Conductivity of Plexiglas
Bull. Am. Phys. Soc. 1 321 (November 23, 1956)

Munick, R. J.
Transient Electric Currents from Plastic Insulators
J. Appl. Phys. 27 1114-1117 (1956)

Nebel, B. R., Lesher, S. E., and Papierski, D. H.
Effects of Continuous Exposure to Gamma Radiation on Mouse
Spermatogenesis
Rad. Res. 5 587 (November 1956)

Nebel, B. R., and Minick, O. T.
Embedding Aid for Coverslip Mounts in Electron Microscopy
J. Biophys. Biochem. Cytol. 2 (4) 61-63 (July 1956)

Neubert, T. J., and Burton, M.
Effect of Fast Neutron Bombardment on Physical Properties of Graphite: A Review
J. Appl. Phys. 27 557 (1956)

Neutron Induced Discomposition of Graphite
J. Appl. Phys. 27 568 (1956)

Nobles, R. G., and Smith, A. B.
Fission Chamber Measures Neutron Distribution Quickly, Accurately
Nucleonics 14 60-62 (January 1956)

Norris, W. P., and Woodruff, L. A.
The Fundamentals of Radioautography
Annual Review of Nuclear Soc. 5, ed. J. G. Beckerly (Stanford: Annual Reviews, Inc., 1955) p. 297-326

Norris, W. P. (See Speckman, T. W.)

Novey, T. B., Freedman, M. S., Porter, F. T., and Wagner, F., Jr.
Beta-Gamma Directional Correlation in Re^{186}
Phys. Rev. 103 942-948 (1956)

Novey, T. B. (See Freedman, M. S.)
(See Krohn, V. E.)
(See Porter, F. T.)

Novick, M. (See Zinn, W. H.)

Okrent, D. (See Cerutti, B. C.)

Osborne, D. W., Abraham, B. M., and Weinstock, B.
Thermodynamic Properties of Liquid He^3 between 0.23° and 2°K
Proc. Conference de Physique des Basses Temperature, Paris, September 2-8, 1955 pp. 26-29

Osborne, D. W. (See Abraham, B. M.)

Ostrander, H.
Fixture Generates Large Radius
Am. Mach. 100 118-119 (July 2, 1956)

Pahis, L. E. (See Erickson, G. F.)

Peleg, L. G., and Gordon, S. A.
Phenol-Mediated Conversion of Tryptophan to IAA
Plant Physiol. 31 (Suppl.) 26 (August 26, 1956)

Papierski, D. H. (See Nebel, B. R.)

Patt, H. M.
Further Studies on the Influence of Temperature on Radiation Lethality in the Frog
Rad. Res. 5 610 (November 1956)

Patt, H. M., and Straube, R. L.
Measurement and Nature of Ascites Tumor Growth
"Ascites Tumors as Tools in Quantitative Oncology," Ann. New York Acad. Sci. 63 728-738 (1956)

Patt, H. M. (See Straube, R. L.)

Peppard, D. F., Mason, G. W., and Maier, J. L.
Interrelationships in the Solvent Extraction Behavior of Scandium, Thorium, and Zirconium in Certain Tributylphosphate-Mineral Acid Systems
J. Inorg. Nucl. Chem. 3 215-228 (1956)

Perlow, G. J.
Recoil Type Neutron Spectrometer for 0.05 to 1 Mev
Rev. Sci. Instr. 27 460-467 (1956)

Perlow, G. J. (See Lach, E. J.)

Pettitt, E. N. (See Brunson, G. S.)

Porter, F. T., Freedman, M. S., Novey, T. B., and Wagner, F., Jr.
First Forbidden Nonunique Beta Transitions in Re^{186}
Phys. Rev. 103 921-942 (1956)

Porter, F. T. (See Freedman, M. S.)
(See Huizenga, J. R.)
(See Novey, T. B.)

Porter, R. F. (See Chupka, W. A.)
(See Inghram, M. G.)

Powers, E. L., Ehret, C. F., Roth, L. E., and Minick, O. T.
The Internal Organization of Mitochondria
J. Biophys. Biochem. Cytol. 2 341-346 (1956)

Powers, E. L., Greiff, D., and Pinkerton, H.
The Effect of X-Rays on the Rickettsiostatic Activity of Streptomycin, Aureomycin, and Penicillin
Rad. Res. 5, 480 (1956)

Powers, E. L. (See Ehret, C. F.)
(See Katz, E. J.)
(See Tahmisian, T. N.)

Primak, W.
Fast Neutron Damage in Quartz and Vitreous Silica
Bull. Am. Phys. Soc. 1 (March 15, 1956)

Primak, W.
Gamma-Ray Dosage in Inhomogeneous Nuclear Reactors
J. Appl. Phys. 27 54-62 (1956)

Primak, W.
Kinetics of Processes Distributed in Activation Energy
Phys. Rev. 100 1677-1689 (1955)

Primak, W.
C-Axis Electrical Conductivity of Graphite
Phys. Rev. 103 (3) 544-546 (1956)

Primak, W.
Fast-Neutron Damaging in Nuclear Reactors: Its Kinetics and the Carbon Atom Displacement Rate
Phys. Rev. 103 1681-1692 (1956)

Primak, W.
Gouy Modulator for Thermocouples
Rev. Sci. Instr. 27 877 (1956)

Primak, W., and Fuchs, L. H.
Radiation Damage to the Electrical Conductivities of Natural Graphite Crystals
Phys. Rev. 103 (3) 541-544 (1956)

Primak, W., Fuchs, L. H., and Day, P. P.
Radiation Damage in Diamond and Silicon Carbide
Phys. Rev. 103 1184-1192 (1956)

Primak, W., and Quarterman, L. A.
Heat of Reaction of Irradiated Graphite with Potassium
J. Am. Chem. Soc. 78 3879-3881 (1956)

Primak, W. L., and Szymanski, H.
Radiation Damage in Vitreous Silica: Annealing of the Density Changes
Phys. Rev. 101 1268-1271 (1956)

Pringsheim, P.
Varied Behavior of F-Centers in Natural and Synthetic NaCl
Ztschr. Phys. 144 31-38 (1956)

Pyle, G. L. (See Engelkemeir, D.)
(See Fields, P. R.)
(See Fried, S. M.)

Quarterman, L. A. (See Primak, W.)

Quevedo, W. C., Jr.
Effect of Biotin Deficiency on Follicular Melanocytes of Mice
Proc. Soc. Exptl. Biol. Med. 93 260-263 (November 1956)

Raboy, S. (See Ferentz, M.)
(See Huizenga, J. R.)
(See Krohn, V. E.)
(See Monahan, J. E.)

Ramler, W. J. (See Andre, C. G.)
(See Hart, E. J.)

Rauh, E. G. (See Andre, C. G.)

Raz, B. J.
An Interpretation of New dp Experimental Data in Terms of the j-j Coupling Shell Model
Bull. Am. Phys. Soc. 1 336 (November 23, 1956)

Reardon, W. A., and Martens, F. H.
Some Experimental Aspects of Coupling Slow and Fast Reactor Systems
Bull. Am. Phys. Soc. Series II, Vol. 1 68 (January 30, 1956)

Reed, G. W., and Turkevich, A.
The Uranium Content of Two Iron Meteorites
Nuclear Processes in Geologic Settings. Nucl. Sci. Ser. Report 19. Natl. Acad. Sci. Natl. Res. Counc. Publication 400, Washington, July 31, 1956. pp 97-99

Rice, R. E. (See Cerutti, B. C.)

Ringo, G. R. (See Eggler, C.)
(See Krohn, V. E.)

Robinson, J. E.
First Occurrence Probabilities in Stochastic Physical Processes
Bull. Am. Phys. Soc. 1 145 (March 15, 1956)

Rodger, W. A., and Hampson, D. C.
Operating Characteristics and Economics of a 100 Cubic Foot/Day Incinerator for Radioactive Wastes
J. Air Pollution Control Assoc. 6 41-44 (May 1956)

Rodger, W. A., Trice, V. G., Jr., and Rushton, J. H.
Interfacial Area in Liquid-Liquid Dispersions Related to Fluid Motion in Mixing Vessels
Chem. Eng. Prog. 52 515-520 (1956)

Rodger, W. A. (See Shor, A. J.)
(See Trice, V. G., Jr.)

Rose, D., and Hamermesh, B.
Preliminary Studies with the 7.7-Meter Bent-Crystal Gamma-Ray Spectrometer
Bull. Am. Phys. Soc. 1 189 (April 26, 1956)

Rose, J. E. (See Miller, C. E.)

Rosen, C., Banks, E., and Post, B.
The Thermal Expansion Phase Transitions of WO_3
Acta Cryst. 9 475 (1956)

Rosen, C., Banks, E., and Post, B.
The Thermal Expansion of Cubic Sodium Tungsten Bronzes
Acta Cryst. 9 477 (1956)

Rosenthal, M. W. (See Fried, J. M.)

Rosenzweig, N.
On the Level Density of a System of Fermi Particles
Bull. Am. Phys. Soc. 1 304 (June 21, 1956)

Roth, L. E.
Aspects of Ciliary Fine Structure in Euplotes patella
J. Biophys. Biochem. Cytol. 2 235-240 (July 1956)

Roth, L. E. (See Powers, E. L.)

Rothman, S. J., and Hall, L. D.
Diffusion in Liquid Lead
J. Metals 8 199 (1956)

Rowland, R. E.
Detection of Radium in Vivo by Means of Gamma-Gamma Coincidence Techniques
Rad. Res. 3 342 (November 1955)

Rowland, R. E. (See Miller, C. E.)

Ruther, W. E. (See Draley, J. E.)

Sacher, G. A.
Mathematical Analysis of the Behavior of Cellular Systems
Rad. Res. 5 587 (November 1956)

Sacher, G. A.
A Sign of Severe Radiation Injury Observed in the Erythrocyte Sedimentation of Dogs
Blood: the Journal of Hematology 11 174-183 (1956)

Sacher, G. A.
On the Statistical Nature of Mortality with Especial Reference to Chronic Radiation Mortality
Radiology 67 250-258 (1956)

Sacher, G. A., and Miller, M.
Hematologic Responses of LAF1 Mice given Daily Dosage of Gamma Rays
Rad. Res. 5 491 (October 1956)

Sacher, G. A., and Schweisthal, R.
The Stochastic Theory of Lethality: Applications in Mammalian Radiobiology
Rad. Res. 3 343 (November 1955)

Sacher, G. A. (See Grahn, D.)
(See Lesher, S.)

Sadauskis, J. (See Jesse, W. P.)

Sanderson, M. (See Stearner, S. P.)

Saplakoglu, A., Bollinger, L. M., and Coté, R. E.
Neutron Cross-Section Measurements on Niobium
Bull. Am. Phys. Soc. 1 347 (November 23, 1956)

Sato, T. R. (See Strain, H. H.)

Schlenk, F., and DePalma, R. E.
Metabolism of Thetins in Yeast (Torulopsis utilis)
Fed. Proc. 15 348 (1956)

Schubert, J.
Removal of Radioelements from the Mammalian Body
Ann. Rev. Nuclear Sci. 5 369-412 (1955)

Schubert, J. (See Fried, J. M.)

Schumann, R. W.
A 1024-Channel Neutron Time-of-Flight Analyzer
Bull. Am. Phys. Soc. 1 188 (April 26, 1956)

Schumann, R. W.
A 1024-Channel Neutron Time-of-Flight Analyzer
Rev. Sci. Instr. 27 686-689 (1956)

Schumann, R. W., and McMahon, J. P.
The Argonne 256-Channel Pulse Height Analyzer
Rev. Sci. Instr. 27 675-685 (1956)

Schweisthal, R. (See Sacher, G. A.)

Scully, N. J. (See Skok, J.)

Sheft, I., Martin, A. F., and Katz, J. J.
High Temperature Fluorination Reactions of Inorganic Substances with Bromine Trifluoride Addition Compounds
J. Am. Chem. Soc. 78 1557-1559 (1956)

Shor, A. J., Ward, H. T., Miller, D., and Rodger, W. A.
Power Reactor Experiments: Borax-III
Nucleonics 14(8) 38-40 (August 1956)

Shuck, A. B. (See Kelman, L. R.)

Sidhu, S. S., Heaton, L., and Zauberis, D. D.
Neutron Diffraction Studies of Hafnium-Hydrogen and Titanium-Hydrogen Systems
Acta Cryst. 9 607-614 (1956)

Sidhu, S. S., Heaton, L., Zauberis, D. D., and Campos, F. P.
Neutron Diffraction Study of Titanium-Zirconium System
J. Appl. Phys. 27 1040-1041 (1956)

Siegel, S.
The Crystal Structure of $KBrF_4$
Acta Cryst. 9 493-495 (1956)

Siegel, S.
The Structure of TiF_3
Acta Cryst. 9 684 (1956)

Siegel, S.
The Structures of Cs_2ThCl_6 and Cs_2UCl_6
Acta. Cryst. 9 827 (1956)

Sjoblom, R. (See Friedman, A. M.)

Skok, J.
Relationship of Boron Nutrition to Radiosensitivity of Sunflower Plants
Plant Physiol. 31 (Suppl.) 13 (August 26, 1956)

Skok, J., and Scully, N. J.
Nature of the Photoperiodic Responses of Buckwheat
Botanical Gazette 117 134-141 (December 1955)

Smaller, B., Delbecq, C., and Yuster, P.
Paramagnetic Resonance Absorption in Irradiated Thallium-Activated Potassium Chloride
Bull. Am. Phys. Soc. 1 324 (November 23, 1956)

Smaller, B., Yuster, P. H., and Delbecq, C. J.
Paramagnetic Resonance Investigation of Irradiated KCl Crystals Containing U-Centers
Bull. Am. Phys. Soc. 1 124 (March 15, 1956)

Smaller, B. (See Delbecq, C. J.)
(See Hennig, G. R.)

Smith, A. B., Fields, P. R., and Friedman, A. M.
Fission Modes of the Even-Even Isotopes Cm^{244} and Pu^{242}
Bull. Am. Phys. Soc. 1 281 (June 21, 1956)

Smith, A. B., Fields, P. R., and Friedman, A. M.
Prompt Gamma Rays Accompanying the Spontaneous Fission of Cf^{252}
Phys. Rev. 104 699-702 (1956)

Smith, A. B., Friedman, A. M., and Fields, P. R.
Spontaneous Fission Kinetics of Cf^{252}
Phys. Rev. 102 813-815 (May 1, 1956)

Smith, A. B. (See Nobles, R. G.)

Smith, D. E.
The Nature of the Secretory Activity of the Tissue Mast Cell
Proc. 20th Physiol. Cong., Brussels, 1956. Bruges: The St. Catherine Press, 1956, p. 274

Smith, D. E., and Lewis, Y. S.
Electronmicroscopy of Mast Cells after X-Irradiation and Treatment with Chemical Agents
Am. J. Physiol. 183 662 (1955)

Smith, D. E., and Tyree, E. B.
The Influence of X-Irradiation upon Water Consumption by the Rat
Am. J. Physiol. 184 127-133 (1956)

Smith, D. E., and Tyree, E. B.
Attempts to Provide the Rat with Nutrition During Post-Irradiation Anorexia
Rad. Res. 4 435-448 (May 1956)

Sokoloff, J., and Hamermesh, M.
Calculation of Neutron Scattering from the Complex Potential Model
Bull. Am. Phys. Soc. 1 303 (June 21, 1956)

Speckman, T. W., Norris, W. P., and Woodruff, L. A.
Radiation Damage of Bone from Deposited Radium
Rad. Res. 3 350 (November 1955)

Spinrad, B. I. (See Katzin, L. I.)

Stanton, H. E.
Secondary Beryllium Ions Produced by Ion Bombardment
Bull. Am. Phys. Soc. 1 341 (November 23, 1956)

Stanton, H. E., Chupka, W. A., and Inghram, M. G.
Electron Multipliers in Mass Spectrometry: Effect of Molecular Structure
Rev. Sci. Instr. 27 109 (1956)

Stearner, S. P., Sanderson, M., Christian, E. J., and Brues, A. M.
The Initial Radiation Syndrome in the Adult Chicken
Am. J. Physiol. 184 134-140 (1956)

Stearner, S. P., and Tyler, S.
An Analysis of the Role of Dose and Exposure Time in the Radiation Response of the Chick
Rad. Res. 5 597 (November 1956)

Stearner, S. P. (See Bernstein, E. Katz)

Stehney, A. F., and Lucas, H. F., Jr.
Retention of Environmental Radium by Young Humans
Rad. Res. 3 351 (November 1955)

Stehney, A. F., and Wallace, D. E.
Dibutyl Phosphate as an Extractant of Radiothorium from Bone
Rad. Res. 5 598 (November 1956)

Stein, L., and Vogel, R. C.
Behavior of Uranium and Other Selected Materials in Fluorinating Reagents
Ind. Eng. Chem. 48 418-421 (1956)

Steinberg, E. P. (See Flynn, K. F.)

Steunenberg, R. K., and Vogel, R. C.
The Absorption Spectrum of Fluorine
J. Am. Chem. Soc. 78 901-902 (1956)

Stevens, C. M. (See Engelkemeir, D.)
(See Fields, P. R.)
(See Fried, S. M.)
(See Stoughton, R. W.)
(See Mech, J. F.)

Stewart, D. C., and Faris, J. P.
Preparation of Rare Earth Concentrates
J. Inorg. Nuclear Chem. 3 64-66 (August 1956)

Stoughton, R. W., Halperin, J., Stevens, C. M., Ferguson, D. E., and Overholt, D. C.
An Effective Capture Cross Section of Np^{239} for Thermal Reactor Neutrons
Nuclear Science and Engineering 1 108 (1956)

Stoughton, R. W. (See Katzin, L. I.)

Strain, H. H., and Sato, T. R.
Chromatography and Electrochromatography
Anal. Chem. 28(4) 687-694 (April 1956, Part II)

Strain, H. H. (See Evans, G. H.)

Straube, R. L., and Hill, M. S.
Ascites Tumor Growth in Partially Hepatectomized Mice
Proc. Am. Assoc. for Cancer Res. 2 150-151 (April 1956)

Straube, R. L., Hill, M. S., and Patt, H. M.
Mechanisms of Fluid Accumulation in Ascites Tumor Growth
Fed. Proc. 15 181 (1956)

Straube, R. L. (See Patt, H. M.)

Stroud, A. N.
The Effects of Continuous Irradiation by Tritium on Cells Cultivated in vitro
Ann. N. Y. Acad. Sci. 67 11-34 (August 29, 1956)

Stroud, A. N.
The Effects of Continuous Irradiation by Tritium on Cells Cultivated in Vitro
Trans. N. Y. Acad. Sci. 18 228-229 (January 1956)

Stroud, A. N., Brues, A. M., and Chatterley, D. M.
Serial Transplantation of Krebs Mouse Ascites Tumor to Rats
Proc. Am. Assoc. for Cancer Res. 2 151 (April 1956)

Studier, M. H. (See Fields, P. R.)
(See Mech, J. F.)

Stutz, R. E.
The Indoleacetic Acid Oxidase from Lupinus alba L.
Plant Physiol. 31 (Suppl.) 26 (August 26, 1956)

Sullivan, J. C., Cohen, D., Hindman, J. C.
The Behavior of Uranyl and Neptunyl Ions with Dowex-50 Cation-Exchange Resin
J. Am. Chem. Soc. 77 6203 (1955)

Sullivan, J. C. (See Cohen, D.)

Svihla, G., and Malizia, E.
I. La Microfotografia a Raggi Ultravioletti con Transposizione a Colore Nello Studio Della Patologia Clomerulare. II. Assorbimento Ultravioletto Dello Stroma di Glomeruli di Polli Trattati con Cortisone. III. Applicazioni della Microfotografia a Raggi Ultravioletti con Transposizione a Colore Allo Studio Dell' Ipertrofia Glomerulare e del Circolo Intraglomerulare.
Bollettino della Societa' Italiana di Biologia Sperimentale 31 (10) 1-7 (1955)

Swank, R. K., and Buck, W. L.
A Technique for Determining the Performance of Liquid Scintillators under a Controlled Atmosphere
Bull. Am. Phys. Soc. 1 183 (April 26, 1956)

Swick, R. W., and Handa, D. T.
The Incorporation of Fixed Carbon into Amino Acids
J. Biol. Chem. 218 577-585 (1956)

Swick, R. W., Handa, D. T., and Koch, A. L.
The Measurement of Nucleic Acid Turnover in Rat Liver
Arch. Biochem. Biophys. 63 226-242 (July 1956)

Swick, R. W., and Koch, A. L.
Turnover Rate of RNA in Rat Liver
Fed. Proc. 15 534 (1956)

Swick, R. W. (See Klein, P. D.)

Tahmisian, T. N., Powers, E. L., and Devine, R. L.
Light and Electron Microscope Studies of Morphological Changes of Mitochondria during Spermatogenesis in the Grasshopper
J. Biophys. Biochem. Cytol. 2 325-330 (July 1956)

Tahmisian, T. N., and Wright, B. J.
The Immediate Effect of X-Rays on the DPN-DPNH Relationship in Grasshopper Eggs
Fed. Proc. 15 184 (1956)

Tahmisian, T. N., Wright, B. J., and Devine, R. L.
The Effect of X Irradiation on the Dry Weight and Protein Content of Regressing Embryos
Rad. Res. 3 352 (November 1955)

Tahmisian, T. N. (See Beams, H. W.)

Tanaka, K., and Ekstein, H.
Insensitivity of the Scattering Matrix
Bull. Am. Phys. Soc. Series II, Vol. 1 66 (January 30, 1956)

Tanaka, K. (See Ekstein, H.)

Teng, L. C.
Constant Frequency Multi-Bev FFAG Accelerators
Bull. Am. Phys. Soc. 1 178 (April 26, 1956)

Teng, L. C.
Continuous Injection into Circular Ion Accelerators
Rev. Sci. Instr. 27 106 (1956)

Thalgott, F. W. (See Cerutti, B. C.)

Thomas, G. E., Jr.
Potting of Photomultipliers for Use with Liquid Scintillation Detectors
Rev. Sci. Instr. 27 878 (October 1956)

Thomas, G. E., Jr. (See Bollinger, L. M.)
(See Cote , R. E.)

Thomson, J. F., Ginski, J. M., and Omachi, A.
Influence of Temperature, Anaerobiosis, Iodoacetate, and Cyanide on Phosphate Release from Dog Erythrocyte
Fed. Proc. 15 74 (1956)

Thomson, J. F., and Moss, E. M.
The Intracellular Distribution of a Bound Acid Phosphatase of Rat Liver as Studied by Gradient Centrifugation
Arch. Biochem. Biophys. 61 456-460 (1956)

Thorn, R. J. (See Ackermann, R. J.)
(See Winslow, G. H.)

Tomkins, F. S. (See Fred, M.)
(See Manning, T. E.)

Treshow, M.
A Preliminary Study of Superheating Boiling Reactors
Nuclear Science and Engineering 1 167-173 (May 1956)

Trice, V. G., Jr., and Rodger, W. A.
Light Transmittance as a Measure of Interfacial Area in Liquid-Liquid Dispersions
A.I.Ch.E. Journal 2 (2) 205-210 (June 1956)

Trice, V. G., Jr. (See Rodger, W. A.)

Tyler, S. (See Stearner, S. P.)

Uphaus, R. (See Crespi, H.)

Vogel, H. H., Jr., Clark, J. W., and Jordan, D. L.
Some Effects of Protraction and Fractionation Dose of Co^{60} Gamma Radiation on 30-Day Mortality in the Mouse
Fed. Proc. 15 193 (1956)

Vogel, H. H., Jr., Clark, J. W., and Jordan, D. L.
Comparative Mortality Following Single Whole-Body Exposures of Mice
Rad. Res. 3 355 (November 1955)

Vogel, H. H., Jr., Clark, J. W., and Jordan, D. L.
Fractionation and Protraction of Co^{60} Gamma-Radiation--A Study of Acute Lethality in Mice
Rad. Res. 5 601 (November 1956)

Vogel, H. H., Jr. (See Jordan, D. L.)
(See Klein, R. M.)

Vogel, R. C.
Processing of Irradiated Enriched Reactor Fuels using Uranium Hexafluoride
Progress in Nuclear Chemistry. Series III, Process Chemistry, ed. F. R. Bruce, J. M. Fletcher, H. H. Hyman, and J. J. Katz. London: Pergamon Press, Ltd. pp. 286-290.

Vogel, R. C. (See Fischer, J.)
(See Hyman, H. H.)
(See Stein, L.)
(See Steunenberg, R. K.)

Wagner, F., Jr. (See Freedman, M. S.)
(See Magnusson, L. B.)
(See Novey, T. B.)
(See Porter, F. T.)

Wallace, D. E. (See Stehney, A. F.)

Walsh, P. D. (See Hart, E. J.)

Walton, H., Jr. (See Grahn, D.)

Warheit, I. A.
Evaluation of Library Techniques for the Control of Research Materials
Am. Documentation 7 267-275 (October 1956)

Wasserman, F.
The Intercellular Components of Connective Tissue: Origin, Structure and Interrelationship of Fibers and Ground Substance
Ergebnisse der Anatomie und Entwicklungsgeschichte Springer-Verlag (Berlin: January 1956) p. 240-333

Wasserman, F., and Kubota, L.
Observations on Fibrillogenesis in the Connective Tissue of the Chick Embryo by the Aid of Silver Impregnation
J. Biophys. Biochem. Cytol. 2 67-70 (July 1956)

Wasserman, F., and Lindenbaum, A.
Experiments Concerning the Effect of Enzymes on the Reconstitution of Collagenous Fibrils in vitro
J. Biophys. Biochem. Cytol. 2 (4) 299-302 (July 1956)

Watanabe, R.
Paper Chromatographic Studies of Induced and Vegetative Xanthium
Plant Physiol. 31 (Suppl.) 35 (August 26, 1956)

Weeks, J. L., and Matheson, M. S.
The Primary Quantum Yield of Hydrogen Peroxide Decomposition
J. Am. Chem. Soc. 78 1273-1278 (1956)

Weinstock, B., and Malm, J. C.
Properties of Plutonium Hexafluoride
J. Inorganic Nuclear Chem. 2 380 (July 1956)

Weinstock, B. (See Abraham, B. M.)
(See Claassen, H. H.)
(See Gruen, D. M.)
(See Malm, J. G.)
(See Osborne, D. W.)

West, J. M.
Power Reactor Experiments: EBWR
Nucleonics 14 (8) 40-41 (August 1956)

Wexler, S. (See Goodman, L. S.)

Whitham, G. K. (See Zinn, W. H.)

Wilkinson, W. D. (See Kelman, L. R.)

Wing, J. (See Huizenga, J. R.)

Winslow, G. H., Thorn, R. J., and Ackermann, R. J.
Optical Absorption by UO_{2+x} Film
Bull. Am. Phys. Soc. 1 341 (November 23, 1956)

Wright, B. J. (See Tahmisian, T. N.)

Young, H. D.
Atomic Info on Tap
Chem. Eng. News 34 5076-5077 (1956)

Yuster, P. H. (See Delbecq, C. J.)
(See Smaller, B.)

Zauberis, D. D. (See Sidhu, S. S.)

Zinn, W. H.
A Letter on EBR-I Fuel Meltdown
Nucleonics 14 35, 103 (June 1956) also p. 104, 119

Zinn, W. H., Lichtenberger, H. V., Novick, M., Whitham, G. K., Zitek, G. J. B., Feldes, J. G., and Haroldsen, R. O.
Power Reactor Experiments: Borax-III
Nucleonics 14 (8) 38-40 (August 1956)

Zinn, W. H., Lichtenberger, H. V., Novick, M., Whitham, G. K., Zitek, G. J. B., Feldes, J. G., Hall, V. C., Jr., and Haroldsen, R. O.
Operational Experience with the Borax Power Plant
Nuclear Sci. Eng. 1 420-437 (October 1956)

Zitek, C. J. B. (See Zinn, W. H.)